SYNTHESIS AND EVALUATION OF SURFACTANT AND BIODIESEL FROM SESAME OIL

BY

CHERUTO RODAH SOY

THESIS SUBMITTED TO THE SCHOOL OF SCIENCE IN PARTIAL FULFILMENT OF THE REQUIREMENTS FOR THE AWARD OF THE DEGREE OF MASTER OF SCIENCE IN CHEMISTRY, UNIVERSITY OF ELDORET.

2014

DEDICATION

To my loving family: Dad William Soi, mum Grace Soi and brothers Ben, Japheth and David, for their unreserved love and support.

DECLARATION

Declaration by candidate:

I declare that this is my original work and it has never been presented, exhibited or published anywhere for any awards in an academic institution. No part of this thesis may be reproduced without prior permission of the author and/or University of Eldoret.

Signature…….. Date……..…….

Cheruto Rodah Soy SC/PGC/009/10

Declaration by supervisors:

This thesis has been submitted for examination with our approval as the University supervisors:

Signature…….. Date……..…….

Professor Pius Kipkemboi,

Department of Chemistry and Biochemistry,

University of Eldoret.

Signature…….. Date……..……

Dr. Y. Mitei Cheruiyot,

Department of Chemistry and Biochemistry,

University of Eldoret.

ABSTRACT

The search for alternative biodegradable and sustainable raw materials from renewable sources for industrial chemicals to replace the depleted commercially available petrochemicals raw materials has become an area of great research interest. Triglycerides obtained from oil seed crops such as sesame are key potential raw materials for the energy and chemical industry using renewable resources. The objective of this work was to extract oil from sesame seeds, and use it to synthesise biodegradable biodiesel and surfactant. The extracted sesame oil was trans-esterified to SEFAMEs biodiesel, then sulphonated using chlorosulphonic acid and neutralized by sodium hydrogen carbonate to form the anionic sodium sesame fatty methyl ester sulphonate (SEFAMESO) surfactant. The structures of Sesame oil, SEFAMEs biodiesel and the SEFAMESO surfactant were characterized by elemental, HPLC-MS, ^{1}H-NMR, ^{13}C-NMR and FT-IR spectroscopic studies. The peaks at 1418 to 1376 cm^{-1} and a singlet at 3.647 ppm in the SEFAMEs biodiesel FT-IR and ^{1}H-NMR spectra, respectively, corresponded to methyl ester group (-O-CH_3); which confirmed successful trans-esterification of sesame oil to biodiesel. Whereas, the intense peak at 1419 cm^{-1} and 4.690 ppm in the SEFAMESO surfactant FT-IR and ^{1}H-NMR spectra, respectively, corresponded to sulphonate group (S=O), thus, confirmed the presence of sulphonate esters group. The obtained fuel properties of SEFAMEs biodiesel were; density of 840 kg/m^3, flash point of 160 ^{o}C, kinematic viscosity of 3.6 mm^2/s, pour point of -8 ^{o}C and calorific value of 3950 kJ/kg. These values compared well with those of commercially available diesel and it can be used in the existing diesel engine without modification. The evaluated SEFAMESO surfactant solution properties were Krafft temperature, foam-ability and micellar properties. The obtained Krafft point was 19.75 ^{o}C and foam-stability was 54.48 %. Conductivity and viscosity as functions of the SEFAMESO surfactant concentration in aqueous solution at temperature of 298.15, 303.15, 313.15 and 323.15 K were used to determine micellar properties: the critical micelle concentration (CMC) values, thermodynamic parameters of micellization and ionisation degree of micellization of the surfactant. The CMC value was 1.435 $x10^{-4}$ mol/L, change in free energy of micellization -53.78 kJ/mol, and the counter-ion binding degree 0.687 at 298.15 K. The solution properties of SEFAMESO surfactant were good and showed that the synthesized surfactant could be applied as a cleansing agent. This work showed that sesame oil is a potential and viable feedstock for industrial chemicals which can supplement or replace non-biodegradable petroleum based diesel and surfactants in some applications.

TABLE OF CONTENTS

LIST OF TABLES

LIST OF FIGURES

LIST OF APPENDICES

LIST OF SYMBOLS AND ABBREVIATIONS

AOCS- American Oil Chemists' Society.

ASTM- American Standard for Testing Materials.

CMC- Critical Micelle Concentration

C_n-MES-Methyl Ester Sulphonate

^{13}C-NMR-Carbon 13 Nuclear Magnetic Resonance spectroscopy

FAME- Fatty Methyl Esters

FFA- Free Fatty Acid.

FTIR- Fourier Transform Infra-Red Spectroscopy

HPLC-MS- High Performance Liquid Chromatography and Mass Spectroscopy.

^{1}H-NMR- ^{1}H-Proton Nuclear Magnetic Resonance spectroscopy

k- Specific Conductivity

LAB- Linear Alkyl Benzene

n_{sp}- Specific Viscosity

SDS- Sodium Dodecyl Sulphate

SEFAMEs- Sesame Fatty Methyl Esters

SEFAMESO-Sodium Sesame fatty methyl esters Sulphonate

ΔG°_{mic} -Change in free Gibbs energy of micellization.

ΔH°_{mic} - Change in enthalpy of micellization.

ΔS°_{mic} - Change in entropy of micellization

ACKNOWLEDGEMENT

My sincere gratitude and indebtedness goes to my supervisors, Professor Pius Kipkemboi and Dr. Yulita Mitei Cheruiyot. Thank you very much for being my inspirational role models, your guidance, critical comments, advice and encouragements have been valuable throughout this study. Thanks for giving me the opportunity to learn with you and for believing in me.

I salute all the lecturers in the department of Chemistry and Biochemistry who taught me during course work. I also owe a deep debt of gratitude to the technical staff of the department of Chemistry and Biochemistry of University of Eldoret for providing friendly and fruitful working atmosphere. I extend my sincere gratitude to Dr. David Bwambok of Harvard University, USA, for the assistance in the Elemental Analysis, FTIR, HPLC-MS and NMR analysis of the research samples. I acknowledge the assistance of Kenya Pipeline Company Eldoret for giving me the opportunity to use its Laboratory facility in the analysis of fuel properties of SEFAMEs biodiesel.

I acknowledge the National Commission for Science, Technology and Innovation (NACOSTI), for supporting this work by funding the research, the Kenya grant number NCST/ST&I/RCD/4th CALL M.Sc/212.

I am deeply indebted to my dearest friends and all those who believe in me for their support. I would like to express my deep gratitude to my dear friend Denis Magero for his support and always being there for me.

.

CHAPTER ONE

INTRODUCTION

1.1 Background of the Study

The search for renewable and biodegradable raw materials for energy source and industrial production is a research area of intensive interest. This is because of increasing conservation of finite energy resources, environmental pressure to counter global warming caused by greenhouse gases, and a decrease in dependency on foreign trade. Increasing demand for renewable, biodegradable and sustainable products has considerably spark interest in the development of oleo-chemical or bio-based products (Garrier and Packet, 2012).

Bio-based raw materials or oleo-chemical chemicals are of great significance especially in food, biodiesel, cosmetics, polymers, lubricants and pharmaceutical formulation applications, which if exploited can be of great economic importance (Kirk-Othmer, 2012). Therefore, use of renewable raw materials such as vegetable oil crops can reduce greenhouse effect, if grown and harvested sustainably (Wool, 2008). However, due to competition in uses of vegetable oil as food, its application in energy and industrial chemicals has remained limited over decades (Salih *et al.*, 2011).

Sesame (*Sesamum L. indicum*) is recognized as one of the oldest crops in the world history. Archaeological records indicate that it has been used in India for more than 5000 years (Bedigian, 2004). Sesame is widely used in food, nutraceutical, pharmaceutical and industrial applications in many countries because of its high oil, protein and antioxidant contents. In countries like Germany, China, India and Turkey it is used for

ethno-botanical uses against health problems such as cancer, cold and colic (Koca *et al*., 2007).

The crop in the East African region is grown mainly for grains and oil extraction (Were *et al*., 2006). The plant is highly resistant to drought and can produce good yields, when soil moisture is adequate. The crop matures in 3-4 months. Sesame seed has an oil content of 35-63 % which is among the highest of any oil crop (Baydar *et al*., 1999). Sesame has been listed among the neglected and underutilized crop species by The International Plant Genetic Resources Institute (IPGRI), as a crop with high potential (Hawtin, 2007). Hence, using renewable feedstock such as sesame oil as the main raw material for the industrial synthesis of surfactant and biodiesel is of great importance.

1.2 Surfactant System

Surface active agent (surfactant) is a substance that is active at the interface. Surfactants are long organic molecules that have a water soluble (hydrophilic) head and a water insoluble (hydrophobic) tail. The surfactant molecules form oriented monolayers at interfaces and show surface activity; that is they lower the surface or interfacial tension of medium in which they are dissolved (Hill, 2000). Surfactants can be derived from both petrochemical feed-stocks (synthetic organic materials) and renewable resources (oleochemicals that is vegetable oil or fat) (Kjellin and Johansson, 2010).

Surfactants from oleochemical origin are nontoxic and biodegrade better than petrochemical products, giving them an environmental benefit in addition to being derived from renewable resources (Holmberg, 2003). Oleochemical surfactants therefore, have ecological and economic benefits compared to petrochemical

surfactants. Nevertheless, using oleo-chemical feedstocks to produce surfactants is a technology that has been around for many years. However, the potentials of oleo-chemical feedstocks have not been exploited especially in producing oleo-chemical surfactants commercially because they could not compete with low cost petrochemical commodity surfactants (Kjellin and Johansson, 2010).

Vegetable oils can be chemically modified to produce various derivative compounds, which provides the chemical structures that are building blocks for various applications (Salih *et al*., 2011). The oleo-chemical derivative compounds such as fatty acid esters, fatty alcohols, fatty ethoxylates, fatty amines, and glycerol can be formed through various chemical reactions. These compounds have wide ranging surfactant properties (Kjellin and Johansson, 2010). For instance, vegetable oil fatty acids and esters are key precursors in the oleo-surfactant synthesis. This is because they can be easily converted into various derivative compounds through the reaction at the carboxyl group or the double bonds (Yao, 2009). Largely, because of economic reasons, trans-esterification of vegetable oil with methanol to obtain fatty methyl esters (FAMEs) is a cost economical process of synthesizing surfactants on a large scale (Garrier and Packet, 2012). Hence, FAMEs represent more favourable starting materials for production of oleo-chemical surfactants.

Surfactants are of a great practical importance and have diverse applications in the industry area which include: processing of foods, agrochemicals, pharmaceuticals, personal care and laundry products, petroleum, mineral ores, fuel additives and lubricants, paints, coatings and adhesives, and in photographic films. They are also

applied in soil remediation techniques and oil recovery, environmental, health and safety applications (Schramm *et al.*, 2003; Carretti *et al.*, 2003).

Nevertheless, most commercially available surfactants used widely as cleaning agents are from petrochemical (synthetic) origin and they perform well in all types of water(Holser, 2005). Therefore, they are alternatives to soaps which are from oleo-chemical (natural) origin which do not perform well in hard water. However, synthetic detergents cannot be biodegraded by microbes in the sewage treatment systems, thereby causing pollution in water sources. Nevertheless, many synthetic surfactants remain in common use because of their low prices and high effectiveness (Kjellin and Johansson, 2010).

Surfactants are widely used because of their favourable physicochemical characteristics such as: wetting, foaming/defoaming, emulsification/demulsification, dispersion/aggregation of solids, solubility and solubilisation (hydrotropic properties), adsorption, micellization, detergency (which is a complex combination of several of these properties), and synergistic interactions with others. Many surfactants possess a combination of these properties. Furthermore, depending on the chemical composition of a particular surfactant, it may possess important ancillary properties such as: corrosion inhibition, substantivity to fibres and surfaces, biocidal properties, lubricity, stability in highly acidic or alkaline media and viscosity modification. Thus, by defining the properties required to meet a specific application need, the choice of surfactant is narrowed down (Farn, 2008).

A fundamental understanding of the physical chemistry of surfactants, their unusual properties and their phase behaviour is essential for most industrial chemists. In

addition, an understanding of the basic phenomena involved in the application of surfactants, such as in the preparation of emulsions and suspensions and their subsequent stabilization, in micro emulsions, wetting spreading and adhesion is of vital importance in arriving at the right composition and control of the system involved (Tadros, 2005).

The thermodynamic and transport properties such as the activity, enthalpy, volume and compressibility changes on dilution, electrical conductivity, viscosity, and transport numbers are important in understanding useful surfactants interactions behaviour in solution. These properties are used for both examining theories and providing data for technology that is to test various theories and models of surfactant solutions (Holmberg *et al*., 2003; Schramm *et al.*, 2003).

One of the important properties of surfactants is that, at a given surfactant concentration, called critical micelle concentration (CMC), the surfactant molecules self-assemble or aggregate into nanostructures called micelles. CMC is the concentration of surfactant where the micelles start to form. CMC is of great interest because at concentrations above this value the adsorption of surfactant at interfaces usually increases very little. Hence, CMC represents the solution concentration of surfactant from which nearly maximum adsorption occurs. Therefore, CMC is of great significance in consideration of the practical use of surfactants (Svenson, 2004).

In this study, sodium sesame fatty methyl ester sulphonate (SEFAMESO) was synthesised from sesame fatty methyl esters biodiesel. The solution properties of the surfactant which include Krafft temperature, foam-ability, and the CMC values, counter-ion binding degrees and thermodynamic properties of micellization were

evaluated. The CMC values of the SEFAMESO surfactant were determined using electrical conductivity and viscosity measurements as functions of surfactant concentration at temperature range of: 298.15, 303.15, 313.15, and 323.15 K. From the electrical conductivity data, the thermodynamic parameters: change in free Gibbs energy (ΔG°_{mic}), entropy (ΔS°_{mic}), and enthalpy (ΔH°_{mic}) of micellization were calculated. From these data, an understanding and optimum applications of the synthesised surfactant were established.

1.3 Biodiesel

The indiscriminate extraction and consumption of fossil fuels has led to a reduction in petroleum reserves which are limited, finite and highly concentrated in certain regions of the world. In addition, currently need for clean energy to counter global warming have become critical drivers in energy use. Therefore, the search for alternative renewable source of energy is of great concern. These concerns include: feedstock availability as related to the security of the supply and using domestic energy sources, price volatility and continuing depletion of the reserves of non-renewable petroleum and greenhouse gas emissions (Dincer, 2008). Hence biodiesel is a viable alternative fuel for diesel engines.

Biodiesel is defined as mono alkyl esters of long fatty acids obtained from renewable lipid feedstock such as vegetable oils or animal fats (Zhang *et al*., 2003; Demirbas, 2000; Kinney and Clemente, 2005). Biodiesel has physical properties very similar to petroleum-derived diesel fuel, but its emission properties are superior. Biodiesel has more advantages compared to diesel fuel, such as: it is renewable; energy efficient; biodegradable; non-flammable and nontoxic; offers the same performance and engine

durability as petroleum diesel fuel; reduces tailpipe, unburnt hydrocarbons, carbon monoxide, sulphates, polycyclic aromatic hydrocarbons, nitrated polycyclic aromatic hydrocarbons, thus reduce global warming and particulate matter emissions. In addition, its life expectancy is thinner than regular diesel and serves as a better lubricant thus, increasing engine life (Meher *et al.*, 2006; Srivastava and Prasad, 2000). Biodiesel is usually produced by the trans-esterification of vegetable oils or animal fats with methanol or ethanol (Knothe *et al*., 2005).

A complete understanding of the physical and chemical properties of biodiesel raw materials is important to the development of biodiesel. The properties of the various individual fatty esters that make biodiesel determine the overall fuel properties. Structural features that influence the physical and fuel properties of a fatty ester molecule include: chain length, degree of unsaturation and branching of the chain. These affects cetane number and exhaust emissions, heat of combustion, cold flow, oxidative stability, viscosity, and lubricity (Anand *et al*., 2011; Garnica *et al.*, 2009; Knothe, 2005). Factors such as geography, climate, and economics determine which vegetable oil is of greatest interest for potential use in biodiesel fuels (Knothe *et al*., 2005**).**

In this study, sesame oil was used as the raw material to synthesize the sesame fatty methyl esters (SEFAMEs). The synthesized sesame biodiesel (SEFAMEs) was then used to synthesise the anionic surfactant. This study showed the influence of raw material composition on the biodiesel properties. A comparative study of the properties of the SEFAMEs biodiesel and those of other biodiesel and diesel fuel in literature was done.

1.4 Problem Statement

The depletion of non-renewable petroleum reserves, increasing demands for diesels, uncertainty in their availability and also products from petrochemicals being less biodegradable; hence, persisting in environment, thus, causing pollution have become urgent drivers for search for alternative sources of energy and chemicals. Vegetable oil crops therefore, represent readily available, renewable and biodegradable raw materials with zero or low greenhouse gases emission, thus, has minimal impact on the climate. Vegetable oil can therefore, supplement or replace the finite fossil fuels and petrochemicals. Biodiesel is an alternative to petroleum-derived diesel fuel, it has very similar physical properties to petroleum diesel, but its emission properties are superior. However, its applications as fuel and industrial chemical has remained limited and unexploited. Similarly, use of oleo-chemicals in surfactants making has remained limitedly applied and unexploited for decades.

Sesame plant on the other hand, has been listed among underutilized crop with high potentials in industrial applications. This study therefore, sought to investigate the viability and potentiality of sesame oil as raw material for industrial production of biodiesel and surfactant. This was done by synthesizing and evaluating properties of the synthesized biodiesel and surfactant from the renewable and biodegradable sesame oil.

1.5 Justification of the Study

The significance of renewable sources as an alternative energy and surfactant source is based on the fact they are carbon neutral. This is because growing of vegetable oil crops remove CO_2 from the atmosphere during the process of photosynthesis that occurs naturally, hence, have less impact on climate. On the other hand, fossil fuels and petrochemicals release carbon dioxide into the air without the benefit of concurrent carbon dioxide absorption, thus, causing global warming. Renewable, biodegradable and carbon neutral vegetable oil crops are readily available if grown and harvested sustainably. Hence, use of vegetable oils as the main raw materials for surfactant and biodiesel synthesis allow the development of competitive and powerful products, which are both consumer and environment friendly.

Sesame plant has been listed among neglected and underutilized crop species of great potential for industrial applications. Therefore, planting this crop for commercial use for biodiesel and surfactant should be encouraged because it can highly stimulate rural economic development. This is because farmers would benefit from increased demand for the vegetable oils. Hence, bio-based raw materials can have important impact on the environmental, social and economic impacts on the agriculture-based economies.

It is of practical importance to determine the fuel properties of new biodiesels and the micellar properties of new surfactants. This is because it is of great importance to the manufactures in optimising the properties, cost of production and applications. In addition, studying the thermodynamic properties of surfactants provide vital information on the technical uses as detergents, dispersants, emulsifiers or forming agents.

1.6 Objectives

1.6.1 General Objective

The main objective of the study was to use the extracted oil from sesame seeds to synthesise biodegradable biodiesel and surfactant and thus, evaluate the potentiality of sesame oil as an alternative source of feedstock for biodiesel and surfactant synthesise.

1.6.2 Specific Objectives

i. To determine the yield and physicochemical properties of the extracted sesame oil and SEFAMEs biodiesel.
ii. To determine the fuel properties of SEFAMEs biodiesel and compare with those of commercial petroleum diesel and biodiesels available in literature.
iii. To synthesize and characterize SEFAMEs biodiesel and SEFAMESO surfactant and the extracted sesame oil.
iv. To determine the Krafft point, foam-ability and the thermodynamic parameters of micellization of the SEFAMESO surfactant.

CHAPTER TWO

LITERATURE REVIEW

2.1 Significance of Physicochemical Characteristics of Vegetable Oils

Vegetable oils or triglycerides are esters of three molecules of fatty acids and one of glycerol. Vegetable oils contain substantial amounts of oxygen in their structures. The side chains of triglycerides are either saturated, monounsaturated or polyunsaturated. Triglycerides can further be characterized by the length and saturation degree of their side chains. Saturated oils have better oxidation stability and higher melting points than unsaturated ones. A higher degree of unsaturation also means a higher reactivity (Srivastava and Prasad, 2000). The building blocks of triglycerides are shown in Figure 2.1.

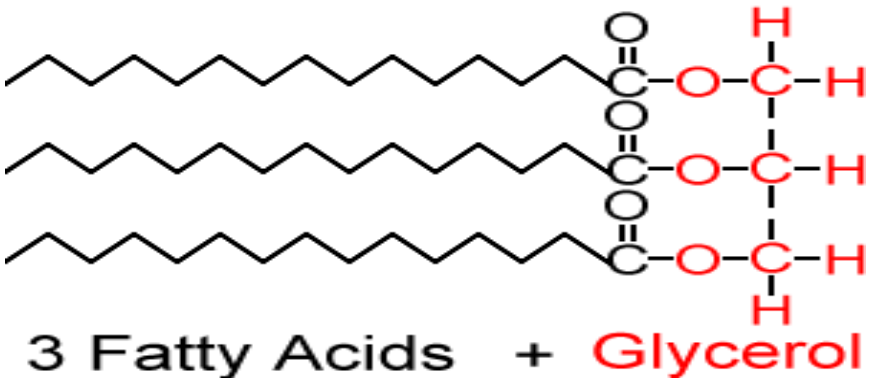

Figure 2.1: Building blocks of triglycerides

(Source: Lim, 2012).

The triglycerides fatty acids are almost entirely straight chain aliphatic carboxylic acid with chain lengths of C_4 to C_{22}, with most commonly C_{16}, C_{18}, and C_{22} fatty acids dominating in most plant oils (Ali *et al.,* 2005). The properties of fatty chains of the

vegetable oils such as the carbon chain, degree of saturation, and the position of double bonds are the important variables that determines the functional properties of the oils (Lim, 2012).

Essentially, the properties of triglycerides depend on the fatty acid composition and the relative location of fatty acids on the glycerol. The compositional properties of vegetable oils are of great significance, especially the types of fatty acids, which determines the key applications of the oil. The predominant fatty acids in the triglycerides alkyl chains of vegetable oil are palmitic ($C_{16:0}$), oleic ($C_{18:1}$) and linoleic ($C_{18:2}$) fatty acids (Srivastava and Prasad, 2000).

The physicochemical properties of vegetable oil determine the quality and therefore, overall applications of the oils (Ali *et al.*, 2005). These physicochemical properties include oil yield, density and specific gravity, free fatty acid value or acid value, saponification value, iodine value, peroxide value, and viscosity.

Density and viscosity of oil are directly related to the molecular weights and fatty chain length of oils (Garnica *et al.*, 2009; Knothe, 2005). Vegetable oils have high viscosity due to their long fatty chain structure. In addition, the viscosity of oil is also related to the level of unsaturation. The viscosity of oils tends to decrease when there is an increased presence of double bonds. On the other hand, viscosity grows with an increase in the length of the hydrocarbon chain and according to the level of polymerisation in the oil (Knothe and Steidley, 2005).

Iodine value indicates the degree of unsaturation in the fatty acids of triglycerides. This value can be used to quantify the amount of double bonds present in the oil, which

signifies the susceptibility of oil to oxidation. Whereas free fatty acid or acid value is a reflection of pH value of oil, as the acid value increases the pH of oil decreases (Ali *et al.*, 2005). Peroxide value shows vegetable oil's ability to get rancid because of oxygen absorption during storage or processing (Hill, 2000).

Saponification value gives the ability of oils to form soap and it is also an indicator of molecular weight or size as a function of the chain lengths of the constituent fatty acids (Ali *et al.*, 2005). It has an inverse relationship with molecular weight of lipids. The saponification value increases with decreasing molecular weight (Lim, 2012). Conversely, the unsaponifiable matter of seed oils naturally consists of hydrocarbons, terpene alcohols, sterols, tocopherols and other phenolic compounds which may act as oxidation inhibitors or antioxidants under a range of conditions. Hence, high unsaponifiable value guarantee the use of oil in cosmetics since it repairs damaged skins (Kirk-Othmer, 2012).

2.1.2 Physicochemical Properties of Sesame Oil and its Common Uses

Several studies on the composition and physicochemical analysis of sesame oil from a variety of sesame seeds grown worldwide that have been done showed that there are significant differences in the physicochemical properties. The researchers explained that the variation in the oil yield and compositional properties of sesame oil are due to the differences in variety of the plant, climatic conditions, soil type, maturity/ ripening stage of plant, the harvesting time of the seeds and the extraction method used (Nzikou *et al*., 2009; Gulla and Waghray, 2011; Mohammed and Hamza, 2008; El Khier *et al*., 2008; Alyemeni *et al*., 2011; Rahman *et al*., 2007; Were *et al*., 2006; Onginjo and Ayiecho, 2009).

Sesame oil extracts contain high levels of unsaturated fatty acids especially oleic and linoleic and low levels of saturated fatty acids. The dominant saturated acids are palmitic and stearic. The approximated amounts of various fatty acids in sesame seeds oil are presented in Table 2.1.

Table 2.1: Approximated fatty acids composition of sesame oil.

Name of Fatty acid	Percentage range (%)
Oleic $C_{18:1}$	35- 50
Linoleic $C_{18:2}$	35- 50
Palmitic $C_{16:0}$	7 - 12
Stearic $C_{18:0}$	3.5 - 7.7
Linolenic $C_{18:3}$	< 0.5
Eicosenoic $C_{20:1}$	< 1
Myristic $C_{14:0}$	< 0.1
Palmitoelic $C_{16:1}$	< 0.1
Arachidic $C_{22:0}$	< 0.2

Source fatty acids composition of sesame oil: (Nzikou *et al.*, 2009; Gulla and Waghray, 2011; Mohammed and Hamza, 2008; El Khier *et al.*, 2008; Alyemeni *et al.*, 2011; Rahman *et al.*, 2007; Were *et al.*, 2006; Onginjo and Ayiecho, 2009).

Some of the physicochemical properties of sesame oil are presented in Table 2.2.

Table 2.2: Physicochemical properties of sesame oil.

Property	Range	
Proteins (%)	18-25	
Carbohydrates (%)	11-14	
Ash (%)	3-5	
Oil (%)	34-63	
Density (kg m^{-3}) (at 25ºC)	880-940	
Specific gravity (at 25°C)	0.88-0.941	
Viscosity (mPa.s)	(at 25ºC) 48-56	(at 37 ºC) 33
Refractive Index (at 25°C)	1.469-1.474	
Iodine Value (g I_2/100 g of oil)	103-120	
FFA (mg/g of KOH)	0.2- 3	
Saponification Value (mg of KOH/g of oil)	160-197	
Unsaponifiable Matter Content (%)	1.5-2.3	
Peroxide value (meqO_2/kg of oil)	1.84- 16	

Source of physicochemical properties of sesame oil: (Nzikou *et al.,* 2009; Gulla and Waghray, 2011; Mohammed and Hamza, 2008; El Khier *et al.,* 2008; Alyemeni *et al.,* 2011; Rahman *et al.*, 2007; Were *et al.*, 2006; Onginjo and Ayiecho, 2009).

Sesame is an excellent source of high quality oil and protein, its oil is odourless and close in quality to olive oil (Lim, 2012). It is used widely as cooking oil and as raw material in the manufacture of inks, paints, margarine and pharmaceuticals (Adebowale *et al.*, 2011). Also used in the production of the paste (tehineh) and in food formulations such as Halaweh (sweetened tehineh), java beans and salads (Abou-Gharbia *et al*., 2000; Abu-Jdayil *et al*., 2002).

Sesame oil is rich in vitamin A and E, hence, protects the skin. It is high in antioxidants that protect against the sun and air pollution. The sterolins in sesame oil are valuable moisturizers and skin conditioning agents (Shyu and Hwang, 2002; Kahyaoglu and Kaya, 2006).

Studies on blending of the sesame oil with other vegetable oils showed that when blended to less stable vegetable oils, it improves their stability and longevity because it has antioxidants such as sesamin, sesamolin and sesamol. Blends therefore have nutritional merits and have more stability during heating (Suja *et al*., 2004; Chung *et al*., 2004; Adebowale *et al*., 2011; Gulla and Waghray, 2011).

Researchers suggested that the good physicochemical properties of sesame oil extracts can be very useful in the industrial applications. They recommended that the high unsaponifiable matter content guarantees the use of the sesame oils in the cosmetics industry (Mohammed and Hamza, 2008; El Khier *et al*., 2008; Alyemeni *et al.*, 2011; Nzikou *et al*., 2009).

2.2 Trans-esterification of Vegetable Oils and Applications of Trans-esterified Oils

Vegetable oils are raw materials in various industrial applications. However, one of the structural drawbacks in using vegetable oils or triglycerides as raw materials is their thermal stabilities due to the presence of a hydrogen on the β carbon on the glycerol backbone (Yao, 2009). This limits the applications of vegetable oils structures. Consequently, to increase the industrial applications of vegetable oils, chemical modification must be carried out. Hence, chemical modification of vegetable oils is an attractive way of obtaining valuable commercial products from renewable raw materials (Salih *et al*., 2011).

Vegetable oils chemical modification routes include hydrolysis, esterification, trans-esterification, and hydrogenation among others. Some of these processes introduces branched or bulky moieties into the structure of esters or various fatty acids which

enhances fundamental properties that are required for numerous practical applications of oils such as the bio-lubricants and cosmetics (Texter, 2001). For example, the hydrogenation of both fatty acids and their methyl esters gives fatty alcohols, which are applied in surfactant synthesis (Ali *et al.,* 2005).

However, the irreversible nature and production of side-reaction products in the oleo-chemical synthesis routes are the main challenges which have limited the use of oleo-chemical raw materials for industrial application. This is due to the fact the synthesis methods/routes which can avoid side-reactions have not been fully developed and understood. Hence, designing appropriate synthesis routes through continuous fundamental research studies is necessary in order to better the understanding and designing of optimized oleo-chemical or bio-based synthesis routes. This include modifying oleo-chemical structures through polymerization and using natural enzymes catalyst to catalyse various reactions (Garrier and Packet, 2012).

Trans-esterification is the process of separating the fatty acids from their glycerol backbone to form fatty acid esters and free glycerol. It is the process of reacting a triglyceride molecule (vegetable oil) with an excess of alcohol in the presence of a catalyst either acid or base such as concentrated H_2SO_4, KOH or NaOH to produce glycerol and Fatty Methyl Esters (biodiesel). It is the process of transforming one type of ester into another type of ester (Meher *et al*., 2006). This reaction occurs stepwise, with mono-glycerides and di-glycerides as intermediate products (Sekhar *et al*., 2010). The trans-esterification reaction scheme is presented in Figure 2.2.

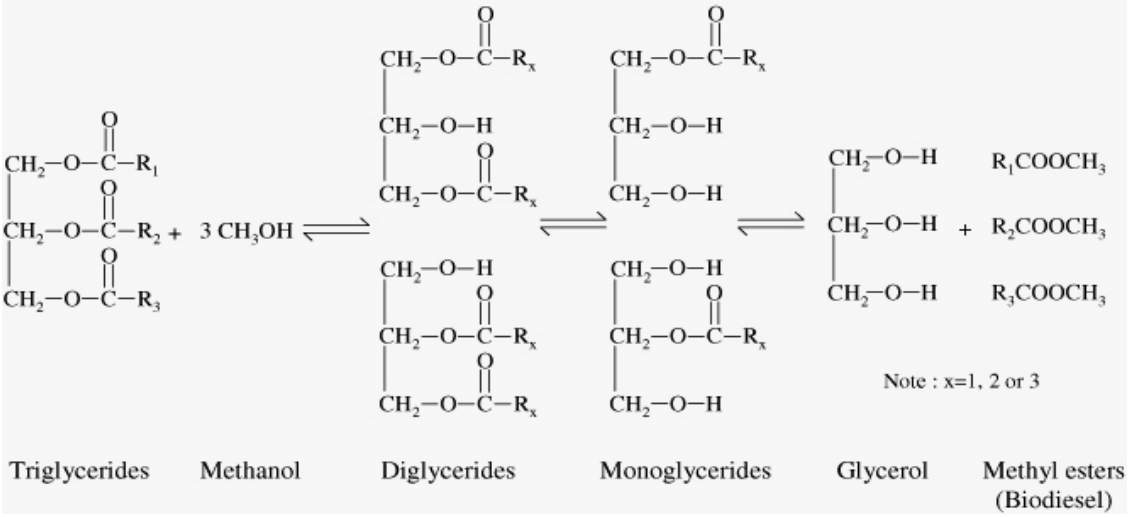

Figure 2.2: Trans-esterification of triglycerides

(Source: Pedro *et al*., 2006).

Trans-esterification methods are classified as: base catalysed, acid-catalysed, and acid-base catalysed (two stage), non-catalysed super critical methanol, enzyme catalysed, and heterogeneous catalyst trans-esterification process. Studies show that the method of trans-esterification selected depends on the amount of free fatty acid and water content of the feedstock (Demirbas, 2007; Math *et al*., 2010).

The base catalysed trans-esterification process is the mostly used method in converting triglycerides into esters when free fatty acids (FFA) level is less than 1% wt. or 2 mg/g of KOH (Knothe, 2006). However, when the FFA content of feedstock is greater than 1 %wt., then an acid-base catalysed trans-esterification process is the most effective (Math *et al.*, 2010). Bases can catalyse the reaction by removing a proton from the alcohol, thus making it more reactive. Methanol is mostly used as the alcohol for producing fatty methyl esters because it is the least expensive alcohol and also sodium hydroxide is

widely used as catalyst because of its low cost and high product yield (Demibras, 2007). A base-catalysed trans-esterification scheme is shown in Figure 2.3.

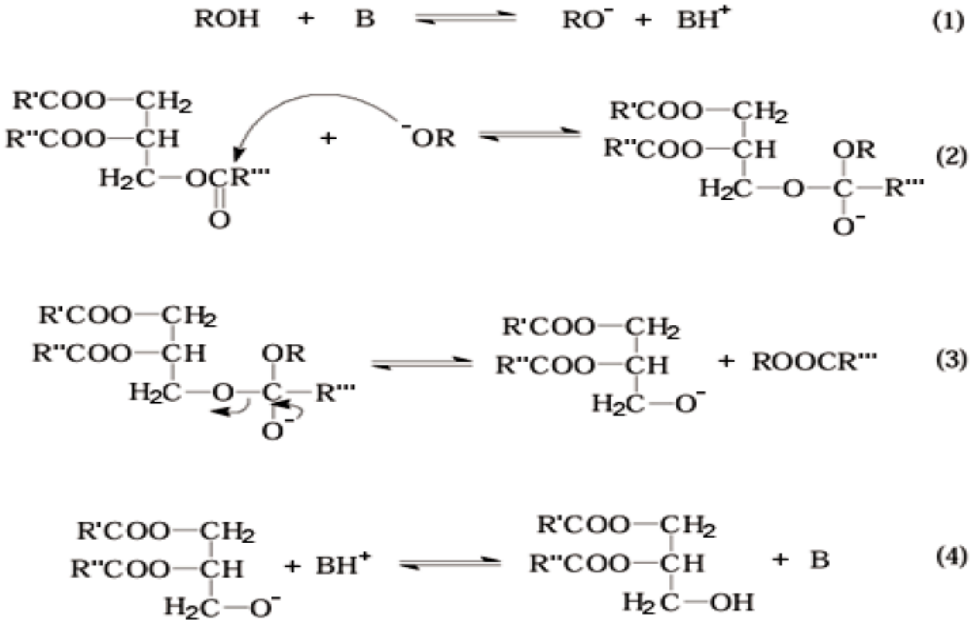

Where, R = alkyl chain of fatty acid or alcohol and B = base catalyst

Figure 2.3: Base-catalysed trans-esterification scheme of vegetable oil

(Source: Demirbas, 2008a).

The use of methyl esters rather than fatty acids as starting materials for many oleo-chemical applications is significantly gaining grounds because of the following advantages. First, in trans-esterification process, for example, the production of the methyl esters, low energy is consumed compared to splitting of fats and oil to produce fatty acids. This is because production of methyl esters requires much lower reactor temperatures and pressures than the splitting of fats and oils to obtain fatty acids (Kirk-Othmer, 2012). Secondly, glycerol a by-product resulting from trans- esterification of oils to give methyl esters is more concentrated. Hence, trans-esterification process is a dry reaction and yields concentrated glycerine, whereas fat splitting produces glycerine

water, which has more than 80 % water; thus, recovery of the latter uses more energy. Thirdly, it is easier to subject methyl esters to fractional distillation compared to fatty acids because they have lower boiling points and are more heat stable than the corresponding fatty acids. Fourthly, esters are better chemical intermediates compared to fatty acids in some application such as in the production of alkanoamides esters. This is because trans-esterification can produce superamides, with more than 90 % purity compared to fatty acids, which can only produce amides with a purity of 65-70 % (Kirk-Othmer, 2012).

Generally, fatty acids esters find applications in many areas. The choice of fatty esters for an application particularly depends on the alcohol added. For example, simple alcohols such as methyl, ethyl, propyl, isopropyl and butyl esters are completely oil soluble and have very good properties as emollient. Conversely, poly-functional alcohols such as sorbitol, ethylene glycol esters are used in food, paper and personal care (Ali *et al.,* 2005). Hydrogenation of both fatty acids and their fatty esters gives fatty alcohols, which are used for the production of surfactants. Therefore, the main applications of fatty esters include as emollients in cosmetics, solvents and metal working fluids (Garrier and Packet, 2012).

Fatty Methyl Esters (FAMEs) consists of fatty acid carbon chain of about C_{12}-C_{22}. The saturated fatty acid methyl esters and unsaturated fatty acid methyl esters, can have side chains, the carbon chain can also have a hydroxyl group and other groups (Ali *et al.,* 2005). Principally the most common application of FAMEs is as biodiesel. FAMEs are also used as solvents, lubricants, carrier fluids or they are converted to other oleo-chemical derivatives such as fatty alcohols which are used as intermediate product in

the production of special esters. Therefore, FAMEs are important chemical intermediates, widely applied in food, pharmaceutical, cosmetic and industrial applications (Garrier and Packet, 2012).

2.2.1 Application of FAMEs as Biodiesel

Biodiesel is an alternative fuel for diesel engines. Biodiesel is becoming increasingly important due to diminishing petroleum reserves and the environmental consequences of exhaust gases from petroleum-fuelled engines. Biodiesel is a methyl or ethyl esters of fatty acid made from renewable biological resources such as vegetable oils (both edible and nonedible), recycled waste vegetable oil and animal fats (Demirbas, 2000; Kinney and Clemente, 2005).

Vegetable oils cannot be used directly as fuel in diesel engines mainly because of their high viscosity, high density and low volatility; since these causes serious problems such as severe engine deposits, injector coking, and piston ring sticking (Meher *et al*., 2006; Murugesan *et al.*, 2009; Barnwal and Sharma, 2005; Demirbas, 2008b). Hence, ways of reducing the viscosity and density of the vegetable oil include: dilution, micro-emulsification, pyrolysis and trans-esterification. Trans-esterification is the most common methods used to reduce oil viscosity in the biodiesel industry (Meher *et al.*, 2006; Demirbas, 2008b).

The trans-esterification process reduces the molecular weight to one-third, reduces the viscosity by about one-eighth, and increase the volatility marginally. Biodiesel contains 10-11 % oxygen (w/w), thereby enhancing the combustion process in an engine (Demirbas, 2008a).

The physical and chemical properties of the biodiesel depend on the chemical composition of vegetable oil and it influences its behaviour and the performance of the vehicle engine. These include the composition and amounts of each fatty acids present in the molecules that influences critical parameters of the biodiesel, such as cetane number and cold flow properties. Chain length and number of double bonds determine the physical characteristics of both fatty acids and triglycerides (Garnica *et al*., 2009; Ramadhas *et al*., 2006; Anand *et al*., 2011).

The presence of double bonds and the length of the fatty acid chain influences the melting point, flash point, and pour point including the cloud point and cetane number. Long, saturated and unbranched chains have a high cetane number. Cetane number gives the ignition quality of a diesel fuel. Whereas, cloud point and pour point have implications on the use of biodiesel in cold weather applications (Knothe, 2005).

Flash point is the minimum temperature at which the vapours of a fuel catch fire if in contact with a flame. The higher the flash value is, the safer the storage, transportation and manipulation of the biodiesel is. The longer the hydrocarbon chain and the higher the level of unsaturation of the vegetable oil is, the higher the flash point will be (Knothe, 2005).

Acid value of biodiesel indicates the concentration of free fatty acids. However, the higher the acid value at high temperatures, the free fatty acids form salts with the metal and may damage the engine or the tanks (Garnica *et al*., 2009).

The study of the influence of fatty acid composition of vegetable oils on the quality of biodiesel synthesized showed that low cetane numbers have been associated with more

highly unsaturated components ($C_{18:2}$ and $C_{18:3}$). Polyunsaturated fuels that contain high levels of these components include soybean, sunflower and grape seed oils. These biodiesels showed high iodine values. Furthermore, their oxidation stability decreased with the increase of the content of polyunsaturated methyl esters. Conversely, this was not the case for the cold filter plugging point of biodiesels rich in long carbon chain saturated methyl esters. It was therefore, concluded that biodiesel of almond, olive, corn, rapeseed and high oleic sunflower oils have the global better properties because they have the greater monounsaturated content (Ramos *et al.*, 2009).

Density and viscosity are the most important characteristics of the liquids used as fuels in diesel engines. These properties influence the atomization and combustion processes that take place in the diesel engine, and the flow properties. High viscosity and density affects the atomization of a fuel upon injection into the combustion chamber and thus leads to the formation of engine deposits. Thus, when viscosity is low, efficiency of the biodiesel is enhanced (Demirbas, 2008b).

Density and viscosity are used to calculate indexes that provide a basis for comparison between fuels for diesel engines, like cetane index and ignition index. Cetane index is used to evaluate the combustion quality (ignition delay) of a fuel like light distillate diesel oils or biodiesels, used for high-speed diesel engines. Calculated ignition index is used to evaluate ignition quality of fuels like heavy fuel oils or vegetable oils used for low-speed diesel engines. An increase in density from 848 to 885 kg/m^3 of methyl esters increase the viscosity from 2.83 to 5.12 mm^2/s and the increase is highly regular (Demirbas, 2008b).

One of the limitations of biodiesel is that there is an inverse relationship between biodiesel's oxidative stability and its cold flow properties. The oxidation process produces hydroperoxides, aldehydes, ketones, and acids that change the fuel's properties. Saturated compounds are less prone to oxidation than unsaturated compounds but they raise the cloud point of the fuel. Research findings have shown that ability of biodiesel to get oxidised increases with increase in peroxide value, acid value, and viscosity of vegetable oil (Knothe, 2005). Biodiesel oxidative stability can be improved by adding additives against oxidative damage by a combination of peroxide-destroying and chain- breaking antioxidants such as tri-phenyl phosphine and propyl gallate (Larson and Marley, 2011). The fuel properties of some of the biodiesels in the literature are presented in Table 2.3.

Table 2.3: Fuel properties of some biodiesels.

Vegetable Methyl Esters	**Density** at 15-25ºC ($kg\ m^{-3}$)	**Kinematic viscosity** at 40ºC (mm^2/s)	**Flash point** (ºC)	**Pour point** (ºC)	**Cloud point** (ºC)	**Cetane NO.**	**Calorific Value** (kJ/kg)
Jatropha	840	4.82	128	-2	8	-	4280[a]
	877.4	4.43	147.4	-	-	55.03	4075[b]
Corn	864.2	4.0694	168	-30	-15	52.48	3992[c]
Peanut	883	4.9	176	-	5	54	3360[d]
Coconut	870	3	118		-3	51	3781[e]
Olive oil	860	4.18	174	-	-	-	4135[f]
Soya bean	885	4.5	178	-7	1	45	3350[d]
Palm	855	4.5	174	16	16	65	4013.5[g]
	880	5.7	164	-	13	62	3350[d]
Sunflower	884	3.6	170	-7	-5	49.2	3858[h]
Cotton seed oil	871	3.75	172	-	-	-	4118[f]
Rapeseed	857	4.60	180	-	-	-	4155[f]
Sesame	880	3.04	143	-	-	-	4090[f]
	867.2	4.20	170	-14	-6	50.48	4040[i]
	850	5.47	185	-8	-5	40	3460[j]
	870	3.60	162	-9.5	-19	-	4021[k]

Source: ([a]Raja *et al.,* 2011; [b]Wagutu *et al.,* 2009; [c]Aydin *et al.,* 2011; [d]Barnwal and Sharma, 2005; [e]Ozawa *et al.,* 2011; [f]Demibras, 2008b; [g]Nagi *et al.,* 2008; [h]Mojtaba and Ahmad, 2012; [i]Saydut *et al.,* 2008; [j]Ferdous and Uddin, 2012; [k]Bhave *et al.,* 2013).

2.3 General Classification and Applications of Surfactants

Generally, both surfactants from petrochemical and oleo-chemical sources can be classified into four main groups depending on the type of the charge of the head namely: anionic, non-ionic, cationic and amphoteric (zwitterionic) surfactants (Rosen and Kunjappu, 2012). Nevertheless, the continuous search for improving surfactant properties have recently resulted in development of new structures that exhibit interesting synergistic interactions, enhanced surface and aggregation properties (Holmberg, 2003).

The current trends in developing new surfactants involve synthesizing surfactants from natural building blocks and making cleavable surfactants that can biodegrade easily, in addition to developing surfactants with less dermatological effects (Holmberg, 2003; Banno *et al.,* 2010). New surfactant class also referred as novel surfactants or speciality surfactants have attracted much interest. These surfactants include: fluorocarbon and silicone, Gemini, polyol, cleavable, polymerizable and polymeric surfactants (Holmberg *et al*., 2003; Schramm *et al.,* 2003; Tadros, 2005; Banno *et al.,* 2010).

2.3.1 Anionic Surfactants

Anionic surfactants have the surface-active portion of the molecule bearing a negative charge. For example, the Carboxylates: $C_nH_{2n+1}COO^-X^+$, Sulphates: $C_nH_{2n+1}OSO_3^-X^+$,

Sulphonates: $C_nH_{2n+1}SO_3^- X^+$, and Phosphates: C_nH_{2n+1} OPO $(OH)O^-X^+$ (Rosen and Kunjappu, 2012). Anionic surfactants constitute 60 % of surfactants applications, mainly because of the ease to use and low cost of manufacturing. Their main applications are in detergency, personal care products, emulsifiers and soaps (Schramm *et al.*, 2003; Tadros, 2005).

Anionic surfactants are generally not compatible with cationic surfactants (although there are some exceptions). They are generally sensitive to hard water. Sensitivity decreases in order carboxylates > phosphate > sulphate ≈ sulphonates. Surfactants with heads of sulphates or sulphonates, are soluble in the presence of most cations. A short polyoxypropylene chain between the anionic group and hydrocarbon improves salt tolerance considerably and also improves solubility in organic solvents (but may reduce rate of biodegradation. Sulphates are readily hydrolysed by acids in autocatalytic process (Holmberg *et al*., 2003).

2.3.1.1 Alkyl Esters Sulphonates

Alkyl esters sulphonates are anionic surfactants derived from natural fats and oils, hence, from renewable sources (Holser, 2005). These surfactants can potentially replace or substitute very cheap, abundant and commercially available linear alkyl benzene based anionic surfactants (LABS). The LABS have good surface-active properties. However, LABS, are toxic and have lower biodegradability, and hence, persist in environment for a long time; thus, causing environmental degradation. Therefore, alkyl esters sulphonates represents unexploited class of anionic surfactants from renewable sources with favourable, wetting, emulsifying and dispersant properties (Maurad *et al.*, 2006; Aparicio *et al.*, 2012; Kirk-Othmer, 2012).

The advantages of alkyl esters sulphonates are as follows: they are derived from renewable resources, hence, from reproducible sources. They are mild to skin, hence, they are not skin irritants; nontoxic orally and therefore, can be applied in drug delivery. They biodegrade faster; thus, nontoxic to aquatic organisms; and contains minimal by-products with safety issues (Kjellin and Johansson, 2010). Alkyl esters sulphates and sulphonates can be used as detergents or foaming agents in high value formulations such as shampoos, tooth pastes and hand dishwashing products (Aparicio *et al.*, 2012; Kirk-Othmer, 2012).

Despite the fact that alkyl esters sulphonates have shown good surface active properties and superior environmental degradation properties compared to LABS, the study of properties and production of these surfactants is still limited. Hence, the studies of synthesis, properties and application of alkyl esters sulphonates is area of great research interest currently (Garrier and Packet, 2012, Aparicio *et al.*, 2012; Kirk-Othmer, 2012).

2.3.2 Non-ionic Surfactants

The surface-active portion of non-ionic surfactants bears no apparent ionic charge. For example, $RCOOCH_2CHOHCH_2OH$ (monoglyceride of long-chain fatty acid), $RC_6H_4(OC_2H_4)_xOH$ (polyoxyethylenated alkylphenol), $R(OC_2H_4)_xOH$ (polyoxyethylenated alcohol) (Rosen and Kunjappu, 2012). Basically, non-ionic surfactants are the second largest surfactant class. They are normally compatible with all types of surfactants. However, they are not sensitive to hard water. They are applied in formulation of personal care, cosmetic and detergents, as well as industrial applications in paper processing and thin films (Holmberg *et al.*, 2003).

Contrary to ionic surfactants, the physicochemical properties of non-ionic surfactants are not markedly affected by electrolytes. The physicochemical properties of ethoxylated non-ionic compounds are very temperature dependent. Contrary to ionic compounds, they become less water soluble and more hydrophobic at higher temperature. Sugar based non-ionic surfactants exhibit the normal temperature dependence, which is their solubility in water increases with temperature (Holmberg *et al*., 2003).

2.3.3 Cationic Surfactants

In cationic surfactants, the surface-active portion bears a positive charge, for example, quaternary ammonium compounds ($-RNH_3^+Cl^-$) (Rosen and Kunjappu, 2012). Cationic surfactants are the third largest surfactant class. The major application of cationic surfactants is as a result of their tendency to adsorb at negatively charged surfaces. They find applications in low temperature detergents and emulsifiers (Rosen and Kunjappu, 2012). For example, as anticorrosive agents for steel, flotation collectors for mineral ores, dispersants for inorganic pigments, antistatic agents for plastics, and fabric softeners, hair conditioners, anticaking agent for fertilizers and as bactericides (Tadros, 2005).

Cationic surfactants are generally not compatible with anionic surfactants (although there are important exceptions). However, hydrolytically stable cationic surfactants show higher aquatic toxicity than other classes of surfactants. Cationic surfactants adsorb strongly to most surfaces and their main uses are related to in situ surface modification (Holmberg *et al*., 2003).

2.3.4 Amphoteric (Zwitterionic) Surfactants

Amphoteric (zwitterionic) surfactants may have both positive and negative charges present in the surface-active portion, for example, $RN^{+}H_2CH_2COO^{-}$ (long-chain amino acid), and $RN^{+}(CH_3)_2CH_2CH_2SO_3^{-}$ (sulphobetaine) (Rosen and Kunjappu, 2012). Zwitterionic surfactants are the smallest surfactant class, relatively due to high prices (Holmberg *et al*., 2003).

Essentially, because Zwitterionics, carry both positive and negative charges, they can adsorb onto both negatively charged and positively charged surfaces without changing the charge of the surface significantly (Rosen and Kunjappu, 2012). Hence, they are compatible with all other classes of surfactants. However, they are not sensitive to hard water, but generally stable in acids and bases. For example, betaines retain their surfactant properties in strong alkali. Most zwitterionic surfactants show very low eye and skin irritation. They are therefore well suited for shampoos and personal care products (Holmberg *et al*., 2003).

2.4 General Characteristics of Surfactants

Surfactants have distinct characteristic properties which defines their functionality. These properties include: amphipathic/amphiphilic character, their ability to adsorb and orient their molecules at interfaces and their ability to self-aggregate and form structures such as micelles (Tadros, 2005).

2.4.1 Amphiphilic Character

Surfactants are amphiphilic molecules, generally having a polar head group, either charged or neutral, and a long-chain hydrocarbon tail (Manne and Patterson, 2003). A

surfactant molecule consist of a non-polar hydrophobic portion, which is usually a straight or branched hydrocarbon or fluorocarbon chain containing 8-18 carbon atoms, which is attached to a polar or ionic portion (hydrophilic) or neutral head group (Tadros, 2005). Hence, surfactant molecule has both a water-insoluble hydrocarbon group (non-polar) and a polar head group.

The properties of a surfactant are determined by the balance between the hydrophobic and hydrophilic parts of the molecule. The amphipathic structure of the surfactant therefore, causes not only concentration of the surfactant at the surface and reduction of the surface tension of the water, but also orientation of the molecule at the surface with its hydrophilic group in the aqueous phase and its hydrophobic group oriented away from it. If the hydrophobic chain length is increased then the whole molecule becomes more hydrophobic and micelles will form at lower solution concentration that is the CMC decreases. If the hydrophilic chain length is increased then the molecule becomes more hydrophilic and the CMC will increase (Rosen and Kunjappu, 2012).

2.4.2 Adsorption of Surfactant at Interfaces

A surfactant is a substance that, when present at low concentration in a system, has the property of adsorbing onto the surfaces or interfaces of the system and altering to a marked degree the surface or interfacial free energies of those surfaces (or interfaces) (Rosen and Kunjappu, 2012; Holmberg *et al*., 2003).

The adsorption characteristic of surfactants (the tendency to accumulate at interfaces) is a fundamental property of a surfactant. Surfactant molecules arrange themselves in such a way that both sections of the molecule are in a favourable environment, thus, reducing

the free energy of the system. In principle, the stronger the tendency, the better the surfactant. The degree of surfactant adsorption at the interface depends on surfactant structure and the nature of the two phases that meet the interface (Holmberg *et al*., 2003).

Adsorption of surfactants at the interface changes the interfacial properties including surface tension, which is important in many diverse areas of applications, including biological and biochemical processes. It affects foam ability and foam stability, wettability, coating flows, foam drainage, and many other science and engineering processes (Narayanan, 2008).

2.4.3 Surfactant Aggregation/Self-assembly in Solution

One of the fundamental properties of surfactants is that surfactant molecules in solution tend to form aggregates. In aqueous solution, amphiphile molecules of surfactants self-assemble to form a variety of structures of which are of order nano to micro range (Segar *et al.*, 2007). In essence, the surfactants molecules (monomers) interact to form aggregates such as micelles, vesicles, liquid crystals and reverse micelles and these aggregates exist in equilibrium with the surfactant monomers (Bergstrom, 2011).

The process of surfactant molecules aggregating or self-assembling involves an increase of order in a system; this process is unfavourable from an entropic point of view. The driving force for the self-association of amphiphilic molecules in an aqueous solvent is the hydrophobic effect, which is the principle preventing oil and water to mix in a liquid phase and electrostatic interactions. As a result under certain conditions, amphiphilic molecules may spontaneously form a single disperse phase of thermodynamically stable

self-associated interfaces, in addition to completely mixing as free solute molecules with the solvent or to separate into two or more liquid phases (Bergstrom, 2011).

For formation of a stable surfactant aggregate structure in an aqueous system, the internal part of the aggregate should contain the hydrophobic part of the surfactant molecule while the surface of the aggregate should be made up of the hydrophilic heads. The polar head groups in water, if ionic, will repel each other because of same charge repulsion. The larger the charge the greater the repulsion and the lower the tendency to form aggregates. The hydrophilic heads have also strong affinity for water and they space out to allow water to solvate the head groups. On the other hand, hydrophobic tails attract one another due to hydrophobic effect. When the surfactant concentration is high enough, the surfactant molecules pack together due to the interaction of the two opposing forces between the surfactant molecules (Farn, 2008).

The self-assembled structures change in size and shape, can be transformed between several types of aggregates, with small changes in temperature, pressure, concentration, pH or electrolyte strength (Segar *et al.*, 2007; Farn, 2008). The properties of the solution show sharp changes around the critical aggregation concentration. For instance, formation of self-assembled aggregates is evidenced by an increase in turbidity and solubility, a decrease in electrical conductivity (ionic surfactants only) and stability in surface tension, interfacial tension and osmotic pressure around the critical aggregation concentration (Farn, 2008).

2.5 Micelles

A micelle is an aggregate of long chained hydrocarbon surfactant molecules; it is an organized molecular assembly of surfactants molecules in aqueous solution. Micelles can be cationic, anionic, zwitterionic, or non-ionic depending on the chemical structure of the surfactant (Attwood and Florence, 2012). In aqueous solution, the hydrophilic head of the surfactant is in contact with solvent, and the hydrophobic tail is sequestered within the centre of the micelle (Bergstrom, 2011). In a micelle, the surfactant hydrophobic groups are directed towards the interior of the aggregate and the polar head groups are directed towards the solvent. Thus, the micellar interior is essentially composed of hydrocarbon chains and has properties closely related to the liquid hydrocarbon (Schramm *et al.*, 2003). A schematic diagram of an ionic micelle in aqueous medium is shown in Figure 2.4.

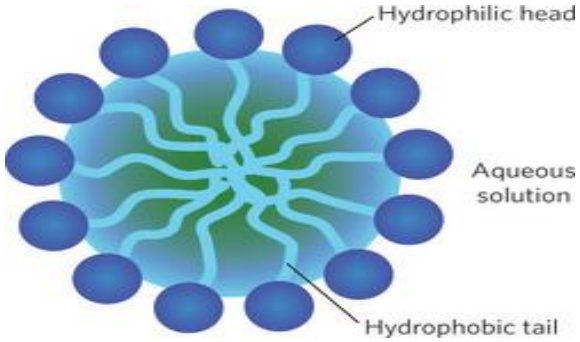

Figure 2.4: An ionic micelle in aqueous medium

(Source: Pasquali, 2010).

The formation of micelles in solution is an important phenomenon, since surfactant molecules behave very differently when present in micelles than as free monomers in solution. A number of important interfacial phenomena, such as detergency and solubilisation, depend on the existence of micelles in solution. In addition, micellization

also affects other interfacial phenomena such as surface or interfacial tension reduction, that do not directly involve micelles (Svenson, 2004; Attwood and Florence, 2012).

Micelles have become a subject of great interest to the organic chemist and the biochemist because of their unusual catalysis of organic reactions and also because of their similarity to biological membranes and globular proteins (Rosen and Kunjappu, 2012). For instance, in drug delivery, the presence of micelles plays a critical role in drug solubilisation, it minimizes drug degradation and loss, prevent harmful side effects, and increase drug bioavailability (Rangel-Yagui *et al.*, 2005; Attwood and Florence, 2012).

2.5.1 Micelle Formation/Micellization

Surfactants dissolve as single molecules in solvent, for example, in water up to a given concentration (dependent on temperature and ionic strength), beyond which they are no longer soluble in water as monomeric units but form aggregates. The monomeric surfactant concentration beyond which added surfactant forms micelles is called the critical micelle concentration (CMC). The CMC represents an equilibrium between monomeric and micellar aggregates of a surfactant at a particular temperature and pressure (Manne and Patterson, 2003). A scheme of surfactant monomers and micelle at equilibrium in aqueous medium is presented in Figure 2.5.

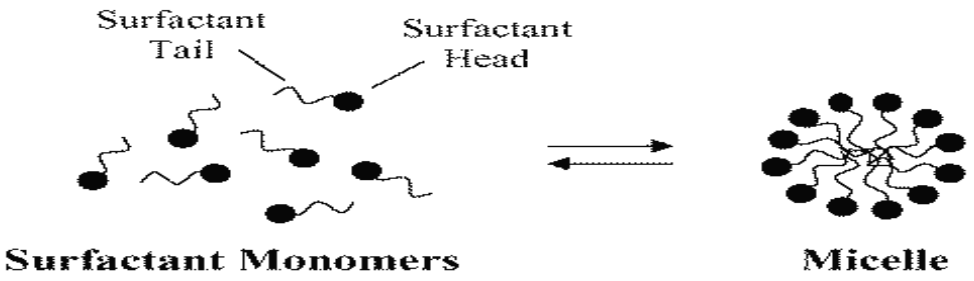

Figure 2.5: Micelle-surfactant monomers equilibrium in aqueous medium

Source: Rangel-Yagui *et al.,* 2005).

Micelles are formed spontaneously when appropriate conditions, such as concentration, temperature, and ionic strength are met. Micelles are generally formed based on the principle of opposing forces. The driving force for micelle formation (or micellization) is the reduction of contact between the hydrocarbon chain and water, thereby reducing the free energy of the system. According to this principle, the attractive forces at the hydrophobic tail regions favour the formation of the micelles while the repulsive forces at the hydrophilic head regions prevent the aggregation (Attwood and Florence, 2012).

The formation of micelles from the constituent monomers involves a rapid, dynamic, association-dissociation equilibrium. These micelles are in dynamic equilibrium and the rate of exchange between a surfactant monomer and the micelle may vary by orders of magnitude, depending on the structure of the surfactant molecule (Zana, 2005). Therefore, formation of micelles is a cooperative process that is spontaneous and reversible (Tadros, 2005; Holmberg *et al*., 2003). Hence, micelles are thermodynamically stable species towards both dissociation and aggregation that are in chemical equilibrium with free surfactants monomers (Zana, 2005).

2.5.1.1 Role of Solvent in Micellization

The role of solvent in micellization is to screen the electrostatic repulsion between polar head groups. The effectiveness of a solvent depends on its ability to form hydrogen bonds. The solvent must have high cohesive energy, density and high dielectric constant. As solvent's cohesive energy or dielectric constant decreases, the driving force for aggregation also decreases. This causes the CMC to increase and become less defined. Studies have shown that water has the highest dielectric constant and cohesive energy and therefore, stand out to be the best solvent in micelle formation. Micelle or liquid crystals have been reported to form in solvents such as water, hydrazine, ethyl ammonium nitrate, formamide and ethylene glycol (Myers, 2005).

2.5.2 Critical Micelle Concentration (CMC)

The critical micelle concentration (CMC) is the surfactant concentration at which the micelles starts to form. Above the CMC, the concentrations of monomers are nearly constant (Schramm *et al.*, 2003). A pseudo phase separation model is a micellar model which treats micelles as a separate but soluble phase, which begins to form at the CMC. According to this model, the CMC value is defined as the concentration of maximum solubility of the monomer in a particular solvent. Thus, the CMC represents a phase separation between the single molecules of surfactant (monomers) and surfactant aggregates in dynamic equilibrium (Holmberg *et al*., 2003).

The CMC is a property of the surfactant which indicates the point at which monolayer adsorption is complete and the surface active properties are at an optimum. Hence, at CMC there are no significant changes in the surfactant surface properties of the solution;

since the monomers are the cause of the surface activity (Farn, 2008). Therefore, CMC value is of interest because it represents the solution concentration of surfactant from which nearly maximum adsorption occurs (Schramm *et al.*, 2003).

The CMC is the single most important characteristic of a surfactant, a very useful tool in the consideration of the practical use of surfactants (Holmberg *et al.*, 2003). The CMC values are important in virtually all of the industrial surfactant applications processes; mineral processing, formulation of personal care products and foods, drug delivery systems and new surfactant remediation technologies. In these processes, surfactant must usually be present at a concentration higher than the CMC because the greatest effect of the surfactant, whether in interfacial tension lowering, emulsification, suspension stabilization, as a delivery vehicle, or in promoting foam stability, is achieved when a significant concentration of micelles is present (Holmberg *et al.*, 2003; Tadros, 2005).

Consequently, CMC is a useful tool for the selection of surfactants for specific applications or properties. Research studies show that surfactants with low CMC values are effective at low concentration. Research studies show that surfactants with low CMC values are effective at low concentration. For example, surfactants with a low CMC are less of an irritant than those with high CMC. The typical CMC values at room temperature are 10^{-3}-10^{-2} M for anionic surfactants, 10^{-3}-10^{-1} M for amphoteric and cationic surfactants and 10^{-5}-10^{-4} M for non-ionic surfactants (Tadros, 2005). It is for this reasons that the CMC value is, feasibly, the most frequently measured and discussed micellar parameter (Attwood and Florence, 2012).

The physicochemical properties of surfactants are very sensitive to surfactant micellization. These properties include surface tension, solubilisation, equivalent conductivity, density, sound velocity, viscosity, apparent or partial molar volume, isentropic and adiabatic compressibility, ultracentrifugation, vapour pressure, activity, osmotic coefficients, osmotic pressure, turbidity, magnetic resonance, fluorescence spectroscopy, self-diffusion, and calorimetery measurements among others.

The physicochemical properties of surfactant vary markedly below and above CMC. When these properties are plotted as a function of surfactant concentration (or its logarithm), a sharp break can be observed in the curves obtained showing the formation of micelles at that point. Therefore, these properties are used to determine the CMC value (Holmberg *et al*., 2003; Schramm *et al.*, 2003). Some of the physicochemical properties dependence on the concentration of anionic surfactant and extrapolation of CMC value are presented in Figure 2.6.

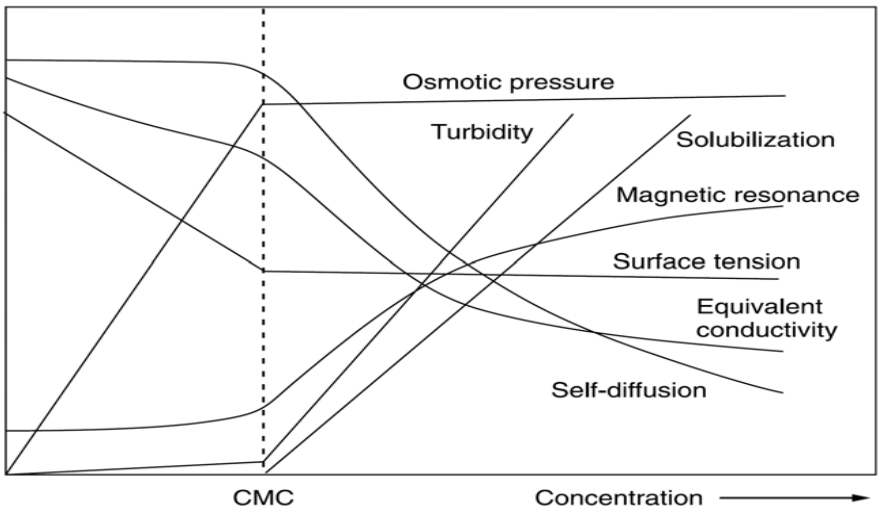

Figure 2.6: Physicochemical properties versus the concentration of anionic surfactant

(Source: Holmberg *et al.*, 2003).

2.5.2.1 Factors Affecting Critical Micelle Concentration

Factors affecting CMC include: length and structure of the hydrophobic group, nature of the hydrophilic group, type of counter-ion, additives (co-solutes), temperature and pressure.

i. Length and structure of the hydrophobic group

Within any class of surfactants, the CMC decreases with increasing chain length of the hydrophobic portion (alkyl group). As the alkyl chain length increases, the decrease in the free energy of micellization becomes larger, thus making the process energetically more favourable. Generally, the CMC decreases by a factor of 2 for ionic surfactants (without added salt) and by a factor of 3 for non-ionic surfactants on adding one methylene group to the alkyl chain (Tadros, 2005).

While alkyl chain branching and double bonds, aromatic groups including other polar character in the hydrophobic part produce sizeable changes in the CMC. A dramatic lowering of the CMC by one or two orders of magnitude results from perfluorination of the alkyl chain. However, partial fluorination may increase the CMC, for example, the fluorination of the terminal methyl group, roughly doubles the CMC. The anomalous behaviour of partially fluorinated surfactants is due to unfavourable interactions between the hydrocarbon and fluorocarbon groups (Holmberg *et al*., 2003).

ii. Nature of the hydrophilic group

Non-ionic surfactants generally have very much lower CMC values and higher aggregation numbers than their ionic counterparts with similar hydrocarbon chains (Tadros, 2005). Zwitterionics appear to have slightly smaller CMCs than ionics with the

same number of carbon atoms in the hydrophobic group (Rosen and Kunjappu, 2012). Cationics typically have slightly higher CMCs than anionics. For non-ionics of the oxyethylene variety, there is a moderate increase of the CMC as the polar head-group becomes larger (Holmberg *et al*., 2003).

iii. Type of counterion

The CMC is also reflected by the degree of binding of the counterion to the micelle. In general, an increased binding of the counterion results in a decrease of the CMC. The extent of binding of the counter-ion increases with increases in its polarity and valence, and decreases with an increase in hydrated radius (Holmberg, 2002).

The valency of the counter ion in ionic surfactants has a significant effect on the CMC. For example, increasing the valency of the counter ion from 1 to 2 reduces the CMC by roughly a factor of 4. Organic counterions reduce the CMC when compared to inorganic ones, more so the larger the nonpolar part (Tadros, 2005; Holmberg, *et al*., 2003). Micellar size increases for a particular cationic surfactant as the counterion is changed according to the series $Cl^- < Br^- < I^-$, and for a particular anionic surfactant according to $Na^+ < K^+ < Cs^+$ (Rosen and Kunjappu, 2012).

iv. Addition of cosolutes such as electrolytes, non-electrolytes

Electrolytes in aqueous solution causes a change in the CMC, the effect being more pronounced for anionic and cationic than for zwitterionic surfactants and more pronounced for zwitterionics than for non-ionics (Rosen and Kunjappu, 2012). The effect of the concentration of electrolyte on CMC of anionic and cationic surfactants is given by Equation 2.1.

$$\text{Log CMC} = -a\log C_i + b \quad \text{.....Equation 2.1}$$

Where 'a' and 'b' are constants for a given ionic head at a particular temperature and C_i is the total counter-ion concentration in equivalents per litre. The depression of the CMC in these cases is due to mainly the decrease in the thickness of the ionic atmosphere surrounding the ionic head groups in the presence of the additional electrolyte and the consequent decreased electrical repulsion between them in the micelle (Rosen and Kunjappu, 2012).

The addition of a 1:1 electrolyte to a solution of anionic surfactant dramatically lowers the CMC, by up to an order of magnitude. The effect is moderate for short-chain surfactants, but is much larger for long-chain ones. At high electrolyte concentrations, the reduction in CMC with increasing number of carbon atoms in the alkyl chain is much stronger than without added electrolyte. This rate of decrease at high electrolyte concentrations is comparable to that of non-ionics. The effect of added electrolyte also depends on the valency of the added counter ions. In contrast, for non-ionics, addition of electrolytes causes only a small variation in the CMC (Tadros, 2005; Holmberg *et al*., 2003).

Addition of non-electrolytes such as alcohols can also cause a decrease in the CMC. The alcohols are less polar than water and are distributed between the bulk solution and the micelles. The more preference they have for the micelles, the more they stabilize them. A longer alkyl chain leads to a less favourable location in water and more favourable location in the micelles. Here, it will act basically as any added non-ionic amphiphile, such as a non-ionic surfactant, in lowering the CMC (Holmberg *et al*., 2003).

v. Temperature

The effect of temperature on the CMC of surfactants in aqueous medium is complex, the value appearing first to decrease with temperature to some minimum and then to increase with further increase in temperature. Temperature increase causes decreased hydration of the hydrophilic group, which favours micellization. However, temperature increase also causes disruption of the structured water surrounding the hydrophobic group, an effect that disfavours micellization. The relative magnitude of these two opposing effects, therefore, determines whether the CMC increases or decreases over a particular temperature range (Rosen and Kunjappu, 2012). Aqueous solutions of many non-ionic surfactants become turbid at a characteristic temperature called the cloud point. At temperatures up to the cloud point there is an increase in micellar size and a corresponding decrease in CMC. Temperature has a comparatively small effect on the micellar properties of ionic surfactants (Holmberg *et al*., 2003).

vi. Pressure

The primary effect of pressure on a micellar system is a change in the CMC, which is closely related to changes in the partial molar volume of micelle formation, aggregation number, and water penetration into the micelles. In general, the CMC increases with pressure, then undergoes a maximum and then tends to decrease again (Holmberg, 2002).

2.5.3 Thermodynamics of Micellization

The process of micellization is one of the most important characteristics of surfactant solution. Determination of the thermodynamics of micelle formation is essential for

better understanding of how to develop stable micelles for use in various pharmaceutical and industrial applications (Bergstrom, 2011).

The driving force of micellization is to obtain the lowest free energy for the system. According to pseudo phase separation model, the micelle formation is considered as being akin to a phase separation with the micelles being the separated (pseudo-) phase, and the CMC is the saturation concentration of surfactant in the monomeric state. Surfactant addition above the CMC consequently only affects the micelle concentration, but not the monomer concentration. This model assumes complete binding of counter ions to the micelles (Holmberg *et al*., 2003). Therefore, above the CMC the phase equilibrium exists with a constant activity of the surfactant in the micellar phase.

The formation of micelles of anionic surfactant at equilibrium is given by Equation 2.2 (Tadros, 2005).

$nS^- + nM^+ \leftrightarrow S_n$ .....Equation 2.2

Where nS^- are monomers, nM^+ counter-ions and S_n are micelles in solution at CMC.

At equilibrium, the equilibrium constant of micellization is given by Equation 2.3.

$K_m = \frac{[s_n]}{[s]^n}$ .....Equation 2.3

Where, [s_n] and [s] are the molar concentration of micelles and monomers, respectively, and n is the aggregation number of surfactant monomers.

Pseudo phase separation model assumes that the chemical potential of the surfactant in the micellar state is constant at a given temperature and may be adopted as the standard

chemical potential, μ°_{mic}, analogous to the standard chemical potential of pure liquid or solid (Tadros, 2005). Equilibrium with the surfactant in solution is then represented by:

$\mu^{\circ}_{mic} = \mu^{\circ}_{I} + RTIna_1$……...Equation 2.4

where, μ°_{mic} is the standard chemical potential of the surfactant micelle, μ°_{1} is the standard chemical potential of the surfactant monomer and *a*, is the activity of surfactant monomer in solution.

By putting $a_1 = X_1 f_1$, the standard free energy of micellization per mole of monomer (ΔG°_{mic}), is given by Equation 2.5.

$\Delta G^{\circ}_{mic} = \mu^{\circ}_{mic} - \mu^{\circ}_{1} = RTInX_1$……...Equation 2.5

where, X_1, is the mole fraction of monomers and the activity coefficient f_1, is taken as unity. Then, CMC, may be identified with X_1. Therefore, ΔG°_{mic} is given by Equation 2.6.

$\Delta G^{\circ}_{mic} = RT\ In[CMC]$……..Equation 2.6

Therefore, ΔG°_{mic} is calculated using the CMC expressed as a mole fraction as indicated by Equation 2.6 (Tadros, 2005). The ΔG°_{mic} represents the free energy difference between monomer in the micelle and some appropriately chosen reference state. This is the convenient starting point for thermodynamic consideration (Holmberg *et al*., 2003).

From the temperature dependence of CMC, one can determine the free energy (ΔG°_{mic}), enthalpy (ΔH°_{mic}) and entropy (ΔS°_{mic}) of micellization using Equations 2.7, 2.8 and 2.9.

$\Delta G^{\circ}_{mic} = RT(1+\beta)\, In\, [CMC]$……Equation 2.7

$\Delta H^{\circ}_{mic} = -RT^2(1+\beta)\frac{\partial ln X cmc}{\partial T}$ ……...……...Equation 2.8

$\Delta S^{\circ}_{mic} = \left(\frac{\Delta H^{\circ}_{mic} - \Delta G^{\circ}_{mic}}{T}\right)$...……..Equation 2.9

2.5.4 General Structure of a Micelle

Nearly all the micellar structures in aqueous media have their surfactant molecules oriented with their polar heads towards the water phase and their tail away from it. An ionic micelle consist of three distinct layers; the hydrophobic core, stern and Gouy-chapman layer (Somasundaran, 2006). The micelle core is hydrophobic, which is water-excluded core with a radius that roughly corresponds to the length of the extended hydrophobic chain. The stern layer of the electrical double layer is formed by the charged terminal groups which is approximately half of the counter ions associated with the micelle and water. Whereas, the Gouy-Chapman layer consists of hydrated counter-ions. The remaining counter ions are contained in the Gouy-Chapman portion of the electric double layer that extends further into the aqueous phase (Attwood and Florence, 2012). Schematic diagrams of the cross-sectional area of an ionic micelle are presented in Figures 2.7a and 2.7b.

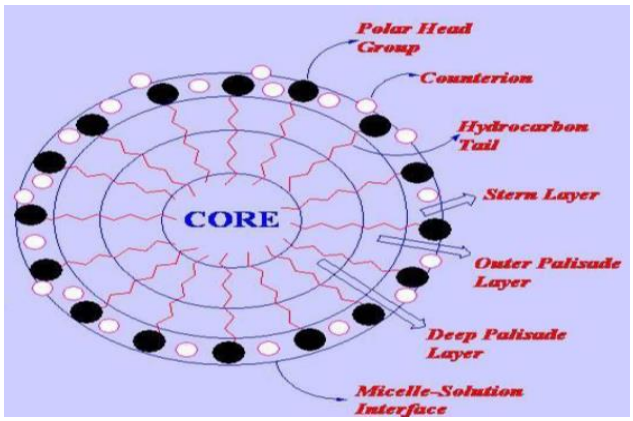

Figure 2.7a: Cross sectional area of an ionic micelle

(Source: Attwood and Florence, 2012).

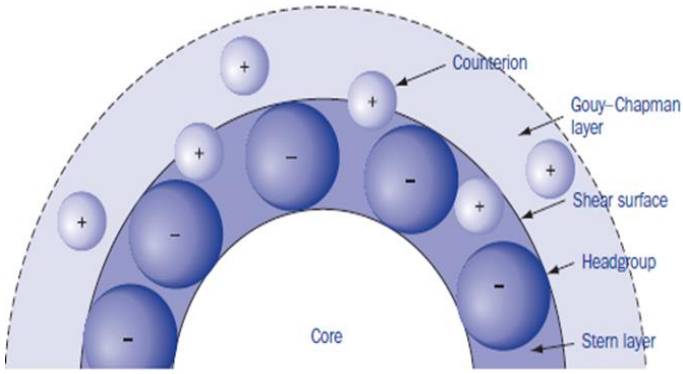

Figure 2.7b: Partial cross-sectional area of an ionic micelle

(Source: Attwood and Florence, 2012).

The layers of the micelle plays significant roles on the various functions of the surfactant micelles. For instance, the micelle structures offers several binding sites for relatively polar and non-polar molecules. The hydrophobic core provides binding site for lipophilic or hydrophobic molecules. The stern region is particularly flexible in binding molecules as it contains highly hydrophilic surfactant head groups and hydrophobic domains in part due to back folding of the surfactant tails. The hydrophobic binding

sites located in the Stern region also provides binding for polar molecules (Somasundaran, 2006; Attwood and Florence, 2012).

The micelle structure, therefore, provides different sites for binding which are important especially in micelles applications in solubilisation, emulsification and catalysis (Goyal and Aswal, 2001; Fendler, 2012). The existence of different sites of binding in the micelle results from the fact that the physical properties such as: micro-viscosity, polarity and hydration degree are not uniform along the micelle (Goyal and Aswal, 2001; Rangel-Yagui *et al.*, 2005).

2.5.5 Shape and Size of Micelle

The shape of the micelle produced in aqueous media is of importance in determining various properties of the surfactant solution such as: its viscosity, its capacity to solubilize water-insoluble material and its cloud point. In aqueous media, surfactants with bulky or loosely packed hydrophilic groups and long, thin hydrophobic groups tend to form spherical micelles, while those with short, bulky hydrophobic groups and small, close-packed hydrophilic groups tend to form lamellar or cylindrical micelles (Rosen and Kunjappu, 2012).

At a concentration very close to the CMC the micelles are spherical or nearly spherical on a time-average basis. As the concentration is increased, the micelles may remain spheroidal or grow and become oblate (disc-like) or prolate (or elongated, cylindrical, or rodlike), with the prolate shape much more often encountered than the oblate shape (Zana, 2005). Thus, any increase in the surfactant concentration does not affect the number of monomers in the solution but affects the structure of micelles (Farn, 2008).

Micelle shape and size can be controlled by changing the surfactant chemical structure as well as by varying solution conditions such as temperature, overall surfactant concentration, surfactant composition (in the case of mixed surfactant systems), ionic strength and pH (Holmberg *et al*., 2003). Micelle growth is controlled primarily by the surfactant heads. Since both one-dimensional and two-dimensional growth require the bringing of the surfactant heads closer to each other in order to reduce the available area per surfactant molecule at the micelle surface, and hence, the curvature of the micelle surface (Holmberg *et al*., 2003; Rangel-Yagui *et al.*, 2005).

2.5.5.1 Packing Parameters of Surfactant Assemblies

Formation of the type of assemblies depends on the geometry of the single surfactant molecule which is well represented by packing parameter 'P'. A collection of monomers of amphiphile arrange itself to form the most favoured structures. The packing parameter depends on 'a' the optimal area of the head (the cross-sectional area occupied by the hydrophilic group) and 'v' is the volume of hydrocarbon chain or chains (hydrophobic group), and 'l' the extended hydrocarbon chain (hydrophobic group) length. Therefore packing parameter p is defined as Equation 2.9.

$$P = \frac{v}{al} \quad \text{Equation 2.9}$$

V and l, based on Tanford approximations is given by Equation 2.10:

$$V = 27.4 + 26.9\text{nÅ} \quad \text{Equation 2.10}$$

where, n is the number of carbon atoms in the chain less one and l is given by Equation 2.11.

$l = 1.5 + 1.265n$ Å……...Equation 2.11

The value of the surfactant packing parameter (‘*P*’), determines the micelle shape (Zana, 2005). The value of packing parameter and shape of micelle are given in Table 2.4.

Table 2.4: Shape and structure of micelle.

Packing parameter (*V/al*)	**Shape**	**Micelle structure**
$< 1/3$	Cone	Spherical
$1/3$ to $< 1/2$	Truncated cone	Cylindrical/Elongated micelles
$1/2$ to < 1	Truncated cone	Lamellar/ Flexible bilayers, vesicles
≈ 1	Cylinder	Planar bilayers
>1	Inverted truncated cone or wedge	Inverted micelles or reverse micelles

Source: (Zana, 2005).

Packing number stresses the importance of surfactant head group in predicting the shape and size of aggregates. Nevertheless, the surfactant tail also control the equilibrium aggregate formation of spherical micelles, rod like micelles, and spherical bilayer vesicles. In cylindrical aggregates, the tail does not affect equilibrium area, the tail influence can only be seen in sphere to rod transitions. The packing parameter and therefore, the shape and size of micelle is influenced by the structure of the hydrophilic head group, length of hydrophobic or hydrocarbon chain, in addition to changes in the electrolyte content, temperature, pH, and the presence of additives in the solution (Zana, 2005; De and Mondal, 2012).

At higher surfactant concentrations, a packing of the micellar aggregates induces the formation of lyotropic liquid crystalline phases, sometimes also called mesophases. These phases are crucial in the manufacture and mode of action of detergents and have

an important role in cosmetics. A dense packing of spherical micelles in a cubic lattice leads to cubic phases. Rod-like micelles form hexagonal phases in which the long axis of the rods is packed on a hexagonal lattice. Bilayers form lamellar phases. At high concentrations inverse phases can also follow. Thus, the sequence of phases with increasing surfactant concentration is usually isotropic micellar (L_1), cubic, hexagonal (H_1), lamellar ($L\alpha$) and reverse. Hence, the transition from one phase to another occurs due to a change in concentration (Farn, 2008).

2.6 Effect of Temperature on Solubility of Surfactants

The effect of temperature on the solubility of surfactants is of great practical significance. The solubility of the ionic surfactant is strongly dependent on temperature. The solubility surfactants may be very low at low temperatures and then increases by orders of magnitude over a relatively narrow temperature range and this behaviour is referred to as the 'Krafft phenomenon'. The temperature for the onset of the strongly increasing solubility is called the 'Krafft point' or 'Krafft temperature'. Kraft point is the temperature at which 1 % solution becomes clear on gradual heating; it is a convenient measure of aqueous solubility (Holmberg *et al*., 2003).

Below the "Krafft point" (temperature), the surfactant solubility increases slowly with increasing temperature because the surfactant dissolves as monomers. The limit to monomer solubility occurs when the chemical potential of the monomers is equal to that of the pure (usually crystalline) surfactant. Above this temperature, the solubility increases very rapidly because the surfactant dissolves as micelles and the contribution of each micelle to the surfactant chemical potential being the same as that of a monomer (Holmberg, 2002).

Surfactants with ionic head groups, or compact highly polar head groups and long straight alkyl chains have high Krafft temperatures. The Krafft temperature increases with alkyl chain length of the surfactant molecule. It can be reduced by introducing branching in the alkyl chains. Using alkyl groups with a wide distribution of alkyl chain length can also reduce the Krafft temperature. The Krafft temperature is very important in the application of surfactants. The solubility of a surfactant increases significantly above the Krafft temperature and, hence, most industrial applications require surfactants with a low Krafft temperature (Holmberg *et al*., 2003; Tadros, 2005).

CHAPTER THREE

MATERIALS AND METHODS

3.1 Introduction

This chapter gives the materials, methods, and procedures of analysis used in the study. Sesame oil was the main raw material used in the synthesis of the eco-friendly SEFAMEs biodiesel and the anionic SEFAMESO surfactant. The procedures used to evaluate the physicochemical and fuel properties of sesame oil and SEFAMEs have been stated in this chapter. The methods used to characterize sesame oil, SEFAMEs and SEFAMESO which include Elemental Analysis, FTIR, HPLC-MS, ^{1}H-NMR and ^{13}C-MNR have been highlighted. The electro conductivity and viscosity procedures which were used to evaluate the CMC, counter-ion binding capacity and the thermodynamic properties of micellization of the surfactant have been stated in this chapter.

3.2 Seed Material

Local sesame (*Sesamum indicum L.*) seeds were purchased from Eldoret market. The seeds were selected according to their condition, where the damaged seeds were discarded before seeds in good condition were cleaned, dried at high temperature of 100-105 ^{o}C overnight in the oven to remove moisture. The seeds were then ground using grinder and weighed prior to extraction of oil.

3.3 Chemical Reagents

Analytical grade reagents from Sigma-Aldrich Company were used, these chemicals included: n-hexane, methanol, sodium hydroxide, carbon tetrachloride, and hydrogen

peroxide, formic acid and chloro-sulphonic acid and sodium hydrogen carbonate. Appendix I gives other chemicals used in the study.

3.4 Oil Extraction

Sesame oil was extracted from sesame seed using solvent extraction method. Solvent extraction was chosen since this method recovers almost all the oils and leaves behind only 0.5-0.7 % residual oil in the raw materials (Liauw *et al*., 2008). In this study, hexane solvent was used to extract oil from sesame seeds, since it is highly efficient and highly volatile hence easily removed through evaporation.

To carry out sesame oil extraction, 300g of sesame seeds were ground and put in a 2.5 L glass bottle and 1.5 L of hexane solvent was added and then corked for three days. After three days, the mixture was filtered and the filtrate concentrated using rotary evaporator at (40-60 ^{o}C). The extracted seed oil was then stored in freezer at -2 ^{o}C for further use.

3.5 Physical and Chemical Analysis of Sesame Oil

Prior to the synthesis of sesame biodiesel and the sesame anionic surfactant, calculation of oil yield, and analysis of physicochemical properties sesame oil was carried out. These physicochemical properties include, density and specific gravity, free fatty acid value, saponification value, iodine value, peroxide value, and viscosity.

3.5.1 Oil Yield and pH

The weight of oil extracted from 300g of sesame seeds powder was measured to determine the oil yield. The result was expressed as the percentage of oil in the dry matter of seed powder as shown by Equation 3.1 (AOCS, 1998).

$$\% \text{ Oil yield} = \frac{Weight\ of\ oil}{Weight\ of\ sesame\ seeds}\ x\ 100 \quad \text{.....Equation 3.1}$$

The pH value of the oil sample was determined using digital pH meter (Hanna HI 2210 model) with platinum electrodes. The pH meter was calibrated with pH buffer solutions. The pH reading was recorded when its fluctuation was less than 1 % within 2 minutes.

3.5.2 Density and Specific gravity

A 25 mL pycnometer was washed thoroughly with detergent, water and petroleum ether, it was then dried and weighed, the weight of bottle obtained was labelled as W_1. The bottle was filled with water and weighed, the obtained weight was labelled W_2. The bottle was then dried and filled with the oil sample and weighed, the obtained weight was referred to as W_3. The density and specific gravity of the oil samples were determined at 25 °C. The specific gravity and relative density of the oil were calculated using Equations 3.2 and 3.3 (AOCS, 1998).

$$\text{Density} = \frac{Weight\ of\ oil - weight\ of\ bottle}{volume} = \frac{W_3 - W_1}{25} \quad \text{.....Equation 3.2}$$

$$\text{Specific gravity} = \frac{Weight\ of\ oil}{Weight\ of\ equal\ volume\ of\ water} = \frac{W_3}{W_2} \quad \text{.....Equation 3.3}$$

3.5.3 Free Fatty Acid Value

Free fatty acid value or acid value was expressed as percentage of free fatty acid and it was calculated as oleic acid. A 2 g oil was weighed and poured in a beaker. A neutral solvent (a mixture of diethyl ether and ethanol (1:1, v/v) was prepared and 50 mL of it was taken and poured into the beaker containing the oil sample. Then 2 drops of phenolphthalein indicator solution was added and the mixture was heated with vigorous stirring for 30 minutes in a boiling water bath. The heating was stopped and the mixture was titrated with 0.1M KOH solution with constant shaking until the pink colour remained constant. From the quantity of 0.5M alkali used, the percentage of free fatty acid present in the oil was calculated according to Equation 3.4 (AOCS, 1998).

Acid value (AV) = $\frac{56.1\ x\ Vx\ M}{W_{Oil}}$ .....Equation 3.4

where, *V* is the volume of the standard alkali used, *M* is the molarity of standard alkali used and W_{oil} is the weight of oil used

3.5.4 Saponification Value

The alcoholic KOH was freshly prepared by dissolving 5.6 g of KOH pellets in 100 mL of ethanol. To a 250 mL conical flask 2g of oil was measured and 25 mL of the alcoholic KOH was added to it. The mixture was then boiled gently under reflux on a water bath for 30 minutes to ensure that the sample dissolve. While refluxing the oil and alcohol KOH mixture, a blank of 25 mL ethanol KOH was titrated against 0.5M HCl, using 1 mL phenolphthalein indicator. The volume of the titrated blank was labelled B. After refluxing the oil sample mixture, 1 mL of phenolphthalein was added to the mixture and

titrated against 0.5M HCl to get the end point, the titre volume was labelled S**.** Saponification value was calculated using Equation 3.5:

Saponification value (SV) = $\frac{56.1\ x\ (B-S) x\ M}{W_{Oil}}$ ……..Equation 3.5

where, *B* is the volume of standard ethanol potassium hydroxide used in blank titration, *S* is the volume of standard ethanol potassium hydroxide used in titration with the oil and *M* is the molarity of standard acid and W_{oil} is the weight of oil used (AOCS, 1998).

The obtained saponification value was used to estimate the molecular weight of oil, which aided in further calculation of reactants in mass balance equations.

3.5.5 Peroxide Value

Peroxide value was determined by weighing 1 g of oil into a clean conical flask. Then, 1g of powdered potassium iodide and 20 mL of solvent mixture of glacial and chloroform 2:1 (2 volume of glacial acetic acid + 1 volume of chloroform) was added. The conical flask was stoppered and placed in a vigorously boiling water bath for 1 minute. The content was quickly poured into a flask containing 20 mL of 5 % potassium iodide solution and the solution kept in the dark for 5 minutes. The mixture was then titrated with 0.025M sodium thiosulphate solution using 1 mL starch indicator. The titration continued until the blue colour disappeared. A blank was also carried out at the same time. The titre volume for $Na_2S_2O_3$ used for the blank and oil sample was labelled V_o and V_1, respectively. Peroxide value was calculated using Equation 3.6 (AOCS, 1998).

Peroxide Value (PV) = $\frac{Molar\ equivalent}{Weight\ of\ oil} = \frac{S\ x\ M\ x1000}{W_{Oil}}$ .....Equation 3.6

where, S is (V_o-V_1) volume of $Na_2S_2O_3$, M is the concentration of the $Na_2S_2O_3$ solution, and W_{oil} is the the weight of oil sample

3.5.6 Iodine Value

Iodine value was determined by weighing 2g of oil sample into a 250 mL Erlenmeyer flask, and 20 mL of carbon tetrachloride was added. Then, 20 mL of Wijs reagent was added into the mixture, stoppered and swirled. The mixture was stored in a dark place at 25 °C for 30 minutes. Then, 15 mL of 10 % potassium iodide solution and 100 mL of purified water was added to the sample solution and the mixture was thoroughly mixed. The sample was titrated with 0.1M $Na_2S_2O_3$ solution until faint yellow colour was observed, after which, 1 mL of starch indicator solution was added to the sample solution. The titration was continued with vigorous swirling until the disappearance of the blue starch-iodine colour. The same procedure was repeated for the blank. Iodine value was obtained using Equation 3.7 (AOCS, 1998).

Iodine value (IV) = $\frac{0.1269(B-S)x\ M\ x100}{W_{Oil}}$ .....Equation 3.7

where, *B* is the volume of $Na_2S_2O_3$ used in blank titration, *S* is the volume of $Na_2S_2O_3$ used in titration with oil, *M* is the molarity of $Na_2S_2O_3$, W_{oil} is the weight of oil used.

3.5.7 Viscosity

Viscosity of sesame oil was carried out using ubbelohde capillary EW-98934-15 viscometer at temperature of 25 ^oC. Acetone was poured first into the viscometer and the time at which the acetone reached the bottom of the equipment was taken. The oil

was then poured into the viscometer and the time taken for the sesame oil to reach the bottom of the equipment was taken. The procedure was repeated 5 times and the average values were taken which were then multiplied with the viscometer calibration to give viscosity in mm^2/s (AOCS, 1998).

According to Poiseulle's Law, the pressure driving the liquid through the capillary at any time during the experiment is directly proportional to the density of the substance and relates flow time t, to the liquid's viscosity (η) (Hummel, 2000) as given by Equation 3.8.

$$\eta = k\rho t \quad \text{.....Equation 3.8.}$$

where, k is the viscometer constant, ρ is density and t is the efflux time.

3.5.8 Unsaponifiable Matter Content

The percentage of unsaponifiable matter, was determined by saponifying oil sample using alcoholic KOH. A 5g of sesame oil sample was measured into 250 mL round bottomed conical flask and 30 mL of 0.5M ethanolic KOH was added and boiled in a water bath under reflux condenser for 1 hour. The mixture was put in a separating funnel, 50 mL of diethyl ether and 50 mL of distilled water containing 5 % $NaHCO_3$ added and shaken vigorously and left to stand to 1 hour. The dissolved soap and water was drained, more distilled water was periodically added to wash the mixture until all the soap and impurities were completely removed. After washing, the sample was dried under vacuum. The obtained sample was then further dried in an oven at 105 ^oC and weighed (AOCS, 1998). Equation 3.9 was used to calculate the percentage of unsaponifiable matter.

Unsaponifiable Matter (*UMS*) = $\frac{S}{M_{Oil}} x100$ %.....Equation 3.9

where, *S* is the mass of the extracted *USM* in g and M_{oil} is the mass of the oil sample saponified.

3.6 Biodiesel Synthesis

The single step base trans-esterification catalysis was carried out. Prior to trans-esterification process, 500 mL of sesame oil was preheated at the temperature of 120 ºC for 90 minutes in a flat bottom flask with constant stirring at 250 rmp by means of magnetic flux heater. The heating was stopped and the oil was made to cool down to 60 °C. In a separate closed glass bottle, 4g of NaOH was dissolved in 50 mL methanol with constant stirring for 15 minutes in a rotary shaker to produce a highly reactive sodium methoxide protonic species.

To synthesise biodiesel, 500 mL of sesame oil was poured into a 1 L three-necked round bottom flask, then 50 mL sodium methoxide was gently added into the flask. A magnetic rod was placed inside the flask. The flask was placed in water bath on a hot magnetic flux heater setup. The flask openings were fitted into a condenser, thermometer, and a cork. The temperatures of the setup was maintained at the range of 60-70 ºC and magnetic revolutions at 250 rmp. The mixture was stirred vigorously and refluxed for 3 hours. The solution was then cooled, and poured into a separating funnel, it was left to stand for 12 hours. The mixture separated into two layers, with the top layer consisting of methyl esters and bottom layer glycerol. Glycerol was removed and sesame methyl esters remained in the separating funnel.

To remove any remaining methanol, glycerine, catalyst, soaps and other impurities, sesame methyl esters was washed. The initial washings was done using warm distilled water containing 10 % H_3PO_4 acid. This was repeated 5 times, thereafter, washing was done using 100 % warm distilled water. This was repeated until the washing water became clear, that is when the pH of the biodiesel became relatively neutral. To remove water/moisture, the obtained SEFAMEs was dried by heating at 100 ^oC for 1 hour on a hot magnetic stirrer plate. The SEFAMEs obtained was then stored in a clean bottle and kept in the freezer at -2^oC for further use.

3.6.1 Determination of Physicochemical Properties of SEFAMEs Biodiesel

The yield of SEFAMEs biodiesel and physicochemical properties evaluated which included: density and specific gravity, acid value, saponification value, peroxide value and iodine value. The procedures used in the determination of biodiesel yield and the physicochemical properties of SEFAMEs were the same as those used to determine the corresponding physicochemical parameter of sesame oil described in section 3.5.1 to 3.5.6.

3.6.2 Analysis of Fuel properties of SEFAMEs Biodiesel

The fuel characteristics of the synthesized SEFAMEs were evaluated according to ASTM standard methods at Kenya Pipeline Company Limited (KPC), Eldoret. The properties analysed were: kinematic viscosity (40 ^oC), pour point, cloud point, cetane index, flash point and calorific value.

3.6.2.1 Kinematic Viscosity: ASTM D 445

A viscometer was inserted into a water bath with a set temperature and left for 30 minutes. The SEFAMEs sample was added to the viscometer and allowed to remain in the bath as long as it reaches the test temperature (40 ^{o}C). The sample was allowed to flow freely and the time required for the meniscus to pass from the first to the second timing mark was taken using a stop watch (ASTM, 2008). The procedure was repeated three of times and the average value are taken which was then multiplied by the viscometer calibration to give the kinematic viscosity as given by Equation 3.8.

3.6.2.2 Flash Point: ASTM D 93

Flash-point analysis was carried out using Pensky-Martens closed cup tester apparatus. The Pensky-Martens cup tester measures the lowest temperature at which application of the test flame causes the vapour above the sample to ignite. A sample of the SEFAMEs biodiesel was heated in a close vessel and ignited. When the sample burns, the temperature was recorded. The biodiesel was placed in a cup in such quantity as to just touch the prescribed mark on the interior of the cup. The cover was then fitted onto the position on the cup and Bunsen burner was used to supply heat to the apparatus at a rate of 50 ^{o}C per minute. During heating, the biodiesel was constantly stirred. As the oil approaches its flashing, the injector burner was lighted and injected into the oil container after every 12 second intervals until a distinct flash was observed within the container. The temperature at which the flash occurred was then recorded, it was repeated three times and the average taken (ASTM, 2008).

3.6.2.3 Cloud Point: ASTM D 2500

The cloud point is the temperature at which crystals first start to form in the fuel (Knothe, 2005). A sample of the biodiesel was placed in a test jar to a mark and then placed inside a cooling bath. The temperature at the bottom of the test jar that is the temperature at which the biodiesel starts to form cloud was taken as the cloud point (ASTM, 2008).

3.6.2.4 Pour Point: ASTM D 97

The pour point is the lowest temperature at which the fuel will still pour from a container when it is cooled (AOCS, 1998). The pour point was determined by heating the biodiesel sample in a test jar up to about 50 ^{o}C. The sample was then cooled slowly at specific rate, and at temperature decrement of 50 ^{o}C, the test jar was constantly tilted to check any movement. The temperature 3 ^{o}C above the point at which the biodiesel stops moving/flowing was recorded as pour point (ASTM, 2008).

3.6.2.5 Cetane Number: ASTM D 4737

Cetane Number is a measure of the fuel's ignition delay. Higher Cetane numbers indicate shorter times between the injection of the fuel and its ignition (Knothe, 2005). Cetane number was determined using Cetane indices. The Cetane indices used was based on formulas in ASTM D 4737. ASTM D 4737 consist of updated correlation that uses the distillation points, and gravity/density to estimate the cetane number.

3.6.2.6 Calorific or Heat Value of SEFAMEs: ASTM D240

Heating Value or Heat of Combustion, is the amount of heating energy released by the combustion of a unit value of fuels (Knothe, 2005). An automated adiabatic bomb calorimeter (Gallenkamp CBA-350 K model) was used to measure the heat of combustion of the biodiesel. Electrical energy was used to ignite 2g of the biodiesel, as the biodiesel was burning, it heated up the surrounding air, which expanded and escaped through a tube that lead the air out of the calorimeter. When the air was escaping through the copper tube it also heated up the water outside the tube. The rise in the temperature of the water allowed for calculating calorie content of the biodiesel (ASTM, 2008).

3.7 Surfactant Synthesis

Prior to surfactant synthesis, the SEFAMEs biodiesel underwent epoxidation. This processes was done in order to generate reactive sites (epoxy group) at the double bonds of the fatty methyl esters. The epoxide group was introduced using per-acids formed *in-situ*, by reacting a carboxylic acid (formic acid) with concentrated hydrogen peroxide.

3.7.1 Epoxidation of Sesame Fatty Methyl Esters

SEFAMEs epoxidation reaction was carried out in a 500 mL three-necked round bottom flask equipped with a thermometer sensor and a magnetic stirrer. A 100 g of SEFAMEs was weighed and mixed with 0.0043 moles of 88 % formic acid. The mixture was placed in an ice bath of temperature range (4-15 ^{o}C) with constant stirring, 0.0098 moles of 30 % hydrogen peroxide was slowly added drop wise. The reaction was then allowed to proceed at 50 ^{o}C with vigorous stirring until a white, powdery solid was observed in the reaction vessel. After the reaction was complete, the mixture was poured into a

separating funnel, and 50 mL of ethyl acetate added to extract epoxidized sesame methyl esters. The mixture was then washed with a solution of sodium bicarbonate (5 wt. %) and after which distilled water was used. The mixture was concentrated using a rotary evaporator to obtain epoxidized SEFAMEs.

3.7.2 Synthesis of SEFAMESO Surfactant

To synthesise the anionic surfactant SEFAMESO, the expoxidized SEFAMEs underwent suphonation using chlorosulphonic acid ($ClHSO_3$) and neutralization using sodium bicarbonate ($NaHCO_3$). A 0.057 moles of epoxidized SEFAMEs was placed in a 500 mL three-necked round bottom flask equipped with a thermometer sensor and a magnetic stirrer, 17 mL of tetra-chloromethane was added. The mixture was then placed in an ice bath and temperature maintained at the range of 0-4 ^oC. Then 0.06 moles of $ClHSO_3$ was added drop-wise to the mixture with continuous stirring for over 30 minutes.

The mixture was subsequently warmed in a steam bath until the solution became clear. Then the reaction temperature was raised and maintained at 60 ^oC for 3 hours under reflux and vigorous stirring. After which the reaction mixture was quenched and the product converted to the sodium salt by pouring the contents into an ice-cooled aqueous $NaHCO_3$ solution and sufficient solid $NaHCO_3$ to keep the solution saturated with inorganic sodium salts.

The product in a separating funnel was extracted twice using 40 mL n-butanol. The solvent was removed from the crude product using a rotary evaporator. The product was then re-dissolved in distilled water and the mixture of suphonated fatty methyl esters

was extracted using diethyl ether, concentrated and dried under vacuum. The synthesised surfactant was then stored in the freezer for further use.

3.8 Characterization of Sesame Oil, SEFAMEs Biodiesel and SEFAMESO Surfactant

The structures of the extracted sesame oil, synthesised SEFAMEs biodiesel and the anionic SEFAMESO surfactant were characterized by Elemental Analysis, FTIR, HPLC-MS, and ^{1}H-NMR and ^{13}C-NMR. Sesame oil and SEFAMEs biodiesel underwent ^{1}H-NMR and ^{13}C-NMR analysis. However, for SEFAMESO surfactant only ^{1}H-NMR was carried out. Elemental analysis of the samples were done using a CHNS/O Elemental analyser (PerkinElmer 2400 Series II CHNS/O Analyser). While FT-IR analysis was done using a Bruker Equinox 55 FT-IR spectrometer with OPUS/IR software, operating at frequency range of 4000- 400 cm^{-1}. The resolution was 1 cm^{-1} and 15 scans.

The ^{13}C NMR) and proton (^{1}H NMR) spectra were recorded on a Bruker Avance Hg400b spectrometer operating at 400 MHz with chloroform-d ($CDCl_3$) as solvent. The molecular masses of the samples were determined by matrix-assisted laser desorption/ionization time-of-flight HPLC-mass spectrometry (LC-MALDI-TOF MS) using a Bruker micrOTOF-Q II mass Spectrometer. The mass resolution was 10 000 FWHM (full width at half maximum). Raw data acquired from LC-MS spectroscopy were interpreted using Bruker Compass Data Analysis 4.0 software to find characteristic compounds molecular features.

The results of all the analyses carried out particularly the spectra, were used to identify the composition of the studied compounds. The interpretation of spectra results was done by comparing the observed results with the available spectra data of the respective analysis database.

3.9 Determination of the SEFAMESO Surfactant properties

The solution surfactant properties which include Krafft point and foam-ability of the synthesised SEFAMESO surfactant were determined. The electro conductivity and viscosity procedures were used to evaluate the CMC, the counter-ion binding capacity of the SEFAMESO. Conductivity and viscosity versus the surfactant concentration data were further used in the evaluation of the thermodynamic properties of micellization of the surfactant.

3.9.1 Determination of Krafft Point and Foam-ability

i. Krafft point

Krafft point was determined by visual observation of 0.2 %wt., of aqueous solution of the synthesized surfactant. The temperature at which the dispersion of surfactant solutions became clear upon gradual heating was noted. The procedure was repeated several times until a clear dispersion temperature was noted.

ii. Foam-ability property

Foam-ability of the synthesized surfactant was evaluated by vigorously shaking 50 mL of 0.1 % wt., of aqueous solution of the surfactant in a 500 mL glass cylinder at 25 °C. Then, the initial height of the foam and after 5 minutes was

evaluated. The procedure was repeated severally until clear heights of the foam was noted. Foaming stability was determined by calculating the difference between the initial and final height of foam that was stable for 5 minutes.

3.9.2 Electrical Conductivity Measurements

Conductance measurements were carried out on a digital conductivity meter (Hanna instrument model HI-8033) and a dipping-type conductivity cell with platinized electrodes. The cell constant was calibrated with aqueous KCl solutions. The measurements of conductivities of the surfactant solution was carried out by continuous dilution of a concentrated solution into water. The conductivity was recorded when its fluctuation was less than 1 % within 2 minutes. The temperature was controlled with a precision of 0.02 K. The obtained absolute conductivity values were multiplied by the cell constant to obtain specific conductivity.

The electro conductivity measurements as a function of concentration of SEFAMESO and the SDS standard were performed at temperatures of 298.15, 303.15, 313.15 and 323 K. This was done by adjusting the temperature of water bath and placing the samples of surfactant solution of varied concentrations in the water bath for 20 minutes, after which the readings were taken. All the readings were done in duplicates and the average values of the measurements were calculated. The specific conductivity versus concentration data of SDS and SEFAMESO surfactants are presented in Appendices II (a) and II (b), respectively. The specific conductivity versus the surfactant concentration curves were plotted using Origin 6.0 program (OriginLab Corporation, US).

The specific conductivity is linearly correlated to the surfactant concentration in both the pre-micellar and in the post-micellar regions. The slope in the pre-micellar region is greater than that in the post-micellar region. The intersection point between the two straight lines gives the CMC (Rosen and Kunjappu, 2012).

The linear relationship between specific conductivity and concentration of surfactant is given by Equation 3.10.

$k = k_o + sC$ .....Equation 3.10

where, k_o is the specific conductivity at infinite dilution, k, is the specific conductivity of the surfactant and s is the slope and C is the concentration of surfactant (Rosen and Kunjappu, 2012). The average specific conductivity values obtained were plotted versus the surfactant concentration to obtain the intersecting lines.

3.9.3 Viscosity Measurements

Viscosity of SEFAMESO was carried out using ubbelohde capillary EW-98934-15 viscometer at the following temperature ranges: 298.15, 303.15, 313.15 and 323.15 K. Acetone was poured first into the viscometer and the time at which the acetone reached the bottom of the equipment was taken.

A viscometer was inserted into a water bath with a set temperature and left for 30 minutes. The SEFAMESO sample was added to the viscometer and allowed to remain in the bath as long as it reaches the test temperature. The sample was allowed to flow freely the time required for the meniscus to pass from the first to the second timing mark was taken using a stop watch. The procedure was repeated three times and the average

value were taken which was then multiplied with the viscometer calibration (constant) to give the kinematic viscosity as given by Equation 3.8.

Relative viscosity is the ratio of the sample viscosity to the solvent's viscosity as shown in Equation 3.11.

$$\eta_r = \frac{\eta}{\eta_s} = \frac{t}{t_s} \quad \text{.....Equation 3.11}$$

where η is the viscosity of the sample and ηs is the viscosity of solvent, while t is the efflux time of sample and t_s is the efflux of the solvent (Rosen and Kunjappu, 2012).

Specific viscosity is the difference between relative viscosity and 1 as defined by Equation 3.12 (Rosen and Kunjappu, 2012):

$$\eta_{sp} = \frac{\eta - \eta_s}{\eta_s} = \frac{t - t_s}{t_s} = \left(\frac{t}{t_s} - 1\right) \quad \text{.....Equation 3.12}$$

The viscosity of the surfactants increases with increase in the concentration of the surfactants (Tadros, 2005). The specific viscosity versus concentration curves shows limited change with increase in concentration up to a point where a break is observed. The breaking point is known as critical micelle concentration, CMC. Therefore, there is minimal change on the viscosity of surfactants with increase in concentration up to the CMC, after which viscosity increases rapidly (Holmberg *et al*., 2003; Tadros, 2005). Appendices III (a) and III (b) give the specific viscosity versus surfactant concentration data of the SDS and SEFAMESO surfactant. The specific viscosity versus the surfactant concentration curves were plotted using Origin 6.0 program (OriginLab Corporation, US).

3.9.4 Determination of Micellar Properties of Surfactant

The electro-conductivity and viscosity data as functions of surfactant concentration were used to evaluate the CMC of the surfactant. The obtained CMC values from viscosity measurements were used for comparison with those obtained from conductivity data. The CMC values obtained from the electro-conductivity versus the surfactant concentration were further used in the calculation of the thermodynamic properties of micellization. This was chosen since conductivity measurement give more precise data for the properties of ionic surfactants than viscosity (Holmberg *et al.*, 2003).

The following micellar properties of surfactant were evaluated:

i. Critical micelle concentration (CMC).
ii. Counter-ion degree of binding (β).
iii. Free Gibbs energy of micellization (ΔG°_{mic}).
iv. Enthalpy (ΔH°_{mic}) and entropy (ΔS°_{mic}) of micellization.

3.9.4.1 Critical Micelle Concentration

On the specific conductivity versus surfactant concentration and the specific viscosity versus surfactant concentration plots, distinct breakpoints of nearly two straights were observed. The CMC value was obtained from the specific conductivity versus concentration curve and specific viscosity versus concentration curve by plotting two straight lines in the curves. The intersection point of the straight lines was taken as the CMC point.

3.9.4.2 Counterion Degree Binding

The ratio between the slopes of the post-micellar region to that in the pre-micellar region gives the counter ion dissociation, β (Rosen and Kunjappu, 2012). From the plot of specific conductivity versus surfactant concentration, the counterion degree binding was calculated using Equation 3.13 (Rosen and Kunjappu, 2012):

$$\beta = 1 - \frac{Slope\ after\ CMC\ \ (post{-}micellar\ region)}{Slope\ before\ CMC\ (pre{-}micellar\ region)} \quad \text{.....Equation 3.13}$$

3.9.2.3 Gibbs Energy of Micellization

The Free Gibbs energy of micellization (ΔG°_{mic}) of the surfactant was calculated using Equation 3.14 (Rosen and Kunjappu, 2012):

$$\Delta G^{\circ}_{mic} = (1 + \beta) RT\ In X_{CMC} \quad \text{.....Equation 3.14}$$

where, X_{CMC}, is the mole fraction.

The mole fraction (X_{CMC}) was determined by converting the CMC values in molarity to CMC in mole fraction by dividing [CMC] by the molar concentration of the solvent, [solvent] (Rosen and Kunjappu, 2012). X_{CMC} was obtained using Equation 3.15.

$$X_{CMC} = \frac{[CMC]}{[Solvent]} \quad \text{.....Equation 3.15}$$

3.9.2.4 Enthalpy and Entropy of Micellization

The temperature dependence of CMC was used to calculate the enthalpy (ΔH^{o}_{mic}) of micellization using Equation 3.16 (Rosen and Kunjappu, 2012).

$$\Delta H^{o}_{mic} = -(1+\beta)RT^{2}\frac{\partial InX_{CMC}}{\partial(^{1}/_{T})} \quad \text{Equation 3.16}$$

where ∂, is the partial differential, $\frac{\partial InX_{CMC}}{\partial(^{1}/_{T})}$ was obtained from the slope of plots of $In\ CMC$ versus the inverse of temperature (Rosen and Kunjappu, 2012).

Entropy (ΔS°_{mic}) of micellization was determined using Equation 3.17.

$$\Delta S^{o}_{mic} = \frac{(\Delta H^{\circ}_{mic} - \Delta G^{\circ}_{mic})}{T} \quad \text{Equation 3.17}$$

CHAPTER 4

RESULTS AND DISCUSSION

4.1 Introduction

This chapter gives the results and discussion of the properties of the extracted sesame oil, sesame biodiesel (SEFAMEs) and the synthesized anionic surfactant (SEFAMESO). The physicochemical properties of sesame oil and SEFAMEs biodiesel including the fuel properties of the SEFAMEs biodiesel are discussed. The compositional properties of the studied compounds obtained from Elemental Analysis, FTIR, HPLC-MS, ^{1}H-NMR and ^{13}C-MNR analysis are discussed.

The electro-conductivity and viscosity measurements versus surfactant concentration data used to evaluate the CMC, counter-ion binding capacity and the thermodynamic properties of micellization of the SEFAMESO and the SDS standard are discussed. The chapter also compares the properties of the synthesised SEFAMEs biodiesel and SEFAMESO surfactant with those of commercially available products.

4.2 Physicochemical Properties of the Extracted Sesame Oil

The physicochemical properties of the extracted sesame oil studied include: oil yield, density and specific gravity, free fatty acid value or acid value, saponification value, iodine value, peroxide value, and viscosity. The physicochemical properties of the extracted sesame oil and the AOCS sesame oil standard are given in Table 4.1.

Table 4.1: Physicochemical properties of the extracted sesame oil and AOCS sesame oil standard.

Property	Present Study Value	AOCS STD Value
Oil Yield (%)	46	-
Density (kg m^{-3}) at 25 ^{o}C	880	913 - 929
pH	7.5	-
Specific gravity	0.88	0.913 - 0.929
Viscosity (mm^2/s) at 25 °C	50	-
Free fatty Acid Value (mg/g of KOH)	0.56	< 3
Iodine Value (g I_2/100 g of oil)	105	104 -120
Saponification Value (mg of KOH/g of oil)	167	186 -195
Unsaponifiable Matter Content (%)	1.67	≈ 2
Peroxide Value, (meq O_2/kg of oil)	1. 84	1.5 - 2.4

Source of AOCS STD values: (Ali *et al.*, 2005).

The extracted sesame oil had a clear yellow colour and pH value of 7.5; hence, relatively neutral. Sesame seeds oil yield was 46 %, this implied that the sesame seeds contained significantly higher amounts of oil. This showed that if commercially exploited, it could serve as one of the major additional sources of oil for industrial applications.

The density and specific gravity of the sesame oil obtained were 880 kg/m^3 and 0.88, respectively. These values were below the AOCS sesame oil standard. The viscosity of sesame oil was 50 mm^2/s at 25 ^{o}C.

The iodine value of the extracted sesame oil was 105 I_2/100 g. The high iodine value indicated that the extracted sesame oil had relatively higher amounts of unsaturated fatty acids such as oleic, linoleic and linolenic acids. This suggested that sesame oil could be used as edible oil for cooking or margarine manufacturing. The obtained iodine value

was greater than 100 g I_2/100 g of oil, which meant that the extracted sesame oil was susceptible to oxidation. However, the value was within the AOCS sesame oil standard.

Sesame oil free fatty acid value was 0.56 mg KOH/g, this value was below the AOCS value. The low acid value of sesame oil showed that sesame oil was stable, relatively neutral and edible. The extracted sesame oil had a peroxide value of 1.84 meq O_2/kg. This indicated that the extracted sesame oil could get rancid because of oxygen absorption during storage or processing. Nonetheless, the peroxide value was within the AOCS sesame oil standard.

The saponification value of sesame oil was 167 mg of KOH/g of oil, this value was lower than the sesame oil AOCS standard. However, the saponification value was relatively high. The high saponification value validates the usage of sesame oil for surfactant making. The unsaponifiable matter value was 1.67 %, this value was within the AOCS reference range. The relatively higher unsaponifiable matter percentage indicated that the extracted sesame oil had valuable antioxidants. Hence, the high unsaponifiable matter value, guaranteed the application of the extracted sesame oil in cosmetics uses. In general, all the physical and chemical properties of the extracted sesame oil were within the range of other sesame oils in the literature as shown in Table 2.2.

4.3 Physicochemical Properties of SEFAMEs Biodiesel

The yield of the synthesised SEFAMEs biodiesel and its physicochemical properties were determined. The evaluated physicochemical properties that influence fuel properties of the biodiesel include: pH, density and specific gravity, kinematic viscosity,

acid value, saponification value, peroxide value and iodine value. The results of physicochemical properties of SEFAMEs biodiesel and that of ASTM biodiesel standard are presented in Table 4.2 which compares the physicochemical properties of SEFAMEs biodiesel with the ASTM biodiesel standard.

Table 4.2: Physicochemical properties of SEFAMEs biodiesel and ASTM biodiesel standard.

Property	SEFAMEs Biodiesel	ASTM Biodiesel STD
Biodiesel yield (%)	95	-
pH	7.2	-
Density (kg m^{-3})	840	880-900
Specific gravity	0.84	0.88-0.9
Kinematic Viscosity (mm^2/s) at 40 °C	3.6	1.9-6
Acid value (mg KOH/g)	0.02	< 0.5
Peroxide value (meq O_2/kg)	0.35	-
Iodine value (g I_2/100 g of biodiesel)	95	-
Saponification value (mg KOH/g of biodiesel)	160	-

Source of ASTM Biodiesel STD values: (Singh and Singh, 2010; Herskowitz *et al.*, 2012).

The yield of the synthesised biodiesel was 95 %. The high yield of synthesised SEFAMEs biodiesel concurred with other studies, which suggested that the optimum conditions in the single step basic catalytic trans-esterification can be achieved when the ratio of oil to methanol is 1:6, using a base catalyst (NaOH or KOH) of 1 % w/v (Knothe *et al*., 2005; Bhave *et al.*, 2013).

The pH of the synthesised SEFAMEs biodiesel was 7.2, this implied that it was relatively neutral. Its density was 840 kgm^{-3}, which was lower than the ASTM biodiesel standard. On the other hand, the viscosity of the SEFAMEs was 3.6 mm^2/s, which was within the range of ASTM biodiesel standard. Therefore, the density and viscosity of SEFAMEs biodiesel implied that SEFAMEs could be applied as fuel in diesel engines.

The acid value of SEFAMEs was 0.02 mg KOH/g, which was within the ASTM biodiesel standard range. SEFAMEs biodiesel showed significantly lower acid value. This suggested that it could not cause damage to engine tanks. The iodine value of SEFAMEs obtained was 95 g I_2/100 g of biodiesel, which was significantly high. This meant that SEFAMEs contains significantly more unsaturated bonds in their carbon chains. Thus, SEFAMEs could undergo a number of reactions because of the existence of reactive double bonds. However, this unsaturation of SEFAMEs is a limitation in its application as fuel; since higher iodine values of biodiesel influences the oxidation and formation of deposits in the diesel engines (Knothe and Steidley, 2005). Therefore, the high iodine value of SEFAMEs biodiesel could limit SEFAMEs application as fuel in diesel engines.

Saponification value of SEFAMEs was 160 mg of KOH/g of biodiesel, which was slightly lower than that of the extracted sesame oil which was 167 mg of KOH/g of oil. The relatively high saponification value suggested that the obtained SEFAMEs biodiesel could be applied in soap or surfactant making.

The peroxide value of SEFAMEs was 0.35 meq O_2/kg. This implied that sesame biodiesel could get rancid because of oxygen absorption during storage or processing. The values of physicochemical properties of SEFAMEs biodiesel compared well with

the values of ASTM biodiesel standard. Hence, the values of physicochemical properties of SEFAMEs biodiesel suggested that it could be used as fuel in diesel engines.

4.4 Fuel Properties of SEFAMEs Biodiesel

The fuel characteristics of the synthesized SEFAMEs biodiesel were evaluated according to the ASTM standard methods. The evaluated fuel properties of SEFAMEs biodiesel include: kinematic viscosity (at 40 ^{o}C), pour point, cloud point, cetane index, flash point and calorific value. The fuel properties of SEFAMEs biodiesel, ASTM biodiesel and commercial petroleum diesel standard are presented in Table 4.3.

Table 4.3: Comparison of fuel properties of SEFAMEs biodiesel, ASTM biodiesel and ASTM petroleum diesel standard.

Property	SEFAMEs Biodiesel	ASTM Biodiesel STD	ASTM Petroleum Diesel STD
Density at 15-25 ^{o}C (kg m^{-3})	840	800-900	826-860
Kinematic viscosity at 40 ^{o}C (mm^{2}/s)	3.6	1.9-6	1.3-4.1
Flash point (^{o}C)	160	100-170	60-80
Pour point (^{o}C)	-8	-15 to 10	-35 to -15
Cloud point (^{o}C)	-6	-3 to 12	-15 to 5
Cetane number	50	47-65	40-55
Calorific Value (kJ/kg)	3950	> 3800	≈ 4200-4500

ASTM Standard Source: (Singh and Singh, 2010; Herskowitz *et al.*, 2012).

The density and viscosity of SEFAMEs biodiesel were within the ASTM standards of biodiesel. The results also indicated that SEFAMEs viscosity and density were very close to that of petroleum diesel. The flash point of SEFAMEs biodiesel was 160 ^{o}C, this was within the ASTM biodiesel standard. The flash point of SEFAMEs biodiesel

was higher than that of petroleum diesel. Consequently, transportation of SEFAMEs is safe; since it cannot catch fire easily compared to petroleum diesel.

The cloud point and pour point of SEFAMEs were -6 and -8 ^{o}C, respectively. SEFAMEs pour point was within the ASTM biodiesel standard range, however, cloud point was not. The result indicated that SEFAMEs biodiesel had a higher tendency of forming cloudy crystals in cold temperature. The cetane number of SEFAMEs biodiesel was 50, which was within the ASTM standard. Cetane number of SEFAMEs biodiesel was higher compared to the conventional petroleum diesel fuel, hence, showed that SEFAMEs biodiesel had higher combustion efficiency.

The calorific value of SEFAMEs was 3950 kJ/kg, this was within both the ASTM standard range of biodiesel and petro-diesel. In general, the fuel properties of SEFAMEs biodiesel were comparable with both the ASTM standard values of biodiesel and petroleum diesel. The present study results support that biodiesel from sesame seed oil can be successfully used as fuels in diesel engines. Appendix IV compares the fuel properties of the SEFAMEs biodiesel with other biodiesels and petroleum diesel in literature.

4.5 Composition Properties of Sesame Oil, SEFAMEs Biodiesel and SEFAMESO Surfactant

The composition properties of sesame oil, the synthesised SEFAMEs biodiesel and the anionic surfactant (SEFAMESO) were determined using Elemental Analysis, FTIR, HPLC-MS, and ^{1}HNMR and ^{13}CNMR. From all the observed spectra, the composition and structural assignments of the compounds were made.

4.5.1 Elemental Analysis Results

Elemental analysis carried out determined the percentages of organic elements C, H, O, and N present in the extracted sesame oil, synthesized SEFAMEs biodiesel and the anionic surfactant SEFAMESO. The amounts of organic elements present in the studied compounds are presented in Table 4.4.

Table 4.4: Percentages of Organic Elements present in Sesame oil, SEFAMEs biodiesel, and SEFAMESO surfactant.

Compound	**C** (%)	**H** (%)	**O** (%)	**N** (%)
Sesame oil	76.41	11.91	11.66	< 0.02
SEFAMEs biodiesel	76.23	12.38	11.37	< 0.02
SEFAMESO surfactant	18.73	2.63	78.62	< 0.02

The results showed that sesame oil consisted of 76.41 % C, 11.91 % H, and 11.66 % O. On the other hand, SEFAMEs biodiesel was found to contain 76.23 % C, 12.38 % H, and 11.37 % O, whereas SEFAMESO surfactant contained 18.73 % C, 2.63 % H, and 78.62 % O. All the three analysed compounds were found to contain nitrogen of less than 0.02 %.

4.5.2 FTIR Results

The FTIR spectra especially in the mid-infrared region were used to determine the chemical functional groups present in the studied compounds. The FTIR spectrum of sesame oil, SEFAMEs biodiesel and the anionic SEFAMESO surfactant are shown in Figures 4.1, 4.2 and 4.3, respectively.

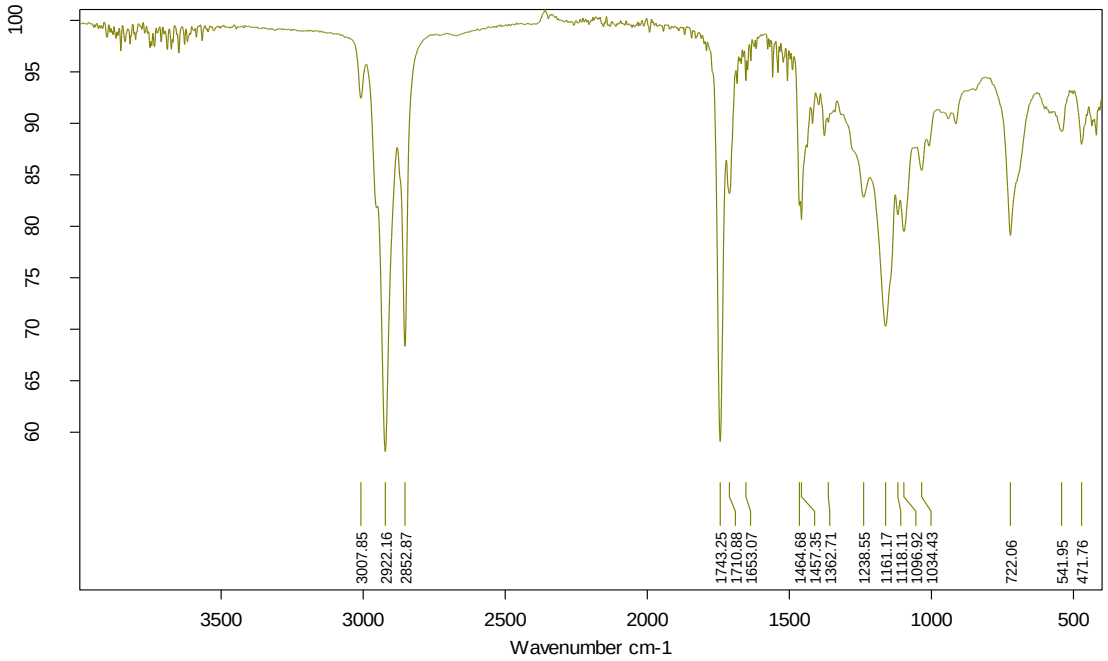

Figure 4.1: FTIR spectrum of Sesame oil.

The weak absorption peak observed at 3008 cm^{-1} in the sesame oil FTIR spectrum was assigned (-C-H) stretching of unsaturated carbon-carbon double bonds. Whereas, the strong peaks at 2922 cm^{-1} and 2853 cm^{-1} were assigned (C-H) stretching of the saturated carbon-carbon bonds. The peak at 1743 cm^{-1} was assigned (C=O) stretching of the carbonyl functionalities. Whereas, the peak at 1653 cm^{-1} was assigned (C=C) stretching of the carbon-carbon double bonds, while the peak at 1457 cm^{-1} was assigned ($-CH_2$) bending (Fadzlillah *et al.*, 2014).

On the other hand, the peak observed at 1239 cm^{-1} was assigned (C-CO-O-) group, while at 1161 cm^{-1} was assigned (C-O-C) stretching of the ester functionalities. The peaks observed at 1118 and 1034 cm^{-1} were assigned ($O-CH_2-C$) stretching of the ester functionalities. The peak observed at 722 cm^{-1} was assigned (C-H) out of the plane stretching of the saturated carbon-carbon bonds. Generally, all the absorption bands observed in the sesame oil FTIR spectrum were in agreement with other reported IR

spectra of sesame oil and other edible oils triacylglycerols bearing saturated and unsaturated fatty acids in their structure (Guillen and Cabo, 1997; Fadzlillah *et al.*, 2014).

The FTIR spectrum of SEFAMEs biodiesel is presented in Figure 4.2.

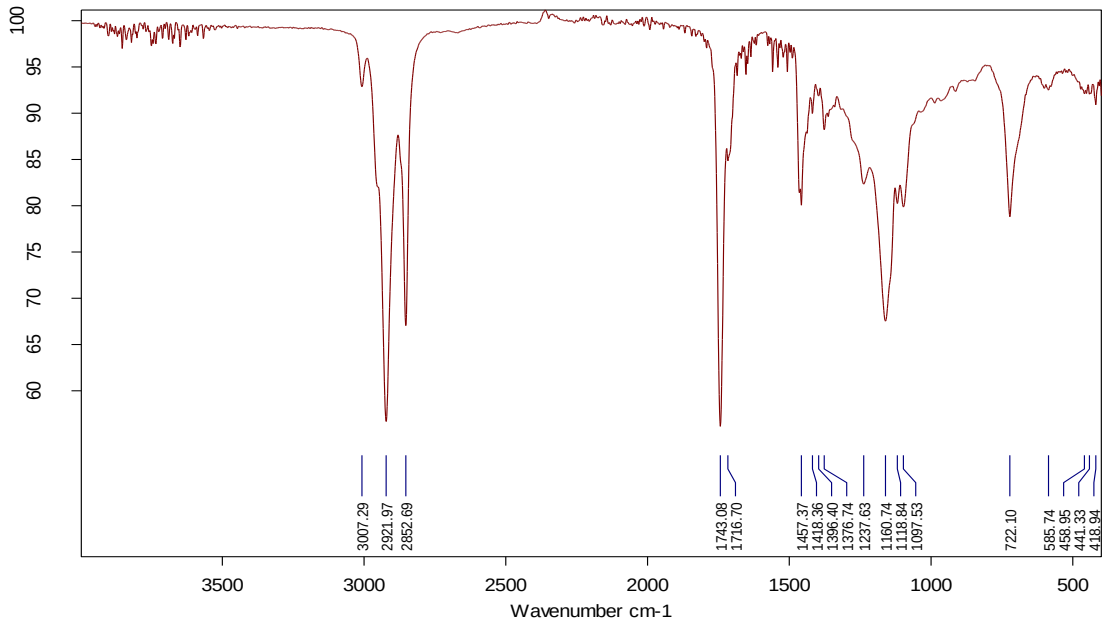

Figure 4.2: FTIR Spectrum of SEFAMEs biodiesel.

In the SEFAMEs biodiesel FTIR spectrum, a weak peak was observed at 3007 cm^{-1}, which was assigned (-C-H) stretching of the unsaturated carbon-carbon double bonds. While the intense peaks observed at 2922 cm^{-1} and 2853 cm^{-1} were assigned (C-H) stretching of the saturated carbon-carbon bonds. Whereas, the peaks at 1743 and 1717 cm^{-1} were assigned (C=O) carbonyl stretching of the ester group. The peak observed at 1457 cm^{-1} was assigned (-CH_2) bending.

The peaks observed at around 1418 to 1376 cm^{-1} were assigned (-O-CH_3) methyl ester group. These peaks indicated that the trans-esterification of sesame oil was successful

and it resulted in formation of fatty methyl esters. Hence, the observed absorption bands between 1418 and 1376 cm^{-1} agreed with other reported IR spectra, which described that this region accounts for the existence of methyl esters, which also differentiate biodiesels from neat vegetable oils (Zhang, 2012; Donnell *et al.*, 2013).

On the other hand, the peak observed at 1238 cm^{-1} was assigned the asymmetric stretching band of C-CO-O-bonds of the ester group, whereas the peak at 1161 cm^{-1} was assigned asymmetric stretching band of (C-O-C) ether bonds of esters functionalities. The peaks observed at 1119 and 1098 cm^{-1} were assigned (O-CH_2-C) stretching of the ester functionalities. Whereas, the peak at 722 cm^{-1} was assigned $(-CH_2)_n$ out of the plane stretching of the saturated carbon-carbon bonds. The obtained sesame biodiesel FTIR spectrum results agreed with other findings on the functional groups of fatty methyl esters biodiesel (Ahmad *et al.*, 2011; Zhang, 2012; Donnell *et al.*, 2013).

The FTIR spectrum of anionic SEFAMESO surfactant is presented in Figure 4.3.

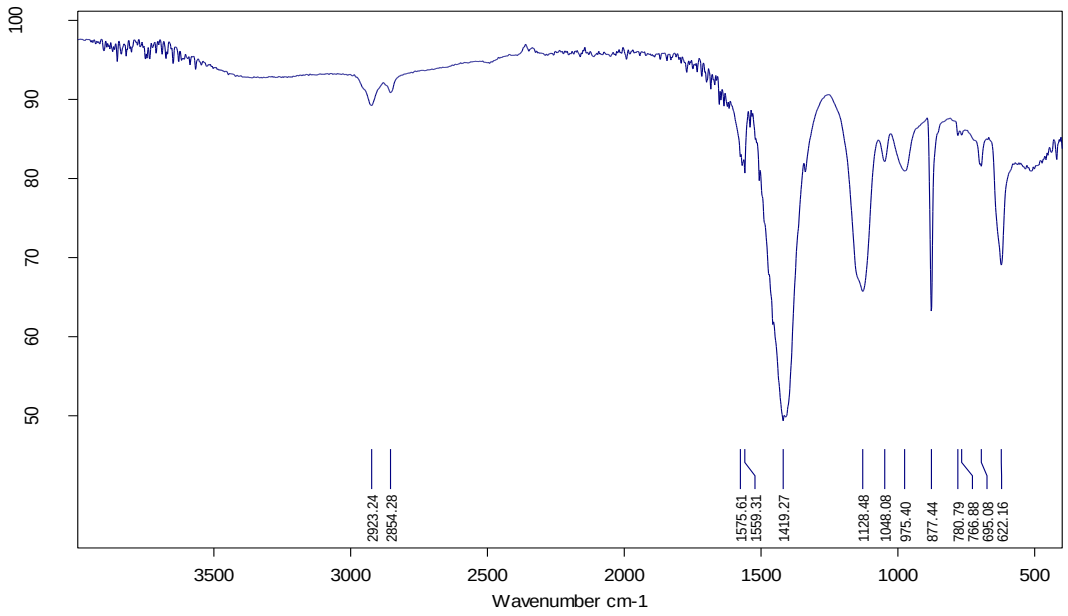

Figure 4.3: FTIR spectrum of SEFAMESO surfactant.

The weak absorption peaks observed at 2923 cm^{-1} and 2854 cm^{-1} in the SEFAMESO surfactant FTIR spectrum were assigned (C-H) stretching of the saturated carbon-carbon bonds. The weak peaks observed at 1576 and 1559 cm^{-1} were assigned asymmetric stretching due to (COO^-) carboxylate esters bonds. Hence, the carboxylate (COO^-) group established the existence of carboxylic acids salts. The observed absorption bands agreed with other reported IR spectra of carboxylic acids, which explained that this region accounts for the existence of aliphatic carboxylic acids salts (Hummel, 2000; Silverstein and Webster, 2006).

The intense peak observed at 1419 cm^{-1} was assigned S=O stretching vibration, thus, indicated the presence of sulphonate group. Similarly, the peaks observed between 1129 to 1048 cm^{-1} also indicated the presence of sulphonate groups due to S=O stretching. These results agreed with other findings that this regions accounts for the existence of sulphonate group (Silverstein and Webster, 2006; Awang and Seng, 2008). Therefore, the presence of sulphonates groups indicated that the fatty methyl esters were successfully converted to fatty methyl esters sulphonate.

The peaks observed at 975 and 877 cm^{-1} corresponded to C-O stretching absorption band, which indicated the presence of asymmetrical epoxy ring in the surfactant. The FTIR result at 975 and 877 cm^{-1} concurred with other reported IR results, which described that the region accounts for the epoxy group (Silverstein and Webster, 2006; Awang and Seng, 2008). A summary of functional groups present in the studied compounds: the extracted sesame oil, SEFAMEs biodiesel and SEFAMESO surfactant are presented in Table 4.5.

Table 4.5: FTIR Frequencies of Sesame oil, SEFAMEs biodiesel and SEFAMESO surfactant.

Sesame Oil		**SEFAMEs Biodiesel**		**SEFAMESO Surfactant**	
Frequency (cm^{-1})	Functional group assignment	Frequency (cm^{-1})	Functional group assignment	Frequency (cm^{-1})	Functional group assignment
3008	-(-C-H) unsaturated stretching	3008	(-C-H) unsaturated stretching	-	-
2923- 2853	-(-C-H) saturated stretching	2922-2853	(-C-H) saturated stretching	2923-2853	-(-C-H) saturated stretching
1743-1711	-(C=O) carbonyl ester group stretching	1743-1717	(C=O) carbonyl ester group stretching	-	-
1653	-(C=C) stretching	-	-	-	-
-	-	-	-	1576-1559	-(COO-) carboxylate esters bonds
1465-1457	-(-CH_2) bending	1457	-(-CH_2) bending	-	-
-	-	1418-1376	-(-O-CH_3) methyl ester group	1419	-(S=O) stretching vibration
1234	-(C-CO-O) ester group	1238	-(C-CO-O) ester group	-	-
1161	(C-O-C) ether group	1161	-(C-O-C) ether group	1129	-(S=O) stretching vibration
1118, 1097, 1034	-(O-CH_2-C) stretching	1119-1098	-(O-CH_2-C) stretching	1049	-(S=O) stretching vibration
-	-	-	-	958-877	-(C-O) stretching
722	-(C-H) out of the plane stretching of saturated carbon-carbon bonds	722	-(-CH_2)$_n$ out of the plane stretching saturated carbon-carbon bonds	-	-

4.5.3 NMR Analysis Results

^{1}H-NMR and ^{13}C-NMR spectra were used to determine the composition of the extracted sesame oil, SEFAMEs biodiesel and the anionic SEFAMESO surfactant. The ^{1}H-NMR spectra of sesame oil are presented in Figure 4.4a and Appendices V (a), V (b) and V (c); whereas, the ^{13}C-NMR spectra of sesame oil are given in Figure 4.4b and Appendices V (d) and V (e). On the other hand, Figure 4.5a, and Appendices VI (a) and VI (b) shows the SEFAMEs biodiesel ^{1}H-NMR spectra. Whereas, the ^{13}C-NMR spectra of SEFAMES biodiesel are shown in Figure 4.5b and Appendix VI (c).

For the anionic SEFAMESO surfactant, only ^{1}H-NMR analysis was carried out and its spectrum is shown in Figure 4.6.

4.5.3.1 ^{1}H-NMR and ^{13}C-NMR Results of Sesame oil and SEFAMEs Biodiesel

The ^{1}H-NMR and ^{13}C-NMR spectra of sesame oil, respectively are shown in Figures 4.4a and 4.4b.

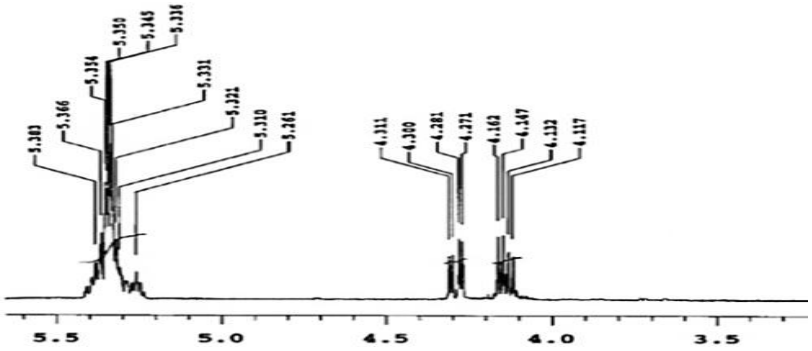

Figure 4.4a: ^{1}H-NMR Spectrum of Sesame oil.

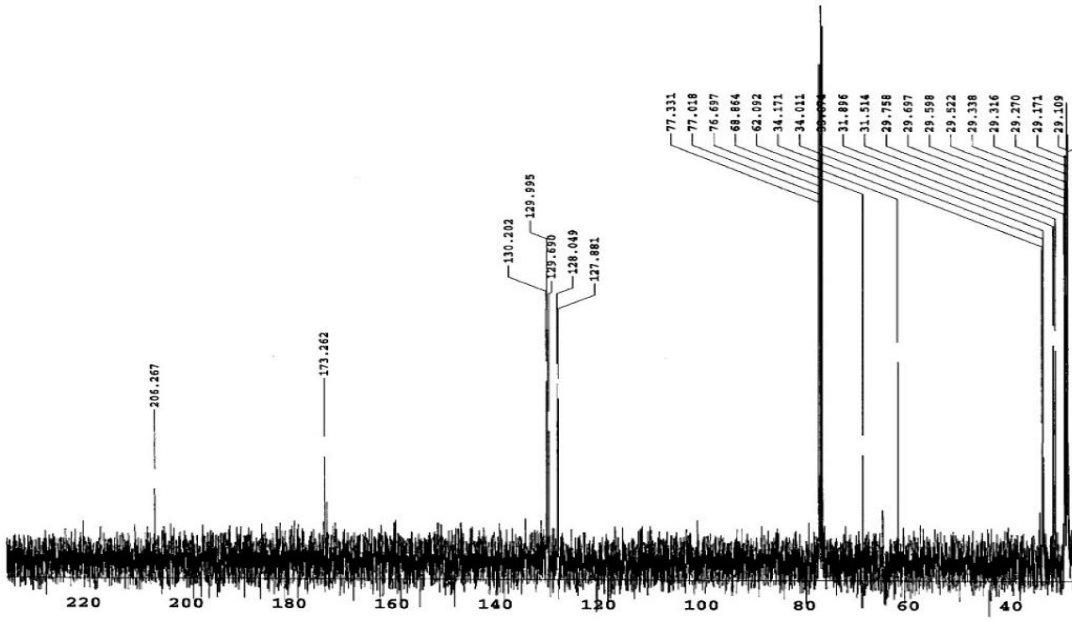

Figure 4.4b: ^{13}C-NMR Spectrum of Sesame oil.

In the sesame oil ^{1}H-NMR spectra, the chemical shifts observed between 0.858 to 0.902 ppm were assigned terminal methyl (-C**H**$_3$) protons of all the fatty acids except linolenic fatty acids. Whereas the chemical shifts observed between 1.250 to 1.367 ppm were assigned methyl protons (-CH_2C**H**$_3$), of linolenic acyl chains. Whereas, the peaks observed at 1.421 to 2.359 ppm were assigned methylene (-C**H**$_2$**)** protons of all fatty acids acyl chains.

The hydrogen protons chemical shifts observed at 2.748 to 2.781 ppm and 5.261 to 5.383 ppm were assigned (-C**H**=CH_2-) due to allylic or methylenic protons of unsaturated fatty acids acyl chains. The peaks observed at 4.117 to 4.162 ppm were assigned methylene (-C**H**$_2$**)** protons, while those at 4.271 to 4.162 ppm were assigned (-C**H**) protons due to the presence of hydrogen protons at the α and β carbons of the glycerol backbone.

In the ^{13}C-NMR spectra of sesame oil, many signals were observed at the range of 14.061 to 34.171 ppm. The signals at 14.061 to 14.107 ppm were assigned terminal

methyl carbon atoms of the fatty acid chains. The peaks at 22.566 to 22.681 and 29.079 to 29.758 ppm were assigned methylene $(CH_2)_n$ chains of all fatty acids. Whereas the allylic (CH=CH) fatty acid chains were observed at 25.566 and 27.185, ppm. The signals at 62.092 and 68.864 ppm were assigned the glycerol of CH_2 and CH carbon atoms, respectively.

The signals at 127.881 to 130.202 ppm were assigned the vinylic (=CH) or diallylic (CH=CHCH=CH) carbon atoms. The signal at 173.262 ppm was assigned the carbonyl (C=O) carbon atoms of the tri-ester functionality. Whereas, the signal at 206.267 ppm was assigned $(CH_3)_2CO$ groups of free fatty acids. Both the ^{1}H-NMR and ^{13}C-NMR spectra of sesame oil agreed with other reported vegetable oils NMR spectra describing the structure of a triacylglycerol bearing saturated and unsaturated fatty acid chains (Guillén and Ruiz, 2003; Barison *et al.*, 2010; Gomez *et al.*, 2011).

The ^{1}H-NMR and ^{13}C-NMR spectra of SEFAMEs biodiesel are given by Figures 4.5a and 4.5b, respectively.

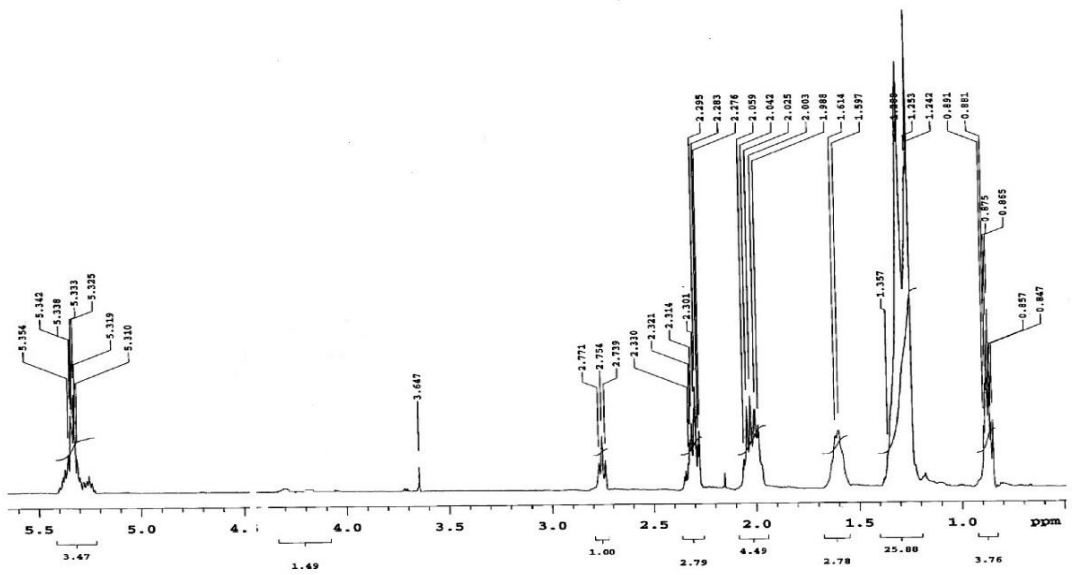

Figure 4.5a: ^{1}H-NMR Spectrum of SEFAMEs biodiesel.

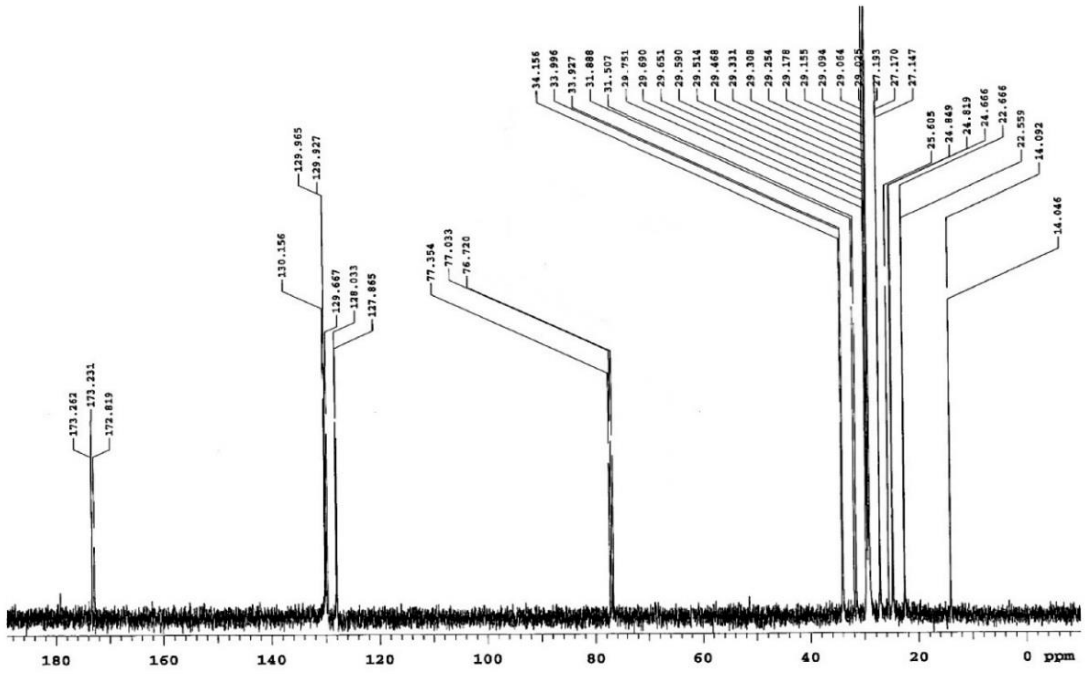

Figure 4.5b: ^{13}C-NMR Spectrum of SEFAMEs biodiesel.

In the ^{1}H-NMR spectra of SEFAMEs biodiesel, the peaks observed at 0.847 to 0.891 ppm were assigned terminal methyl (-C**H**$_3$) protons of all fatty acid chains. While those observed at 1.242 to 1.288 ppm were assigned methyl (-CH_2C**H**$_3$) protons of linolenic fatty acids, while the peaks at 1.346 to 2.330 ppm were assigned methylene (-C**H**$_2$) protons of fatty acids chains. Whereas those observed at 2.739 to 2.771 and 5.310 to 5.353 ppm were assigned allylic (-C**H**=CH protons of fatty acid chains. The peak observed at 3.647 ppm was assigned protons of the methoxy group (-COO-C**H**$_3$).

In the ^{13}C-NMR spectra of SEFAMEs biodiesel, the peaks at 14.046 to 14.092 ppm were assigned terminal methyl carbon atoms of the fatty acid chains. The peaks at 22.599 to 22.666 and 29.025 to 29.751 ppm were assigned methylene $(CH_2)_n$ chains of all fatty acids. Whereas the peaks observed at 25.603 and 27.147 to 27.193 ppm were assigned the allylic (CH=CH) carbon atoms of fatty acid chains. The peaks at 127.865 to 130.156 ppm were assigned the vinylic (=CH) or diallylic (CH=CHCH=CH) carbon atoms of

fatty acid chains. Whereas the signal at 172.819-173.262 ppm were assigned the carbonyl (C=O) carbon atoms of the tri-ester functionality.

In general, the observed sesame oil ^{1}H-NMR and ^{13}C-NMR spectra signals were quite similar to those SEFAMEs biodiesel. The main difference in features of the obtained ^{1}H-NMR spectra of SEFAMEs biodiesel and that of sesame oil, corresponded to the presence of a new singlet at 3.647 ppm in the SEFAMEs ^{1}H-NMR spectra. The new peak was assigned the methoxy group (CH_3O) of the methyl ester functionality. In addition, there was the disappearance of the signals around 4.117 to 4.311 ppm associated with the CH and CH_2 groups of the glycerol moiety.

In the ^{13}C-NMR spectra of SEFAMEs biodiesel, there was also the disappearance of signals at 62.092 and 68.864 ppm associated with the carbon atoms of the glycerol moiety. There was also the disappearance of the peak due to free fatty acids at 206.267 ppm, thus, suggested that the free acids were converted to fatty methyl esters. These observation agreed with other vegetable oil trans-esterification results which explained that the disappearance of glycerol moiety groups confirms the formation of fatty methyl esters (Ahmad *et al.,* 2011; Tariq *et al.,* 2011). These findings clearly confirmed the formation of the fatty methyl esters (biodiesel) from the sesame oil.

The ^{1}H-NMR and ^{13}C-NMR spectra results of sesame oil and SEFAMEs biodiesel including the functional groups assignments are summarized in Tables 4.6 and 4.7, respectively. Thus, compares sesame oil and SEFAMEs biodiesel ^{1}H-NMR and ^{13}C-NMR spectra.

Table 4.6: ^{1}H-NMR chemical shifts and interpretation of Sesame oil and SEFAMEs biodiesel.

Sesame oil Chemical shifts δ (ppm)	SEFAMEs Chemical shifts δ (ppm)	H-proton (s) assignments	Explanation
0.858-0.902	0.847-0.891	- CH_2-CH_2-C**H$_3$**	All fatty acids chains, mainly oleic and linoleic except linolenic.
1.250-1.367	1.242-1.288	-CH=CHCH_2-C**H$_3$**	Linolenic acyl chains
1.421	1.357	- (C**H$_2$**)$_n$	All acyl chains
1.611	1.614	- C**H$_2$**-CH_2COOH	All acyl chains
1.980-2.069	1.988-2.059	- C**H$_2$**-CH=CH-	All unsaturated fatty acids
2.166	-	-OCO-C**H$_2$**	All acyl chains
2.286-2.359	2.276-2.330	-OCO-C**H$_2$**	All acyl chains
2.748-2.781	2.739-2.771	-C**H**=CHCH_2CH=CH	All allylic protons (all unsaturated fatty acids mainly linolely and linolenly)
-	3.647	-O-CH_3	Methoxy group in the fatty acids acyl chains
4.117-4.162	-	-C**H$_2$**-O-COR	Glycerol
4.271-4.311	-	-C**H**-O-COR	Glycerol
5.261-5.383	5.310-5.353	-C**H**=CH-	All unsaturated fatty acids chains
7.261		-$CHCl_3$	Chloroform (solvent)

Table 4.7: ^{13}C-NMR chemical shifts and interpretation of sesame oil and SEFAMEs biodiesel.

Sesame oil Chemical shift δ (ppm)	SEFAMEs Chemical shift δ (ppm)	Functional group	Explanation
14.061,14.107	14.046,14.092	β- CH_3	Terminal carbon atoms of all fatty acids acyl chains
22.566, 22.681,	22.599, 22.666	-(-CH_2-)	All Fatty acids acyl chains
29.079-29.758, 31.514, 31.896	29.025-29.751, 31.507, 31.880	(-CH_2-)n	Fatty acids acyl chains
25.531, 27.185	25.603, 27.147-27.193	-(-CH=CH-)	Allylic and diallylic carbon atoms of unsaturated fatty acids acyl chains
24.666-24.857 33.874-34.171	24.603-24.849, 33.927-34.156	-(OCOCH_2CH_2)	All fatty acids acyl chains
62.092	-	- (CH_2O)	Glycerol
68.864	-	-(CHO)	Glycerol
127.881 130.202	127.865-128.033 129.667 -130.156	-(CH=CH)	Fatty acids acyl chains mainly olely and linoleyl
173.262	172.819-173.262	-(CHCOO-)	Fatty acids
206.267	-	-(CH_3)$_2$CO)	Free fatty acids

4.5.3.2 ^{1}H-NMR Results of Anionic SEFAMESO Surfactant

The peak observed at 0.700 ppm in the SEFAMESO surfactant ^{1}H-NMR spectrum was assigned methyl protons (-CH_2-C**H**$_3$) of the fatty acids chains. While the peaks observed at 1.137-1.785 ppm were assigned methylene $(CH_2)_n$ protons of the fatty acids chains. Whereas the peaks observed between 1.989 to 2.035 ppm were assigned (-CH=CHCH_2-COO-S) esters and sulphur functional groups. The peaks observed at 4.510 to 4.690 ppm were assigned esters sulphonate groups (-CH_2COO-SO_3Na) of fatty acid chains. The ^{1}H-NMR spectrum of the anionic SEFAMESO surfactant is presented in Figure 4.6.

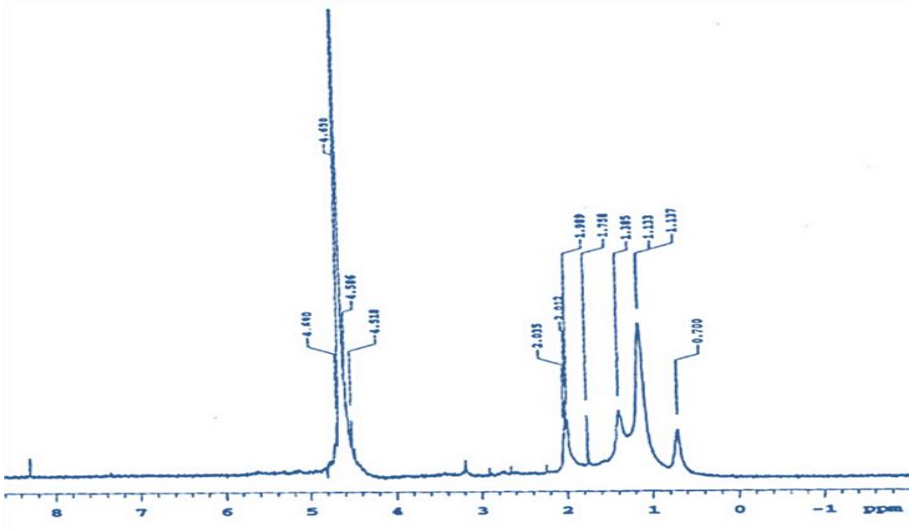

Figure 4.6: ^{1}H-NMR spectrum of the Anionic SEFAMESO surfactant.

The observed ^{1}H-NMR spectrum of SEFAMESO surfactant agreed with other reported chemical shifts of esters and sulphonate groups in the olefin chains (Schmitt, 2001; Cohen *et al.,* 2003).

4.5.4 HPLC-MS Results

HPLC-MS analysis was performed to determine the composition and the molecular weights/masses of the studied sesame oil, SEFAMEs biodiesel and the anionic

SEFAMESO surfactant. The sesame oil HPLC-MS spectra are shown in Figures 4.7 and Appendix VII (a). Whereas, Figure 4.8, and Appendix VII (b) give the SEFAMEs HPLC-MS spectra, while, Figure 4.9 and Appendix VII (c) give the anionic SEFAMESO surfactant HPLC-MS spectra.

4.5.4.1 HPLC-MS Results of Sesame Oil and SEFAMEs Biodiesel

The sesame oil HPLC-MS spectra showed significant peaks at 263.2, 355.3 and 898.8 *m/z*. While for SEFAMEs biodiesel, significant peaks were observed at 277.2, 636.56, 930.8 and 962.8 *m/z*. The molecular ion (m/z = 263) was prominent in both sesame oil and SEFAMEs biodiesel. In the sesame oil mass spectra, it corresponded to loss of glycerol group of linoleic or linolenic fatty acid, whereas, in the SEFAMEs biodiesel it corresponded to the loss of propyloxy ion (-OCH_2) of fatty acids fragments.

Some of the observed HPLC-MS spectra of sesame oil and SEFAMEs biodiesel are presented in Figures 4.7 and 4.8, respectively.

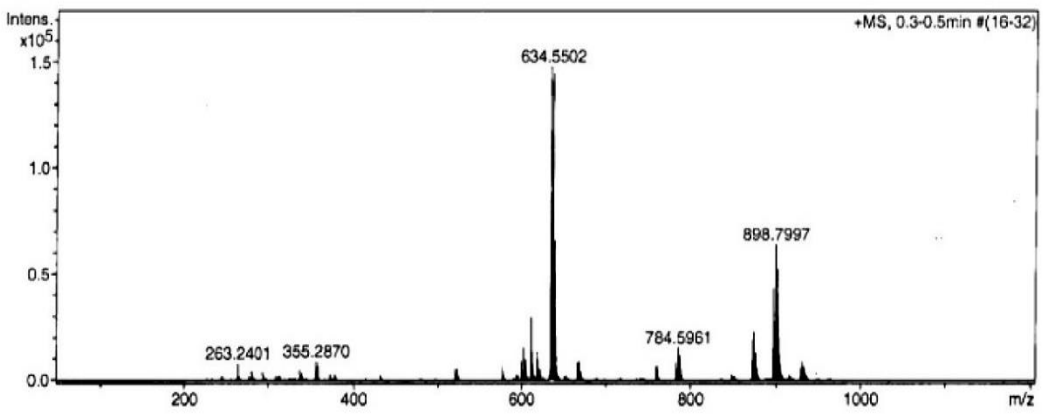

Figure 4.7: HPLC-MS spectrum of sesame oil.

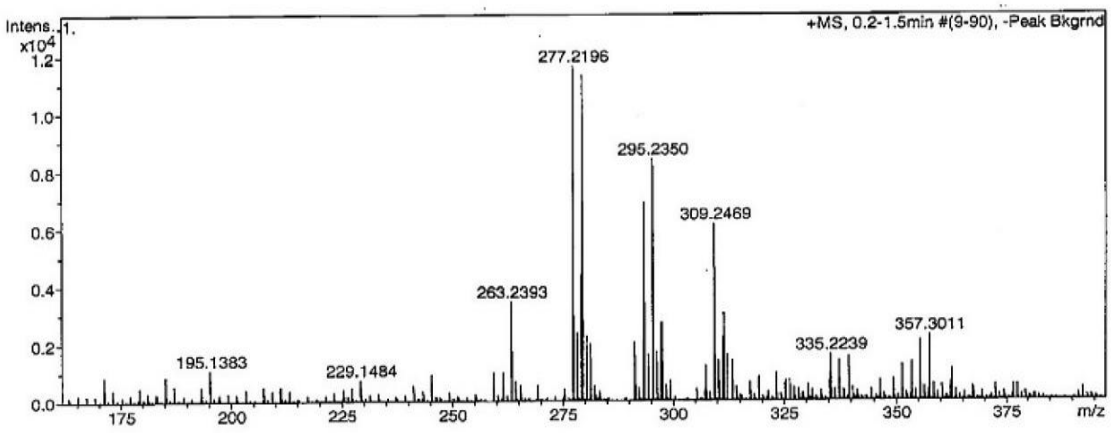

Figure 4.8: HPLC-MS spectrum of SEFAMEs biodiesel.

The observed HPLC-MS molecular ions masses of the sesame oil and SEFAMEs biodiesel and their interpretations are given in Table 4.8. The table compares the sesame oil and SEFAMEs biodiesel HPLC-MS results.

Table 4.8: HPLC-MS molecular ions masses and interpretation of Sesame oil and SEFAMEs biodiesel.

Sesame oil Molecular ion weight (m/z)	SEFAMEs diesel Molecular ion weight (m/z)	Fatty acid carbon atoms	Explanations
229∓1	242∓1	$C_{14:0}$	Myristic fatty acid
254∓1	268∓1	$C_{16:1}$	Palmitoleic fatty acid
256∓1	270∓1	$C_{16:0}$	Palmitic fatty acid
263∓1	293∓1	$C_{18:2}$ or $C_{18:3}$	Linoleic or linolenic fatty acid
278∓1	292∓1	$C_{18:3}$	Linolenic fatty acid
280∓1	294∓1	$C_{18:2}$	Linoleic fatty acid
282∓1	296∓1	$C_{18:1}$	Oleic fatty acids
284∓1	298∓1	$C_{18:0}$	Stearic fatty acid
310∓1	324∓1	$C_{20:1}$	Eicosenoic fatty acid
312∓1	326∓1	$C_{20:0}$	Eicosanoic fatty acid
340∓1	356∓1	$C_{22:0}$	Arachidic fatty acid

The HPLC-MS spectra showed that the extracted sesame oil was mainly composed of mono and poly unsaturated fatty acids, mostly oleic and linoleic which made 84 % of the total fatty acids. Other unsaturated fatty acids included linolenic, eicosenoic and palmitoleic, fatty acids which made 1 % of the total. The most dominant saturated fatty acids were palmitic, and stearic acid which made 14 % of the total fatty acids. Other saturated fatty acids present in very minimal amounts were myristic, eicosanoic and arachidic fatty acids. The observed HPLC-MS spectra concurred with the reported findings that sesame oil consists of mainly unsaturated fatty acids and less saturated fatty acids (Jakab *et al.,* 2002; Bail *et al.,* 2009; Borchani *et al.,* 2010).

The HPLC-MS spectra of the SEFAMEs biodiesel showed that the biodiesel consisted of mixtures of both saturated and unsaturated fatty methyl esters. It showed that the SEFAMEs prominently contained unsaturated fatty methyl esters mainly oleic and linoleic with very minimal amounts of palmitoleic, linolenic and eicosenoic methyl esters. The most dominant saturated fatty methyl esters present in sesame oil was palmitic, and stearic. Other saturated fatty methyl esters present in very minimal amounts included, myristic, eicosanoic, and arachidic methyl esters. The obtained average molecular weight of the SEFAMEs was 291.9852, which was approximately 292 g.

4.5.4.2 HPLC-MS Results of Anionic SEFAMESO Surfactant

The anionic SEFAMESO surfactant mass spectrum showed significant peaks at 269 and 785.9 *m/z*. The peak observed at 269 *m/z* corresponded to palmitate ion derivative (Borchani *et al.,* 2010). Thus, showed that the synthesized surfactant was a triacylglycerol derivative. The peaks observed between 457 to 539 *m/z* represented

fragments of fatty methyl esters sulphonate ions. The results showed that the synthesised surfactant was composed of mixtures of fatty methyl esters sulphonates, with approximately 83 % oleic and linoleic fatty methyl esters sulphonates. The stearic and palmitic fatty methyl esters sulphonates made about 14 % of the total fatty methyl esters. Other methyl esters sulphonates present in very minimal amount were palmitoleic eicosanoic, eicosenoic and arachidic methyl esters sulphonates. The HPLC-MS spectrum of the anionic SEFAMESO surfactant is shown in Figure 4.9.

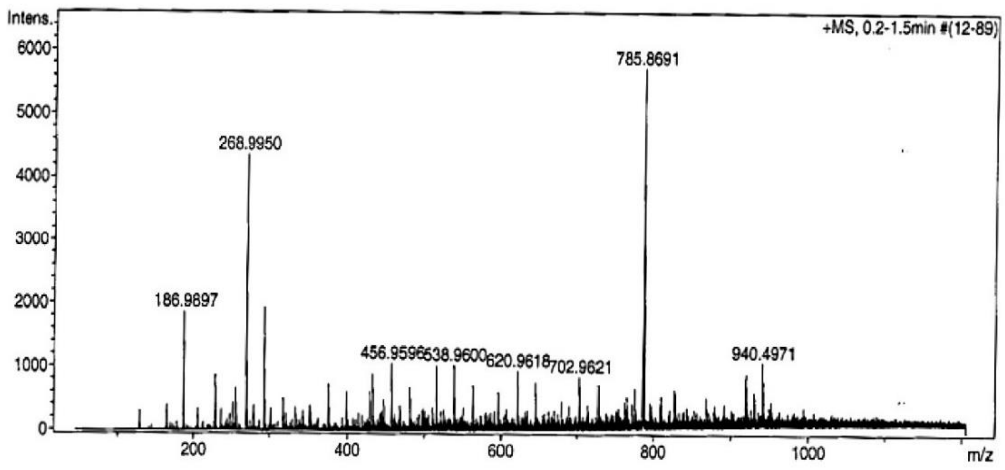

Figure 4.9: HPLC-MS spectrum of Anionic SEFAMESO Surfactant.

The observed peaks agreed with the reported findings on the analysis of sulphoxylated methyl esters (Cohen *et al.*, 2003).

4.6 Properties of Anionic SEFAMESO Surfactant

The evaluated anionic SEFAMESO surfactant solution properties included: the krafft point and foam-ability. The CMC values, counter-ion binding and thermodynamic properties of micellization were also determined using the correlation between specific conductivity and specific viscosity versus the surfactant concentration.

4.6.1 Krafft Temperature of SEFAMESO

The synthesized SEFAMESO surfactant Krafft point was 19.75 ^{o}C, which was relatively low. The Krafft temperature of the synthesized SEFAMESO surfactant showed that the surfactant could be applied as low temperatures detergent. In addition, it showed that the synthesized surfactant consisted of minimal amounts of di-salts. The di-salts are side-reaction products which usually result from hydrolysis of ester groups in the surfactant. The formation of di-salts often causes increased Krafft points and therefore, increased insolubility of the oleo-chemical surfactants (Kjellin and Johansson, 2010). Hence, the quite low Krafft point of the synthesized SEFAMESO surfactant implied that it was relatively soluble and thus, validates its application as low-temperature surfactant. The obtained Krafft point compared well with the reported Krafft points of mixture of $C_{16\text{-}18}$ methyl esters sulphonates which range from 17-30 ^{o}C (Cohen *et al.,* 2008; Aparicio *et al.,* 2012).

4.6.2 Foam-ability of SEFAMESO

The initial foam height of the synthesized SEFAMESO surfactant was 145 cm^3, which after 5 minutes it decreased to 66 cm^3. Hence, the foam stability of the synthesized SEFAMESO surfactant was 79 cm^3, which was 54.48 % of the initial foam height. The foam-ability property results compared well with other reported cleaning and wetting agents that contain mixtures of methyl esters sulphonate (Cohen *et al.,* 2008). Therefore, the SEFAMESO foam-ability results were good, and it showed that the synthesized surfactant could be applied as a cleansing, wetting agent or detergent.

4.6.3 Critical Micelle Concentration (CMC) and the Degree of Counter-ion Binding

From the specific conductivity versus surfactant concentration curves, both the CMC and the counter-ion binding (dissociation) of the synthesized SEFAMESO surfactant and the SDS standard were evaluated. The specific viscosity versus surfactant concentration curves were also used to evaluate the CMC values.

Figures 4.10, 4.11 and 4.14 give the plots of specific conductivity versus the SEFAMESO surfactant concentration whereas, figures 4.12, 4.13 and 4.15 give the plots of specific viscosity versus the concentration of SEFAMESO surfactant. Appendices VIII (a) and VIII (b) give the plots of the specific conductivity versus the concentration, and the specific viscosity versus the concentration of the SDS standard, respectively.

The graph of specific conductivity against the concentration of the anionic SEFAMESO surfactant at 298.15 K is shown in Figure 4.10.

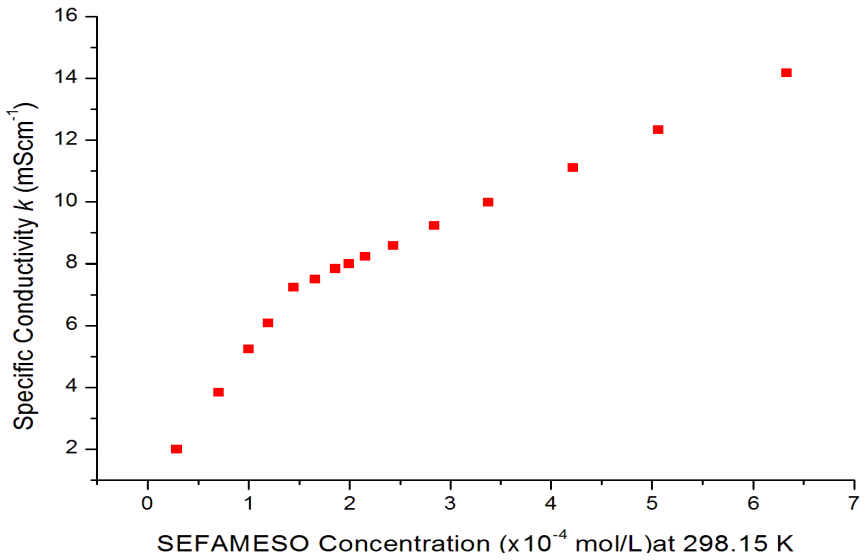

Figure 4.10: Specific Conductivity against SEFAMESO concentration at 298.15 K.

The specific conductivity of the anionic SEFAMESO surfactant increased gradually with increase in the concentration of the surfactant, up to a point where a sharp break was observed in the curve as shown in Figure 4.10. After that point, there was a gradual increase again, however, not as rapid as that observed below that sharp point. The point at which an abrupt break in the curve was observed represented the concentration at which the micelles started forming. Hence, it is the CMC point or value. The observation was in agreement with the reported findings that specific conductivity varies linearly with the concentration of ionic surfactants below and above the CMC (Holmberg *et al.*, 2003; Rosen and Kunjappu, 2012).

The values of CMC at the considered study temperatures were obtained from the specific conductivity against surfactant concentration curves, by drawing two linear lines. The point of intersection of the two lines represented the CMC as shown by the arrow in Figure 4.11.

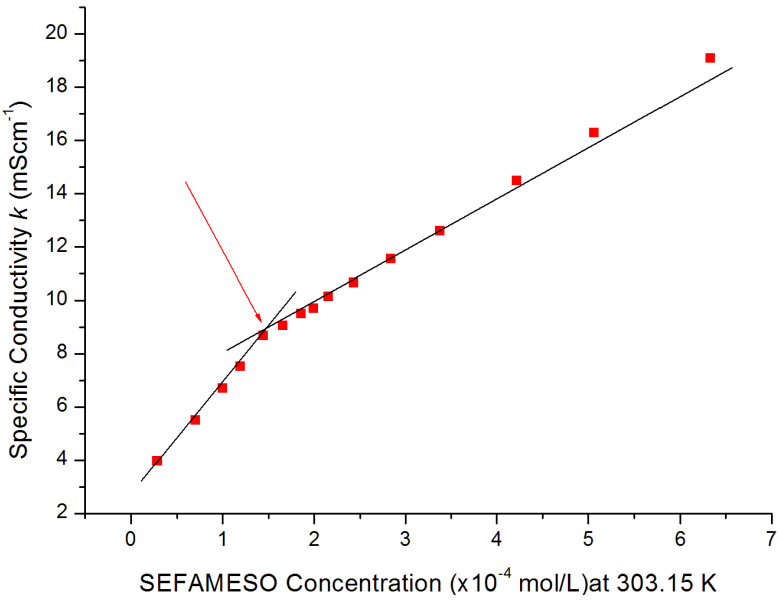

Figure 4.11: Extrapolation of CMC in the specific conductivity versus SEFAMESO concentration curve.

The ratio of the slopes of the post-micellar region (above the CMC) to that in the pre-micellar region (below the CMC) of the specific conductivity versus surfactant concentration curves were used to obtain the counter-ion binding or dissociation (β) constant, according to Equation 3.13.

The change in the electrical conductance of aqueous ionic surfactant solutions at the CMC is due to the different degree of surfactant ionization below and above CMC. Below CMC the surfactant monomers behave as strong electrolytes since the alkyl chains (the anions for anionic surfactant) and the counter-ion (cations) contribute independently to ionization. Thus, the independent contributions of the surfactant monomers ions result in rapid increase in specific conductivity with increase in concentration up to CMC. However, above the CMC, the formation of micelles increases, micelles are partially ionized, thus, above the CMC, the specific conductivity fairly increases with increase in surfactant concentration. Hence, the slope at pre-micellar region is stiffer than the post micellar region (Holmberg *et al*., 2003).

The curve of specific viscosity against the concentration of the anionic SEFAMESO surfactant at 298.15 K is shown in Figure 4.12.

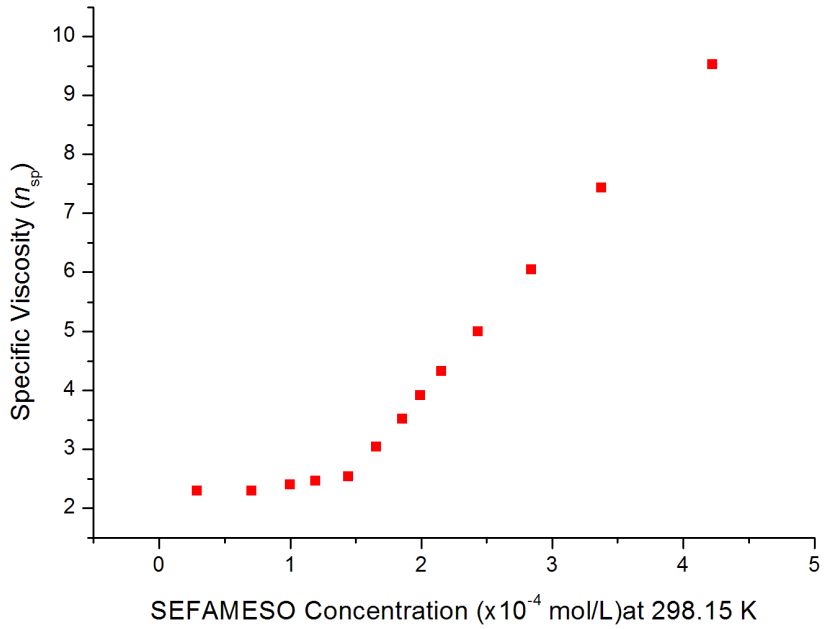

Figure 4.12: Specific viscosity against SEFAMESO concentration at 298.15 K.

It was observed that there was a minimal change in the specific viscosity of the anionic SEFAMESO surfactant with increase in the concentration up to a point where a break, after which a very rapid increase in viscosity was observed as shown in Figure 4.12. The breaking point on the curve was assigned the CMC point. The rapid increase in viscosity after the CMC point was due to the formation of free micelles in the solution and the forces of interaction between micelles molecules. The observation concurred with other reported findings that the rapid growth of the viscosity with surfactant concentration above the CMC is attributed to the considerable cross links among the micelles (Holmberg *et al*., 2003; Tadros, 2005; Wang *et al.*, 2004).

The CMC values were obtained from the specific viscosity versus surfactant concentration curves by extrapolating in the same way as those of the specific conductivity versus surfactant concentration curves as shown in Figure 4.13.

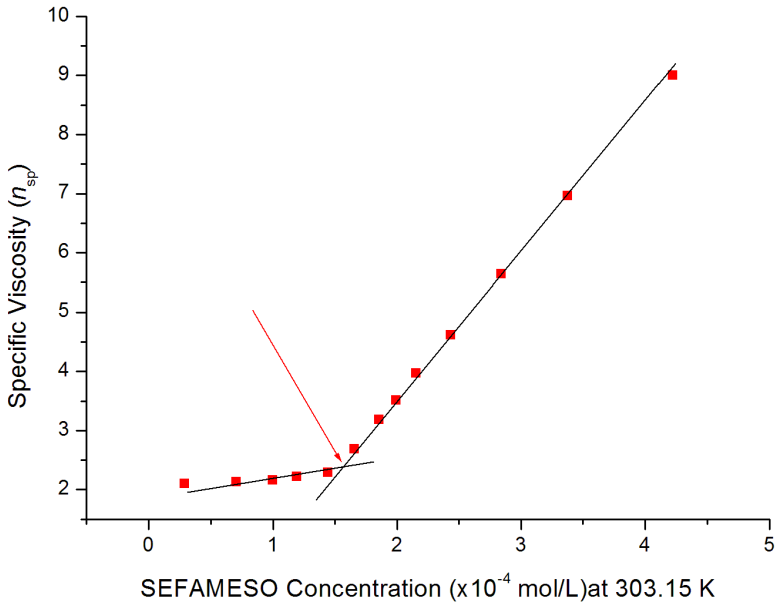

Figure 4.13: Extrapolation of CMC in the specific viscosity versus concentration curve.

4.6.3.1 Effect of Temperature on the CMC and Counter-ion binding Degree

The plots of specific conductivity versus the concentration and specific viscosity versus the concentration of the anionic SEFAMESO surfactant as function of temperature (at study temperatures: 298.15, 303.15, 313.15, and 323.15 K) are presented in Figures 4.14 and 4.15, respectively. The distinct break point observed for each temperature curve give the CMC value.

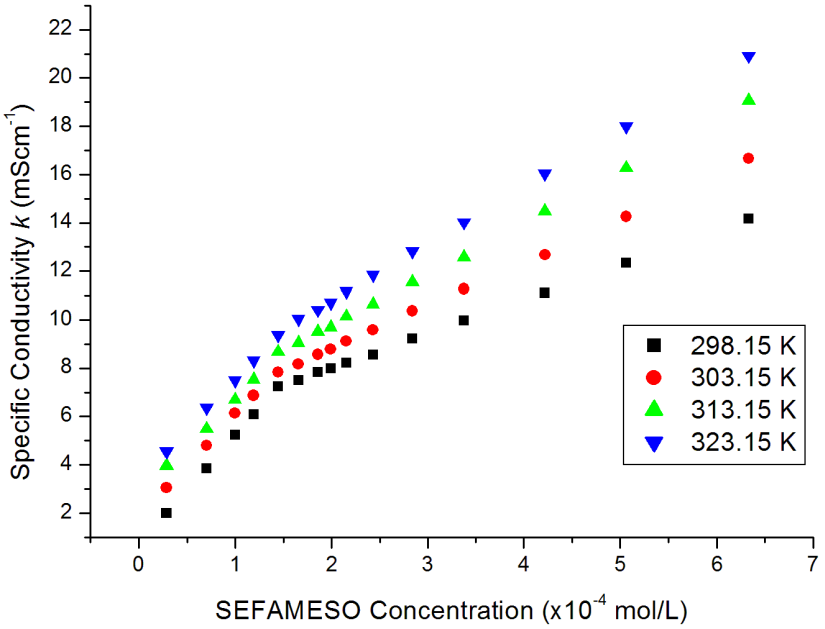

Figure 4.14: Effect of temperature on the specific conductivity against SEFAMESO concentration.

A gradual increase in specific conductivity as a function of SEFAMESO surfactant concentration was observed with increase in temperature as shown in Figure 4.14. This was attributed to an increase in the thermal energy of the molecular entities (Holmberg *et al.*, 2003). The CMC values obtained from the specific conductivity against the concentration of the SEFAMESO as function of temperature initially decreased from 1.435 x 10^{-4} mol/L at 298.15 K to 1.418 x 10^{-4} mol/L at 303.15 K. Then, a significant increase was observed at higher temperatures of 313.15 and 323.15 K; in which CMC values of 1.471 x 10^{-4} and 1.518 x 10^{-4} mol/L were obtained, respectively. This observation concurred with other findings which explained that the change in CMC values with increase in temperature follows a parabolic-shape or U-shape (Mehta *et al.*, 2005; Holmberg *et al*., 2003).

The plots of specific viscosity versus the concentration of the anionic SEFAMESO surfactant as function of temperature are shown in Figure 4.15.

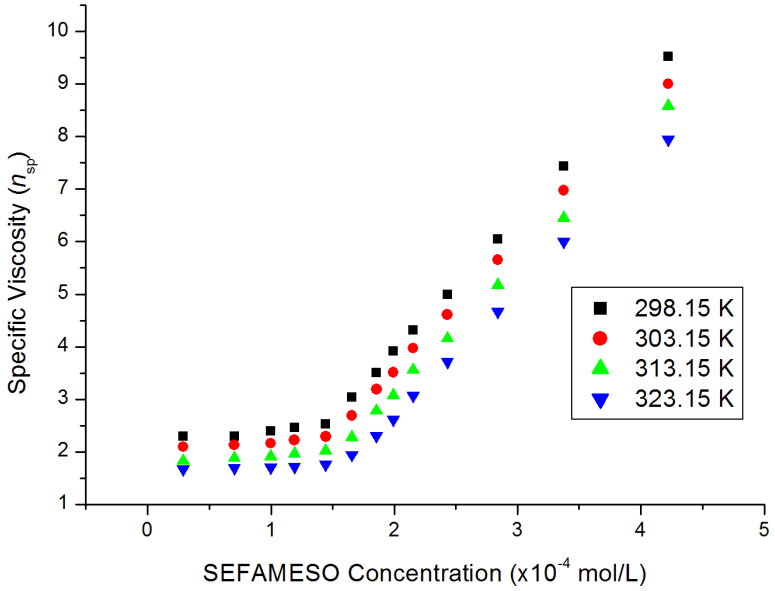

Figure 4.15: Effect of temperature on the specific viscosity against SEFAMESO concentration.

It was observed that the specific viscosity of the anionic SEFAMESO decreased with increasing temperature as shown in Figure 4.15. This behaviour was attributed to the changes in the structure or conformation of the surfactant molecules at higher temperatures; in which surfactant molecules became less polar with increasing temperature and hence the chain contracts, resulting in a decrease in viscosity (Akbas *et al.*, 2003; Wang *et al.*, 2004).

The CMC values obtained from the specific viscosity against the concentration of the SEFAMESO were quite higher than those obtained from the conductivity measurements. In the same way as the CMC values from conductivity measurements, the CMC values as function of temperature from viscosity measurements showed a decreased from 1.535 x 10^{-4} mol/L at 298.15 K to 1.512 x 10^{-4} mol/L at 303.15 K. Then at higher temperatures, a significant increase in the CMC values was observed, in which

CMC values of 1.550 x 10^{-4} and 1.637 x 10^{-4} mol/L were obtained at 313.15 and 323.15 K, respectively.

The CMC values from the conductivity (k) and viscosity (n_{sp}) measurements and the counter-ion binding (β) of the anionic SEFAMESO surfactant and the SDS standard at the study temperatures are presented in Table 4.9. Thus, compares the CMC and β values of SEFAMESO and SDS standard.

Table 4.9: Comparison of CMC values and counter-ion binding degree (β) values of SEFAMESO and SDS.

Temp K	**Anionic SEFAMESO Surfactant**			**SDS Standard**		
	CMC values (x 10^{-4}) mol/L		Counter ion binding degree (β)	CMC values (x 10^{-3}) mol/L		Counter ion binding degree (β)
	From k	From n_{sp}		From k	From n_{sp}	
298.15	1.435	1.512	0.687	8.318	8.535	0.771
303.15	1.418	1.535	0.570	8.200	8.400	0.756
313.15	1.471	1.550	0.476	8.530	8.834	0.722
323.15	1.518	1.637	0.433	8.757	8.843	0.700

The CMC values of the SEFAMESO surfactant were much lower than those of the SDS standard at the study temperatures. This was due to the fact that the CMC values decreases significantly with increase in alkyl chain lengths because of increased hydrophobicity (Holmberg *et al*., 2003; Rosen and Kunjappu, 2012) and SEFAMESO mainly consisted of C_{18} alkyl chains which were longer than C_{12} chains of the SDS.

The counter-ion binding degrees of SEFAMESO surfactant at 298.15, 303.15, 313.15 and 323.15 K were 0.687, 0.570, 0.476 and 0.433, respectively. The counter-ion binding degrees in the SEFAMESO surfactant were lower than those of the SDS standard. This could be due to the presence of longer hydrophobic alkyl chains in the SEFAMESO

than in SDS which result in chain folding inside the micelle core, thus, decreasing counter-ion binding degree (Rosen and Kunjappu, 2012; De and Mondal, 2012).

The SEFAMESO counter-ion binding degree also showed a significant variation with temperature, whereby, with increase in temperature, the counter-ion binding degree of SEFAMESO decreased significantly. This indicated that with increase in temperature, the self-assembly or micellization was much less cooperative in the anionic SEFAMESO molecules and more loosely held aggregates or small aggregates were formed at higher temperatures (Tadros, 2005).

On the other hand, the counter-ion binding degree constant of the SDS standard did not show any significant change with increase in temperature. The observation concurred with the reported findings that the Na^+ ions at the SDS micellar surface is unlikely to change the counter-ion binding constant by more than 35 % with change in environmental conditions such as increase in temperature due to stable absorption in bulk to the stern layer of SDS micelle (De and Mondal, 2012).

The observation made on the variation of the CMC values with temperature was due the fact that increase in temperature, increases two opposing effects in the surfactant solution: (i) the degree of hydration of the head group decreases, thereby favouring micellization, and (ii) the ordered structure of solvent molecules around the hydrophobic tails breaks, thereby disfavouring micellization. Hence, the two opposing forces result in increase in the solubility and the decrease in the hydration of hydrophilic groups. The degree of hydrophillic dehydration, at high temperature, is greater than that of hydrophobic dehydration which enhances the repulsion among hydrophilic groups and

renders micellization difficult consequently increasing the CMC values (Rosen and Kunjappu, 2012; De and Mondal, 2012).

A comparison of the CMC values, counter-ion binding degrees (β) as function of temperature, and the Krafft temperatures of the methyl esters sulphonate in the present study with other reported methyl esters sulphonates in literature are presented in Table 4.10.

Table 4.10: Comparison of CMC, β values and Krafft points of Alkyl Methyl Esters Sulphonates.

Temp K	**Present Study**			**Other studies**		
	CMC (mM)	Krafft (^oC)	β	CMC (mM)	Krafft (^oC)	β
298.15	0.1435	19.75	0.678	C_{12}- 8-8.4[a] C_{14}-2.21[a], 2.8[b] C_{16}-5.5[a],0.4[b], 2.2[c] C_{18}-0.08-0.16[b]	C_{12}-16-17[a], 6[b] C_{14}-36[a] C_{16}-44-45[a], 45[b]	C_{12}-0.74[c] C_{14}- 0.92[c] C_{16}- 0.88[c]
303.15	0.1418		0.570			
313.15	0.1471		0.470	C_{18}-0.16[a]	C_{18}-54-56[a]	
323.15	0.1518		0.433			

Source: ([a]Könnecker *et al.,* 2011; [b] Mazzanti, 2008; [c]Prabha *et al.,* 2013).

The CMC values, counter-ion binding degree, and the krafft temperature of the synthesized SEFAMESO were within the ranges of other reported findings of alkyl methyl esters sulphonates.

4.6.4 Thermodynamic Properties of SEFAMESO Surfactant

The obtained CMC data as a function of temperature from the conductivity measurements were used to determine the thermodynamic properties of micellization: the free Gibbs energy, enthalpy, and entropy terms of micellization of SEFAMESO

surfactant. The CMC values, mole fraction (X_{CMC}), β, and the thermodynamic data of micellization of the SDS standard are presented in Appendix IX.

The CMC values, mole fraction (X_{CMC}), and β values, together with the ΔG°_{mic} of the SEFAMESO as function of temperature and the ΔG°_{mic} of other reported methyl esters sulphonates are presented in Table 4.11.

Table 4.11: Comparison of CMC values, β and ΔG^{o}_{mic} of SEFAMESO with other MES surfactants.

Temp (K)	X_{CMC} (x 10^{-6})	InX_{CMC}	**β**	**Present Study** ΔG°_{mic} (kJmol^{-1})	**Other MES studies** ΔG°_{mic} (kJmol^{-1})
298.15	2.581	-12.867	0.687	-53.780	C_{12}: -30.07[a] C_{14}: -34.49[a], -34.13[b], -40.7[c] C_{16}: -40.80[a] , -35.08[b] $C_{16/18}$: -45.72[a]
303.15	2.550	-12.879	0.570	-50.940	C_{14}: -41.2[c]
313.15	2.646	-12.843	0.476	-49.330	C_{14}: -42.0[c]
323.15	2.730	-12.811	0.433	-49.300	C_{14}: -42.7[c]

Sources of MES ΔG^{o}_{mic}: ([a]Lim and Ramle, 2009; [b] Prabha *et al.,* 2013 [c]Okano *et al.,* 2000).

The change in free Gibbs energy of micellization (ΔG°_{mic}) at each study temperature was negative, which meant that micellization process was spontaneous. The ΔG°_{mic} of the SEFAMESO were much higher and more negative than those of the SDS standard and other reported C_{12}, C_{14} andC_{16}MES, but quite higher than those mixtures of $C_{16}/_{18}$ MES. This observation was in agreement with the established findings that the values of free energies of micellization are affected by the length of hydrocarbon chains (hydrophobic portion) of the surfactant and therefore, micelle formation become more

spontaneous with increase in alkyl chain length (Rosen and Kunjappu, 2012; De and Mondal, 2012). Therefore, the large negative values of ΔG°_{mic} indicated that micellization was thermodynamically favourable process (Zana, 2005). Hence, the formation of micelles by the SEFAMESO molecules was spontaneous mainly because it consisted of longer C_{18} alkyl chains.

The CMC values, β, and thermodynamic properties of micellization (ΔG°_{mic}, ΔH°_{mic} and ΔS°_{mic}) of the SESAMESO surfactant together with the reported ΔH°_{mic} and ΔS°_{mic} data of C_{14}-MES are presented in Table 4.12.

Table 4.12: Thermodynamic properties of micellization of SEFAMESO surfactant and ΔH^{o}_{mic} and ΔS^{o}_{mic} of C_{14}-MES.

Temp (K)	**CMC** (x 10^{-4} mol/L)	**β**	ΔG°_{mic} (kJ mol^{-1})	ΔH°_{mic} (kJ mol^{-1})		ΔS°_{mic} (J $mol^{-1}K^{-1}$)	
				Present study	**C_{14}-MES**	**Present study**	**C_{14}-MES**
298.15	1.435	0.687	-53.780	-24.970	C_{14}: -1.63	96.678	C_{14}: 133
303.15	1.418	0.570	-50.940	-23.970	C_{14}: -6.35	89.010	C_{14}: 106
313.15	1.471	0.476	-49.330	-38.470	C_{14}: -15.3	34.700	C_{14}: 56.6
323.15	1.518	0.433	-49.300	-40.970	C_{14}: -23.7	28.792	C_{14}: 11.8

Source of C_{14}-MES ΔH°_{mic} and ΔS°_{mic}: (Okano *et al.,* 2000).

The ΔG°_{mic} results of SEFAMESO surfactant showed that the values of ΔG°_{mic} became less negative with increase in temperature. This indicated that the spontaneity of micellization process decreased at higher temperature. In general, the ΔG°_{mic} depended on the relative amount of the changes in ΔH°_{mic} and ΔS°_{mic}. It was observed that the values of ΔS°_{mic}were positive, while those of ΔH°_{mic} were negative at each temperature, this meant that micellization is both an entropy and enthalpy driven process (Holmberg

et al., 2003; De and Mondal, 2012). In addition, the negative values of ΔH°_{mic} showed the micellization process of SEFAMESO was exothermic.

The ΔS°_{mic} were more positive at the temperatures of 298.15 and 303.15 K, this region was characterized by lower values of X_{CMC} and also the $T\Delta S^{\circ}_{mic}$ were higher than ΔH°_{mic}. The increased positive entropy below 303.15 K, may be due to the changes in the water solvent structure. The positive entropy resulted from the destruction of the ‘‘iceberg’’ structure that forms water molecules around the hydrophobic chain of surfactant molecule, which led to increased transfer of hydrophobic chains of SEFAMESO from aqueous environment to micelle core (Attwood and Florence, 2012).

Therefore, the removal of hydrophobic groups from the aqueous environment was entropically favourable leading to the disruption of the highly organized water structure and removal of mobility constraints on the hydrocarbon chain (Attwood and Florence, 2012). This consequently, led to increased hydrophobic interactions, thus, favouring micellization. Hence, below 303.15 K, SEFAMESO micellization process was entropy driven.

It was observed that the value of ΔS°_{mic} decreased above the temperature of 303.15 K, while the value of ΔH°_{mic} increased with increase in temperature. This implied that the more ordered structure of water molecules around hydrophobic chains and restriction in vibrations of hydrophobic groups led to a decrease in entropy of the system (De and Mondal, 2012).

Conversely, the increased negative values of ΔH°_{mic} may have been due to increased hydration of water molecules around the hydrophilic heads groups; which became more

favourable at higher temperatures than the destruction of water structure around hydrophobic groups of monomers (Rosen and Kunjappu, 2012). Hence, increase in temperature caused dehydration of hydrophilic groups, thus, making electrostatic repulsion stronger. This observation showed that at higher temperatures, the hydrophobic interactions became weaker while electrostatic ones become stronger (Attwood and Florence, 2012). Thus, at higher temperatures, micellization was enthalpy or energy driven.

The observation made on the considered thermodynamic properties of micellization agreed with other findings that the lengths of hydrophobic alkyl chain significantly affect the CMC values and consequently, the thermodynamic properties of micellization. In addition, it confirmed that the micellization process can either be entropy or enthalpy driven depending on temperature.

CHAPTER FIVE

CONCLUSION AND RECOMMENDATIONS

5.1 Conclusion

This study has considered sesame oil as one of the promising renewable, biodegradable and sustainable oleo-chemical feedstock/raw material, which can supplement or replace the depleted petrochemical feedstock in the industrial production of energy and surfactants. The obtained oil yield of sesame seeds was 46 %, which was relatively high. The physicochemical properties of sesame oil were obtained which included density of 880 kg m^{-3}, viscosity of 50 mm^2/s, free fatty acid value of 0.56 mg/g of KOH, saponification value of 167 mg of KOH/g of oil and unsaponifiable matter content of 1.67 %. These values indicated that the underutilized sesame seeds are viable and potential sources of vegetable oil which can be exploited commercially for industrial applications in biodiesel and surfactant synthesise.

The physicochemical and fuel properties of the synthesized SEFAMEs biodiesel such as; density of 840 kg/m^3, flash point of 160 ^oC, and kinematic viscosity of 3.6 mm/s^2, pour point of -8 ^oC, calorific value of 3950 kJ/kg, saponification value of 160 mg KOH/g of biodiesel were obtained. These values were within the ASTM standards of biodiesel and diesel fuels. Hence, showed that the SEFAMEs biodiesel could be applied as fuel in the diesel engines. In addition, the properties of SEFAMEs biodiesel indicated that it could be applied as industrial chemical, especially its high saponification value indicated that it could be used as a precursor in the surfactant synthesis. In this study,

the SEFAMEs biodiesel was used to synthesize the sodium sesame fatty methyl esters sulphonate surfactant.

The compositional properties of the extracted sesame oil, SEFAMEs biodiesel and the SEFAMESO surfactant were evaluated using Elemental, HPLC-MS, NMR and FTIR analysis. The peaks at 1418 to 1376 cm^{-1} and a singlet at 3.647 ppm in the in the FT-IR and ^{1}H-NMR spectra of SEFAMEs biodiesel, respectively, corresponded to the methyl ester functional group (-O-CH_3). Methyl ester group therefore, confirmed that the trans-esterification of sesame oil to SEFAMEs biodiesel was successful. On the other hand, the intense peak at 1419 cm^{-1} and 4.690 ppm in the SEFAMESO surfactant FT-IR and ^{1}H-NMR spectra, respectively, corresponded to sulphonate group (S=O), thus, confirmed the presence of sulphonate esters group. This indicated that synthesise of the SEFAMEs biodiesel and SEFAMESO surfactant were successful.

The synthesized anionic SEFAMESO surfactant solution properties in water were evaluated. These included the Krafft point, foam-ability and the temperature influence on the CMC values, the counter-ion binding degree, and the thermodynamic properties of micellization: (ΔG°_{mic}, ΔH°_{mic} and ΔS°_{mic}) at temperatures of 298.15, 303.15, and 313.15 and 323.15 K. The Krafft temperature of SEFAMESO was found to be 19.75 ^{o}C, while its foam-stability was 54.48 %.

It observed that the CMC values and thermodynamic parameters of micellization were highly influenced by temperature variation. Minimum CMC value was observed at 303.15 K which was 1.418 x 10-4 mol/L and significantly increased at 313.15 and 323.15 K which were 1.471 x 10^{-4} and 1.518 x 10^{-4} mol/L, respectively. The counter-ion binding degree of the SEFAMESO surfactant decreased significantly with increase

in temperature from 0.687 at 298.15 K to 0.433 at 323.15 K. The value of ΔG°_{mic}, was -53.78 kJ/mol at 298.15 K and reduced to -49.3 kJ/mol at 323.15 K. Similarly, the entropy (ΔS°_{mic}) at 298.15 K was 96.678 J mol^{-1} K^{-1} and reduced to 29.792 at 323.15 K. However, enthalpy showed significant increase with increase in temperature, for instance, at 298.15 K it was -24.97 kJ/mol and increased significantly to -40.97 kJ/mol at 323.15 K.

The thermodynamic properties of micellization; ΔG°_{mic}, ΔH°_{mic} and ΔS°_{mic} showed that the formation of micelles by the SEFAMESO molecules was spontaneous. It was observed that at temperature below 303.15 K, micellization was entropy driven and above this temperature it was enthalpy driven. The thermodynamic properties of micellization therefore, showed that the SEFAMESO molecules could form thermodynamically stable aggregates or micelles which are highly influenced by temperature changes.

The results of this study indicated that sesame oil is a potential raw material for industrial production of biodiesel and surfactant from renewable and biodegradable sources. Thus, indicated that renewable oleo-chemical feed-stocks are viable raw materials sources for energy and surfactant industry.

5.2 Recommendations

In this study, crude sesame oil was used in synthesis, in further studies, crude sesame oil should be separated into its respective fatty acids. Then the separated fatty acids should be used to carry out the studies. In addition, in this study, synthesis routes were catalysed by organic and inorganic chemicals such as sodium hydroxide base in trans-

esterification of sesame oil to SEFAMEs biodiesel. More synthesis research studies using natural enzymes as catalysts in synthesise of biodiesel and bio-based surfactants should be done. Natural enzymes represent potential catalysts for oleo-chemical feedstock that can replace organic and inorganic chemicals. The physicochemical and fuel properties of SEFAMEs biodiesel were good. However, cloud point and pour point were quite high which implied it could limit SEFAMEs biodiesel application of in cold climate. There is need therefore, for more research in optimizing biodiesel properties and thus, improving SEFAMEs biodiesel properties.

The micellar properties of the anionic SEFAMESO surfactant in water were studied using conductivity and viscosity measurements, these techniques are not comprehensive. There is therefore, need for studying the micellar properties using more efficient, comprehensive and specific methods such as diffusional NMR methods, fluorescence probe spectroscopy and light scattering. In addition, SEFAMESO surfactant solution properties should be done in presence of various additives and mixed surfactants. This include studying the effect of additives such salts e.g. NaCl, poly-electrolytes and solvents both organic and inorganic such as, methanol, butanol, and poly-ethylene glycol on the critical micelle concentration and thermodynamic properties of micellization of the SEFAMESO surfactant.

Evaluation of toxicity and biodegradability of SEFAMESO surfactant should also be carried out, including evaluation of its dermatological effects such as skin irritability tests. This will be important in ascertaining the practicality and viability of production and applications of the anionic SEFAMESO surfactant.

Most reported oleo-chemical products synthesis and applications studies have been mainly done in the laboratory with limited large scale synthesis and applications. Therefore, the use of oleo-chemical feed-stocks for industrial applications is still unexploited commercially. Hence, in future more emphasis in large scale oleo-chemical products synthesis should be considered to enhance the feasibility of using renewable, biodegradable oleo-chemical raw materials.

REFERENCES

Abou-Gharbia, H. A., Shehata, A. A. Y., and Shahidi, F. (2000). Effect of processing on oxidative stability and lipid classes of sesame oil. *Food Research International*, **33**, 331-340.

Abu-Jdayil, B., Al-Malah, K., and Asoud, H. (2002). Rheological characterization of milled sesame (tehineh). *Food Hydrocolloides*, **16**, 55-61.

Adebowale, A. A., Sami, S. A., and Falore, O. A. (2011). Varietal difference in physical properties and proximate composition of Elite sesame seeds. *World Journal of Agricultural Sciences,* **1**, 42-46.

Ahmad, M., Ullah, K., Khan, M. A., Ali, S., Zafar, M., and Sultana, S. (2011). Quantitative and qualitative analysis of sesame oil biodiesel. *Energy Sources, Part A: Recovery, Utilization, and Environmental Effects*, **33**(13), 1239-1249.

Akbas, H., Sidim, T., and Iscan, M. (2003). Effect of polyoxyethylene chain length and electrolyte on the viscosity of mixed micelles. *Turkish Journal of Chemistry,* **27**(3), 357-364.

Ali, M. F., El Ali, B., and Speight, J. G. (2005). *Handbook of Industrial Chemistry: Organic Chemicals.* New York: McGraw-Hill Professional Publisher.

Alyemeni, M. N., Basahy, A. Y. and Sher, H., (2011). Physico-chemical analysis and mineral composition of some sesame seeds (*Sesamum indicum* L.) grown in the Gizan area of Saudi Arabia. *Journal of Medicinal Plants Research,* **5**(2), 270-274.

Anand, K., Sharma, R. P., and Pramod, S. M. (2011). A comprehensive approach for estimating thermo-physical properties of biodiesel fuels. *Applied Thermal Engineering*, **31**, 235-242.

AOCS (1998). *Official Methods and Recommended Practices of the American Oil Chemists' Society: Physical and Chemical Characteristics of Oils, Fats and Waxes.* 5th Edition, Champaign: American Oil Chemists' Society.

Aparicio, J., MacArthur, B. W., Sheats, W. B., and Brooks, B. J. (2012). MES -Myths, Mysteries and Perspectives on Properties and Use. *Journal of Detergent and Cosmetics*, **35**(4).

ASTM (2008). *ASTM Standard specification for diesel fuel oil, biodiesel blend*. West Conshohocken: ASTM International press.

Attwood, D., and Florence, A. T. (2012). *Physical Pharmacy*; *FAST track Series:* 2ND Ed. London: Pharmaceutical Press.

Awang, M., and Seng, G. M. (2008). Sulfonation of phenols extracted from the pyrolysis oil of oil palm shells for enhanced oil recovery. *ChemSusChem*, **1**(3), 210-214.

Aydin, F., Kafadar, A. B., Erdogan, S., Saydut, A., Kaya, C., and Hamamci, C. (2011). The basic properties of trans-esterified corn oil and biodiesel-diesel blends. *Energy Sources, Part A: Recovery, Utilization, and Environmental Effects*, **33**(8), 745-751.

Bail, S., Stuebiger, G., Unterweger, H., Buchbauer, G., and Krist, S. (2009). Characterization of volatile compounds and triacylglycerol profiles of nut oils

using SPME-GC-MS and MALDI-TOF-MS. *European journal of lipid science and technology*, **111**(2), 170-182.

Banno, T., Kawada, K., and Matsumura, S. (2010). Creation of novel green and sustainable gemini-type cationics containing carbonate linkages. *Journal of surfactants and detergents*, **13**(4), 387-398.

Barison, A., Pereira da Silva, C. W., Campos, F. R., Simonelli, F., Lenz, C. A., and Ferreira, A. G. (2010). A simple methodology for the determination of fatty acid composition in edible oils through ^{1}H NMR spectroscopy. *Magnetic Resonance in Chemistry*, **48**(8), 642-650.

Barnwal, B. K. and Sharma, M. P. (2005). Prospects of biodiesel production from vegetable oils in India. *Renewable and sustainable energy reviews*, **9**(4), 363-378.

Baydar, H., Turgut, I., and Turgut, K. (1999). Variation of certain characters and line selection for yield, oil, oleic and linoleic acids in the Turkish sesame (*Sesamum Indicum L*.) Populations. *Turkish journal of agriculture and forestry*, **23**, 431-441.

Bedigian, D. (2004). History and lore of sesame in Southwest Asia. *Economic botany*, **58**, 329-353.

Bergström, L. M. (2011). Thermodynamics of self-assembly. *Application of Thermodynamics to Biological and Material Science*, 289-314.

Bhave, N. A., Ugare, V. M., and Andhare, A. M. (2013). Performance and Emission Studies of Sesame Oil Methyl Ester in Compression Ignition Engine. *International Journal of Emerging Technology and Advanced Engineering*, **3**(5), 344-352.

Borchani, C., Besbes, S., Blecker, C., and Attia, H. (2010). Chemical characteristics and oxidative stability of sesame seed, sesame paste, and olive oils. *Journal of Agricultural Science and Technology*, **12,** 585-596.

Carretti, E., Dei, L., and Baglioni, P., (2003). Solubilisation of acrylic and vinyl polymers in nano container solutions. Application of micro-emulsions and micelles to Cultural Heritage conservation. *Langmuir*, **19**, 7867-7872.

Chung, J., Lee, J., and Choe, E. (2004). Oxidative stability of soybean and sesame oil mixture during frying of flour dough. *Journal of food science*, **69**(7), 574-578.

Cohen, L., Soto, F., Luna, M. S., Pratesi, C. R., Cassani, G., and Faccetti, L. (2003). Analysis of sulfoxylated methyl esters (Φ-MES): Sulfonic acid composition and isomer identification. *Journal of surfactants and detergents*, **6**(2), 151-154.

Cohen, L., Soto, F., Melgarejo, A., and Roberts, D. W. (2008). Performance of Φ-Sulfo Fatty Methyl Ester Sulfonate Versus Linear Alkylbenzene Sulfonate, Secondary Alkane Sulfonate and α-Sulfo Fatty Methyl Ester Sulfonate. *Journal of Surfactants and Detergents*, **11**(3), 181-186.

De, S., and Mondal, S. (2012). Micellar Enhanced Ultrafiltration: Fundamentals and Applications. New York: CRC Press.

Demirbas, A. (2000). Conversion of biomass using glycerine to liquid fuel for blending gasoline as alternative engine fuel. *Energy Conversion and Management*, **41**, 1741-1748.

Demirbas, A. (2007). Comparison of trans-esterification methods for production of biodiesel from vegetable oils and fats. *Energy Conversion and Management*, **49**, 125-130.

Demirbas, A. (2008a). Comparison of trans-esterification methods for production of biodiesel from vegetable oils and fats. *Energy Conversion and Management*, **49**(1), 125-130.

Demirbas, A. (2008b). Relationships derived from physical properties of vegetable oil and biodiesel fuels. *Fuel,* **87**, 1743-1748.

Dincer, K. (2008). Lower emissions from biodiesel combustion. *Energy Source Part A,* **30**, 963-8.

Donnell, O.S., Demshemino, I., Yahaya, M., Nwadike, I., and Okoro, L. (2013). A review on the Spectroscopic Analyses of Biodiesel. *European International Journal of Science and Technology*, **2**(7), 137-146.

El Khier, M. K. S., Ishag, K. E. A., and Yagoub, A. E. A. (2008). Chemical Composition and Oil Characteristics of Sesame Seed Cultivars Grown in Sudan. *Journal of Agriculture and Biological Sciences,* **4**(6), 761-766.

Fadzlillah, N. A., Che Man, Y. B., and Rohman, A. (2014). FTIR Spectroscopy Combined with Chemometric for Analysis of Sesame Oil Adulterated with Corn Oil. *International Journal of Food Properties*. **17**(6), 1275-1282.

Farn, R. J. (2008). *Chemistry and Technology of Surfactants.* Oxford: Blackwell Publisher.

Fendler, J. (2012). *Catalysis in micellar and macromoleular systems*. Massachusetts: Academic Press, Elsevier.

Ferdous, K., and Uddin, M. R. (2012). Biodiesel from Sesame oil: Base catalysed Trans-esterification. *International Journal of Engineering and Technology*, **1**(4), 420-431.

Garnica, J. A. G., Da Silva, N. L., and Wolf Maciel, M. R. (2009). Production and purification of biodiesel and glycerine. *Chemical Engineering Transactions*, **17**, 433-438.

Garrier, E., and Packet, D. (2012). 11-Catalytic conversion of oils extracted from seeds: from polyunsaturated long chains to functional molecules. In Aresta, M., Dibenedetto, A., and Dumeignil, F. (Eds.). *Biorefinery: From Biomass to Chemicals and Fuels* (pp 263-276). Berlin: Walter de Gruyter.

Gomez, N. A., Abonia, R., Cadavid, H., and Vargas, I. H. (2011). Chemical and spectroscopic characterization of a vegetable oil used as dielectric coolant in distribution transformers. *Journal of the Brazilian Chemical Society*, **22**(12), 2292-2303.

Goyal, P. S., and Aswal, V. K. (2001). Micellar structure and inter-micelle interactions in micellar solutions: results of small angle neutron scattering studies. *Current Science-Bangalore.*, **80**(8), 972-979.

Guillen, M. D., and Cabo, N. (1997). Characterization of edible oils and lard by Fourier transform infrared spectroscopy. Relationships between composition and frequency of concrete bands in the fingerprint region. *Journal of the American Oil Chemists' Society*, **74**(10), 1281-1286.

Guillén, M. D., and Ruiz, A. (2003). Rapid simultaneous determination by proton NMR of unsaturation and composition of acyl groups in vegetable oils. *European journal of lipid science and technology*, **105** (11), 688-696.

Gulla, S., and Waghray, K. (2011). Effect of Storage on Physico-chemical Characteristics and Fatty Acid Composition of Selected Oil Blends. *Journal of Life Sciences*, **3**, 35-46.

Hawtin, G. (2007). Underutilized plant species research and development activities–review of issues and options. *GFU/ICUC. International Plant Genetic Resources Institute, Rome, Italy*.

Herskowitz, M., Landau, M., Reizner, I., and Kaliya, M. (2012). *Production of diesel fuel from vegetable and animal oils. U.S. Patent No. 8,142,527*. Washington, DC: U.S. Patent and Trademark Office.

Hill, K. (2000). Fats and oils as oleo-chemical raw materials. *Pure and applied chemistry*, **72**(7), 1255-1264.

Holmberg, K. (2002). *Handbook of Applied Surface and Colloid Chemistry.* Vol. (1-2). West Sussex: John Wiley & Sons.

Holmberg, K. (Ed.). (2003). *Novel Surfactants: Preparation Applications and Biodegradability, Revised And Expanded*. New York: CRC Press.

Holmberg, K., Lindman, B., Jonsson, B., and Kronberg, B. (2003). *Surfactants and Polymers in Aqueous Solution.* 2nd Ed. West Sussex: John Wiley & Sons.

Holser, R. (2005). *Synthesis of surfactants from vegetable oil feedstocks*. In, Erhan, S.Z (Ed.) (2005) *Industrial Uses of Vegetable Oils* (p170), Champaign: AOCS Press.

Hummel, D. O. (2000). *Handbook of surfactant analysis: chemical, physicochemical, and physical methods*. New York: John Wiley.

Jakab, A., Nagy, K., Heberger, K., Vekey, K., and Forgacs, E. (2002). Differentiation of vegetable oils by mass spectrometry combined with statistical analysis. *Rapid communications in mass spectrometry*, **16**(24), 2291-2297.

Kahyaoglu, T., and Kaya, S. (2006). Modelling of moisture, colour and texture changes in sesame seeds during the conventional roasting. *Journal of Food Engineering*, **75**,167-177.

Kinney, A. J. and Clemente, T. E. (2005). Modifying soybean oil for enhanced performance in biodiesel blends. *Fuel Process Technol.*, **86**, 1137-1147.

Kirk-Othmer, (2012). *Kirk-Othmer Chemical Technology of Cosmetics*. New York: John Wiley.

Kjellin, M., and Johansson, I. (Eds.). (2010). *Surfactants from Renewable Resources*. London: John Wiley & Sons.

Knothe G. (2005). Dependence of biodiesel fuel properties on the structure of fatty acid alkyl esters. *Fuel Processing Technology*, **86**, 1059-1070.

Knothe, G. (2006). Analyzing biodiesel: standards and other methods. *Journal of the American Oil Chemists' Society*, **83**(10), 823-833.

Knothe, G., and Steidley, K. R. (2005). Kinematic viscosity of biodiesel fuel components and related compounds. Influence of compound structure and comparison to petro-diesel fuel components. *Fuel*, **84**(9), 1059-1065.

Knothe, G., Gerpen, J. V. and Krahl, J. (2005). *The Biodiesel Handbook.* Champaign, IL: AOCS Press.

Koca, H., Bor, M., Ozdemir, F., and Turkan, I. (2007). The effect of salt stress on lipid peroxidation, antioxidative enzymes and proline content of sesame cultivars. *Environmental and Experimental Botany*, **60**(3), 344– 351.

Könnecker, G., Regelmann, J., Belanger, S., Gamon, K., and Sedlak, R. (2011). Environmental properties and aquatic hazard assessment of anionic surfactants: Physicochemical, environmental fate and eco-toxicity properties. *Ecotoxicology and environmental safety*, **74**(6), 1445-1460.

Larson, R. A., and Marley, K. A., (2011). *Optimized Antioxidants for Biodiesel*. Champaign, IL: Illinois Sustainable Technology Centre.

Liauw, M. Y., Natan, F. A., Widiyanti, P., Ikasari, D., Indraswati, N. and Soetaredjo, F. E. (2008). Extraction of Neem Oil (A*zadirachta indica A. Juss*) Using n-Hexane and Ethanol: Studies of Oil Quality, Kinetic and Thermodynamic. *Journal of Engineering and Applied Sciences,* **3**, 3.

Lim, T. K. (2012). *Edible Medicinal and Non-Medicinal Plants*: *Fruits* (Vol. 4). New York: Springer.

Lim, W. H., and Ramle, R. A. (2009). The Behaviour of Methyl Esters Sulphonate at the Water–Oil Interface: Straight-Chained Methyl Ester from Lauryl to Stearyl as an Oil Phase. *Journal of Dispersion Science and Technology*, **30**(1), 131-136.

Manne, S., and Patterson L. K. (2003). *Micelles: Encyclopaedia of Physical Science and Technology.* 3rd Ed (pp 661-677). New York: Academic Press.

Math, M. C., Kumar, S. P. and Chetty, S. V. (2010). Technologies for biodiesel production from used cooking oil -A review. *Energy for Sustainable Development*, **14**, 339-345.

Maurad, Z. A., Ghazali, R., Siwayanan, P., Ismail, Z., and Ahmad, S. (2006). Alpha-sulfonated methyl ester as an active ingredient in palm-based powder detergents. *Journal of surfactants and detergents*, **9**(2), 161-167.

Mazzanti, C. (2008). Introduction: Surfactants from Biorenewable Sources. *Bio-renewable Sources*, **5**.

Meher, L. C., Sagar D. V. and Naik, S. N. (2006). Technical aspects of biodiesel production by trans-esterification-a review. *Renewable Sustainable Energy Review,* **10**, 248-68.

Mehta, S. K., Bhasin, K. K., Chauhan, R., and Dham, S. (2005). Effect of temperature on critical micelle concentration and thermodynamic behaviour of dodecyldimethylethylammonium bromide and dodecyltrimethylammonium chloride in aqueous media. *Colloids and Surfaces A: Physicochemical and Engineering Aspects,* **255**(1), 153-157.

Mohammed, M. I. and Hamza, Z. U. (2008). Physicochemical Properties of Oil Extracts from *Sesamum Indicum* L. Seeds Grown in Jigawa State Nigeria. *Journal of Applied Sciences and Environmental Management,* **12**(2), 99 -101.

Mojtaba, M., and Ahmad, S., (2012). Effect of mixture of alcohols on biodiesel properties which produced from waste cooking oils and compare combustion performance and emissions of biodiesels with petro-diesel. *Advances in Environmental Sciences*, **4**(3).

Murugesan, A., Umarani, C., Subranmanina, R. and Neduchezhian, N. (2009). Biodiesel as an alternative fuel for diesel engines-a review. *Renewable Sustainable Energy Review,* **13**, 653-62.

Myers, D., (2005). *Surfactant science and technology*. 3RD ED. New York: John Wiley & Sons.

Nagi, J., Nagi, F., and Ahmed, S.K (2008). Palm biodiesel an alternative green renewable energy for the energy demands of the future. In *International Conference on Construction and Building Technology, ICCBT* (pp. 79-94).

Narayanan, R. (2008). *Interfacial Process and Molecular Aggregation of Surfactants*: *Advances in Polymer Science.* Vol. 218, p26. New York: Springer.

Nzikou, J. M., Matos, L., Bouanga-Kalou, G., Ndangui, C. B, Pambou-Tobi, N. P. G., Kimbonguila, A., Silou, Th., Linder, M. and Desobry, S. (2009). Chemical Composition on the Seeds and Oil of Sesame (*Sesamum indicum* L.) Grown in Congo-Brazzaville. *Advance Journal of Food Science and Technology*, **1**(1), 6-11.

Okano, T., Tamura, T., Nakano, T. Y., Ueda, S. I., Lee, S., and Sugihara, G. (2000). Effects of side chain length and degree of counter-ion binding on micellization of sodium salts of α-myristic acid alkyl esters in water: a thermodynamic study. *Langmuir*, **16**(8), 3777-3783.

Onginjo, E. O., and Ayiecho, P. O., (2009). Genotypic variability in sesame mutant lines in Kenya. *African crop science journal*, **17**(2).

OriginLab Corporation, US. Origin 6.0: Scientific Data Analysis and Graphing Software Origin Lab Corporation (formerly Microcal Software, Inc.). Web site: www. originlab. com. Commercial price: 595.Academicprice: 446. *Journal of the American Chemical Society*, **122**(39), 9567-9568.

Ozawa, Y., Soma, Y., Shoji, H., Iijima, A., and Yoshida, K. (2011). The Application of Coconut Oil Methyl Ester for Diesel Engine. *International Journal of Automotive Engineering*, **2**, 95-100.

Pasquali, M. (2010). Gelation: Grow with the flow. *Nature materials*, **9**(5), 381-382.

Pedro F.M., Correis J. N., Raposo I., Joao M. F., Berkemeier R., and Bordado J.M., (2006). Production of biodiesel from waste frying oils. *Waste Management*, **26**, 487-94.

Prabha, D. R., Santhaanalakshmi J., and Arun Prasath R. (2013). Analysis of micellar behaviour of a synthesized sodium itaconate monoesters with various hydrophobic chain lengths in aqueous media. *Research Journal of Chemistry Sciences*, **3**(12), 43-49.

Rahman, M. S., Hossain, M. A., Ahmed, G. M., and Uddin, M. M. (2007). Studies on the characterization, lipids and glyceride compositions of Sesame (Sesamum indicum linn.) Seed Oil. *Bangladesh Journal of Scientific and Industrial Research*, **42**(1), 67-74.

Raja, S. A., Smart, D. R., and Robert Lee, C. L. (2011). Biodiesel production from Jatropha oil and its characterization. *Research Journal of Chemical Sciences*, **1**(1), 1-7.

Ramadhas, A. S., Jayaraj, S., Muraleedharan, C. and Padmakumari, K. (2006). Artificial neural networks used for the prediction of the cetane number of biodiesel. *Renewable Energy*, **31**, 2524-2533.

Ramos, M. J., Fernandez, C. M., Casas, A., Rodriguez, L. and Perez, A. (2009). Influence of fatty acid composition of raw materials on biodiesel properties. *Bioresource Technology*, **100**, 261-268.

Rangel-Yagui, C. O., Pessoa Jr, A., and Tavares, L. C. (2005). Micellar solubilization of drugs. *J Pharm Pharm Sci*, **8**(2), 147-163.

Rosen, M. J., and Kunjappu, J. T. (2012). *Surfactants and interfacial phenomena*. 4th Ed. New York: John Wiley & Sons.

Salih, N., Salimon, J., and Yousif, E. (2011). Synthesis of oleic acid based esters as potential basestock for biolubricant production. *Turkish Journal of Engineering and Environmental Sciences*, **35**(2), 115-123.

Saydut, A., Duz, M. Z., Kaya, C., Kafadar, A. B. and Hamamci, C. (2008). Trans esterified sesame (*Sesamum indicum L.*) seed oil as a biodiesel fuel. *Bioresource Technology.*, **99**, 6656-6660.

Schmitt, T. M. (2001). *Analysis of surfactants*.2nd Ed. New York: CRC Press.

Schramm, L. L., Stasiuk, E. N. and Marangoni, D. G. (2003). Surfactants and their applications. *Annual Reports Section" C" (Physical Chemistry)*, **99**, 3-48.

Segar G. H., Arunagirinathan, M. A. and Bellare, J. R. (2007). Self- assembled surfactant nano-structures important in drug delivery- A review. *Indian journal of experimental biology*, **45**,133-159.

Sekhar, M. C., Mamilla, V. R., Reddy, K. V. and Narayana, G. L. (2010). Synthesis of Biodiesel. *International Journal of Engineering Science and Technology*, **2**(8), 3936-3941.

Shyu, Y. S., and Hwang, S. L. (2002). Anti-oxidative activity of the crude extract of lignan glycosides from unfrosted Bruma black sesame meal. *Food Research International*, **35**, 357-365.

Silverstein, R., and Webster, F. (2006). *Spectrometric identification of organic compounds*. New York: John Wiley & Sons.

Singh, S. P., and Singh, D. (2010). Biodiesel production through the use of different sources and characterization of oils and their esters as the substitute of diesel: a review. *Renewable and Sustainable Energy Reviews*, **14**(1), 200-216.

Somasundaran, P. (Ed.), (2006). *Encyclopaedia of surface and colloid science*. Vol.1. New York: CRC Press.

Srivastava, A. and Prasad, R. (2000). Triglycerides-based diesel fuels. *Renewable and Sustainable Energy Reviews*, **4**, 111-133.

Suja, K.P., Abraham, J. T., Thamizh, S. N., Jayalekshmy, A. and Arumughan, C. (2004). Antioxidant efficacy of sesame cake extract in vegetable oil protection. *Food chemistry*, **84**(3), 393-400.

Svenson, S. (2004). Controlling surfactant self-assembly. *Current opinion in colloid & interface science*, **9**(3), 201-212.

Tadros, T. F. (2005). *Applied Surfactants: Principles and Applications.* Weinheim: John Wiley & Sons-VCH.

Tariq, M., Ali, S., Ahmad, F., Ahmad, M., Zafar, M., Khalid, N., and Khan, M. A. (2011). Identification, FT-IR, NMR (^{1}H and ^{13}C) and GC/MS studies of fatty acid methyl esters in biodiesel from rocket seed oil. *Fuel Processing Technology,* **92**(3), 336-341.

Texter, J. (Ed.). (2001). *Reactions and Synthesis in Surfactant Systems*. Surfactant Science Vol. 100. London: CRC Press.

Wagutu, A. W., Chhabra, S. C., Thoruwa, C. L., Thoruwa, T. F., and Mahunnah , R. L. A., (2009). Indigenous Oil Crops as a Source for Production of Biodiesel in Kenya. *Bulletin of the Chemical Society of Ethiopia*, **23**(3), 359-370.

Wang, S. C., Wei, T. C., Chen, W. B., and Tsao, H. K. (2004). Effects of surfactant micelles on viscosity and conductivity of poly (ethylene glycol) solutions. *The Journal of chemical physics,* **120**(10), 4980-4988.

Were, B. A., Onkware, A. O., Gudu, S., Welander, M. and Carlsson, A. S. (2006). Seed oil content and fatty acid composition in East African sesame (*Sesamum indicum L.)* Accessions evaluated over 3 years, Kenya. *Field Crops Research*, **97**, 254-260.

Wool, R. P. (2008). Biobased Materials and Bioenergy. *Journal of Biobased Materials and Bioenergy*, **2**,181.

Yao, L. (2009). Synthesis of fatty acid derivatives as potential biolubricants and their physical properties and boundary lubrication performances. Graduate dissertation, Iowa State University.

Zana, R. (2005). *Dynamics of Surfactant Self-assemblies: Micelles, Microemulsions, Vesicles, and Lyotropic Phases*. Vol. 125. New York: CRC Press.

Zhang, W. B. (2012). Review on analysis of biodiesel with infrared spectroscopy. *Renewable and Sustainable Energy Reviews*, **16**(8), 6048-6058.

Zhang, Y., Dube, M.A., Mclean, D.D. and Kates, M., (2003). Biodiesel production from waste cooking oil: 1.Process design and technological assessment. *Bioresource Technology*, **89**, 1-16.

APPENDICES

Appendix I: Chemicals and reagents used in the study

Chemical	Uses
Solvents - n-hexane - Diethyl-ether - Chloroform - Petroleum ether - Acetone - Carbon tetrachlorometane - Methanol - Ethanol - Propanol - Diethyl acetate - Pyridine - Butanol - Distilled/double distilled H_2O	- Extraction - Calibration - Cleaning
Acids -HNO_3 -HCl -H_2SO_4 -H_3PO_4 -Chlorosulphonic acid ($ClHSO_3$) - Hydrogen peroxide (H_2O_2) - Glacial acetic acid ($C_2H_4O_2$) - Formic acid (CH_2O_2)	- Cleaning and in reaction processes
Bases -NaOH -KOH	- Used as catalysts and neutralization processes
Salts -KCl -KI -NaCl -Na_2SO_4 -$Na_2S_2O_8$ -$NaHCO_3$ -(SDS)-$C_{12}H_{25}NaSO_4$	- Calibration - used to make standards/ stock solutions - used in reaction processes
Reagents Wijis reagent	- used to determine iodine value
Indicators Phenolphthalein Starch indicator Litmus paper	- Used in titration reactions - used to determine acidity or basicity of products

Appendix II (a): Specific conductivity versus concentration data of SDS

Sodium Dodecyl Sulphate					
Concentration (wt %)	**Concentration** (mol/L)	Specific conductivity *k* ($mScm^{-1}$) at a given Temperature (K)			
		298.15	**303.15**	**313.15**	**323.15**
0.034	1.189×10^{-3}	0.800	0.810	1.100	1.560
0.083	2.886×10^{-3}	1.720	1.750	2.200	2.590
0.171	5.594×10^{-3}	3.500	3.600	4.100	4.400
0.196	6.790×10^{-3}	4.080	4.100	4.600	4.890
0.220	7.639×10^{-3}	4.400	4.600	5.100	5.410
0.236	8.195×10^{-3}	4.531	4.740	5.300	5.799
0.255	8.823×10^{-3}	4.690	4.920	5.500	6.150
0.288	1.000×10^{-3}	4.900	5.170	5.760	6.370
0.337	1.170×10^{-2}	5.200	5.500	6.090	6.690
0.400	1.390×10^{-2}	5.600	5.920	6.580	7.200
0.500	1.930×10^{-2}	6.320	6.620	7.298	7.890
0.600	2.600×10^{-2}	6.950	7.250	7.990	8.660
0.750	3.470×10^{-2}	7.950	8.250	9.030	9.830

Appendix II (b): Specific conductivity versus concentration data of SEFAMESO surfactant

SEFAMESO					
Concentration (wt %)	**Concentration** (mol/L)	**Specific conductivity *k* ($mScm^{-1}$) at a given Temperature (K)**			
		298.15	**303.15**	**313.15**	**323.15**
0.0034	2.869×10^{-5}	2.000	3.0488	3.963	4.556
0.0083	7.004×10^{-5}	3.839	4.794	5.494	6.358
0.0118	9.957×10^{-5}	5.246	6.140	6.703	7.487
0.0141	1.189×10^{-4}	6.089	6.878	7.533	8.312
0.0171	1.144×10^{-4}	7.237	7.835	8.682	9.365
0.0196	1.654×10^{-4}	7.497	8.173	9.064	10.037
0.0220	1.857×10^{-4}	7.838	8.568	9.512	10.412
0.0236	1.992×10^{-4}	8.002	8.792	9.701	10.716
0.0255	2.152×10^{-4}	8.230	9.129	10.148	11.166
0.0288	2.430×10^{-4}	8.568	9.581	10.661	11.839
0.0337	2.844×10^{-4}	9.230	10.366	11.551	12.816
0.0400	1.001×10^{-4}	9.971	11.270	12.588	14.015
0.0500	4.219×10^{-4}	11.099	12.670	14.492	16.045
0.0600	5.063×10^{-4}	12.337	14.254	16.275	17.993
0.0750	6.329×10^{-4}	14.170	16.671	19.078	20.918

Appendix III (a): Specific viscosity versus the concentration data of SDS

Sodium Dodecyl Sulphate (SDS)					
Concentration (wt %)	**Concentration** (mol/L)	Specific Viscosity (n_{sp}) at a given Temperature (K)			
		298.15	**303.15**	**313.15**	**323.15**
0.034	1.189×10^{-3}	1.560	1.100	0.810	0.800
0.083	2.886×10^{-3}	2.590	2.200	1.750	1.720
0.171	5.594×10^{-3}	4.400	4.100	3.600	3.500
0.196	6.790×10^{-3}	4.890	4.600	4.100	4.080
0.220	7.639×10^{-3}	5.410	5.100	4.600	4.400
0.236	8.195×10^{-3}	5.799	5.300	4.740	4.531
0.255	8.823×10^{-3}	6.150	5.500	4.920	4.690
0.288	1.000×10^{-3}	6.370	5.760	5.170	4.900
0.337	1.170×10^{-2}	6.690	6.090	5.500	5.200
0.400	1.390×10^{-2}	7.200	6.580	5.920	5.600
0.500	1.930×10^{-2}	7.890	7.298	6.620	6.320
0.600	2.600×10^{-2}	8.660	7.990	7.250	6.950
0.750	3.470×10^{-2}	9.830	9.030	8.250	7.950

Appendix III (b): Specific Viscosity versus the Concentration of Data SEFAMESO surfactant.

SEFAMESO					
Concentration (wt %)	**Concentration** (mol/L)	Specific Viscosity (n_{sp}) at a given Temperature (K)			
		298.15	**303.15**	**313.15**	**323.15**
0.0034	2.869×10^{-5}	2.297	2.098	1.829	1.667
0.0083	7.004×10^{-5}	2.300	2.131	1.884	1.690
0.0118	9.957×10^{-5}	2.400	2.161	1.912	1.700
0.0141	1.189×10^{-4}	2.466	2.225	1.969	1.717
0.0171	1.144×10^{-4}	2.534	2.290	2.024	1.756
0.0196	1.654×10^{-4}	3.040	2.689	2.278	1.941
0.0220	1.857×10^{-4}	3.513	3.189	2.785	2.307
0.0236	1.992×10^{-4}	3.919	3.511	3.080	2.616
0.0255	2.152×10^{-4}	4.324	3.973	3.561	3.066
0.0288	2.430×10^{-4}	4.998	4.614	4.163	3.713
0.0337	2.844×10^{-4}	6.046	5.648	5.176	4.669
0.0400	1.001×10^{-4}	7.430	6.968	6.444	5.996
0.0500	4.219×10^{-4}	9.526	9.000	8.583	7.937

Appendix IV: Comparison of Fuel properties of SEFAMEs biodiesel with Other Biodiesels and petroleum diesel in literature

Vegetable Oil Methyl Esters	**Density** at 15-25 ^oC (kg m^{-3})	**Kinematic viscosity** at 40 ^oC (mm^2/s)	**Flash point** (^oC)	**Pour point** (^oC)	**Cloud point** (^oC)	**Cetane number**	**Calorific Value** (kJ/kg)
Jatropha	840	4.82	128	-2	8	-	4280[a]
	877.4	4.43	147.4	-	-	55.03	4075[b]
Corn	864.2	4.0694	168	-30	-15	52.48	3992[c]
Peanut	883	4.9	176	-	5	54	3360[d]
Coconut	870	3	118		-3	51	3781[e]
Olive oil	860	4.18	174	-	-	-	4135[f]
Soya bean	885	4.5	178	-7	1	45	3350[d]
Palm	855	4.5	174	16	16	65	4013.5[g]
	880	5.7	164	-	13	62	3350[d]
Sunflower	884	3.6	170	-7	-5	49.2	3858[h]
Cotton seed oil	871	3.75	172	-	-	-	4118[f]
Rapeseed	857	4.60	180	-	-	-	4155[f]
Sesame	880	3.04	143	-	-	-	4090[f]
	867.2	4.20	170	-14	-6	50.48	4040[i]
	850	5.47	185	-8	-5	40	3460[j]
	870	3.60	162	-9.5	-19	-	4021[k]
Present study Sesame biodiesel	**840**	**4.10**	**160**	**-8**	**-6**	**50**	**3950**
Biodiesel ASTM STD.	880 -900	1.9-6.0	100-170	-15 to 10	-3 to 12	47-65	≈3800[l,m]
Petroleum Diesel ASTM STD.	826-860	1.3-4.1	60 -80	-35 to -15	-15 to 5	40-55	4200-4500[l,m]

Source: ([a]Raja *et al.,* 2011; [b]Wagutu *et al.,* 2009; [c]Aydin *et al.,* 2011; [d]Barnwal and Sharma, 2005; [e]Ozawa *et al.,* 2011; [f]Demibras, 2008b; [g]Nagi *et al.,* 2008; [h]Mojtaba and Ahmad, 2012; [i]Saydut *et al.,* 2008; [j]Ferdous and Uddin, 2012; [k]Bhave *et al.,* 2013; [l]Singh and Singh, 2010; [m]Herskowitz *et al.,* 2012).

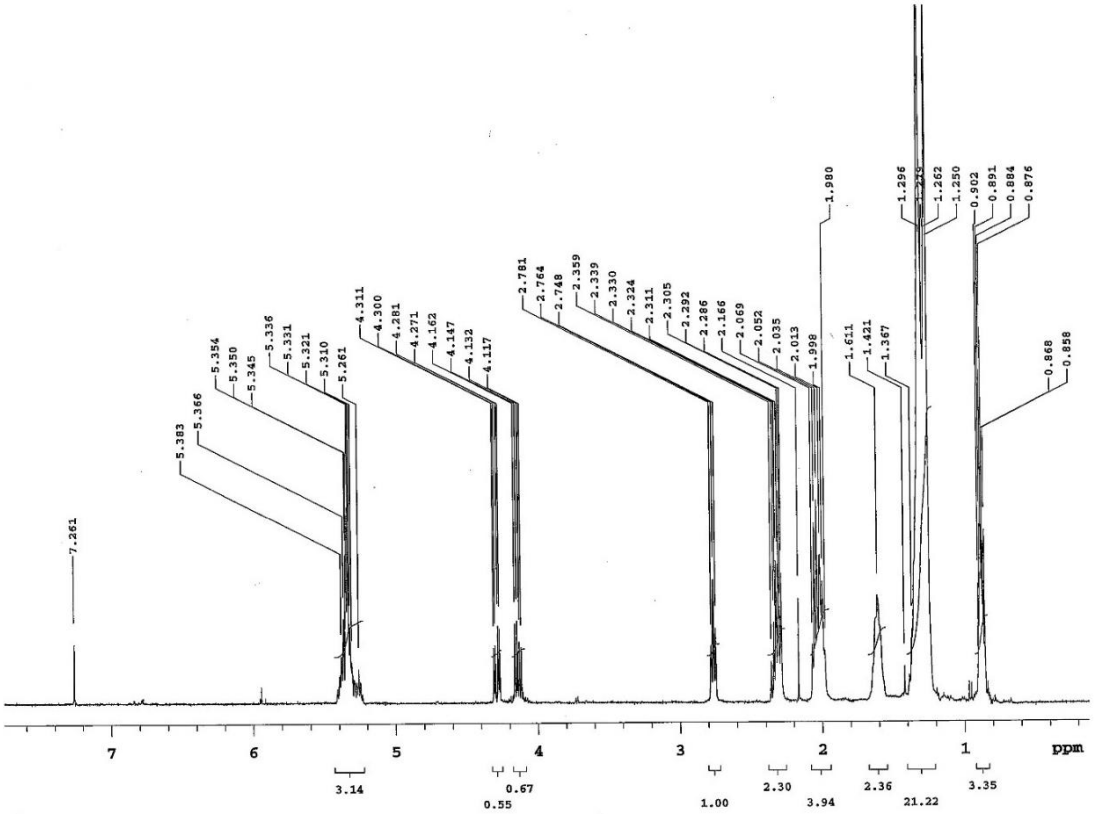

Appendix V (a): ^{1}H-NMR spectrum of Sesame oil (chemical shifts (δ) range 0.000-8.000 ppm).

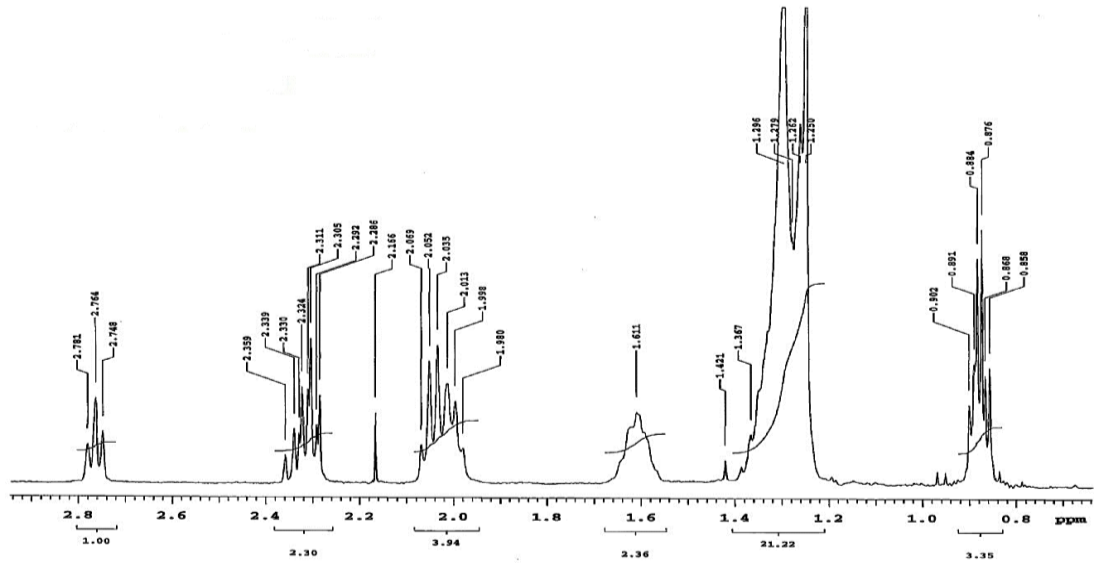

Appendix V (b): ^{1}H-NMR spectrum of sesame oil (chemical shift (δ) range 0.000-3.000 ppm).

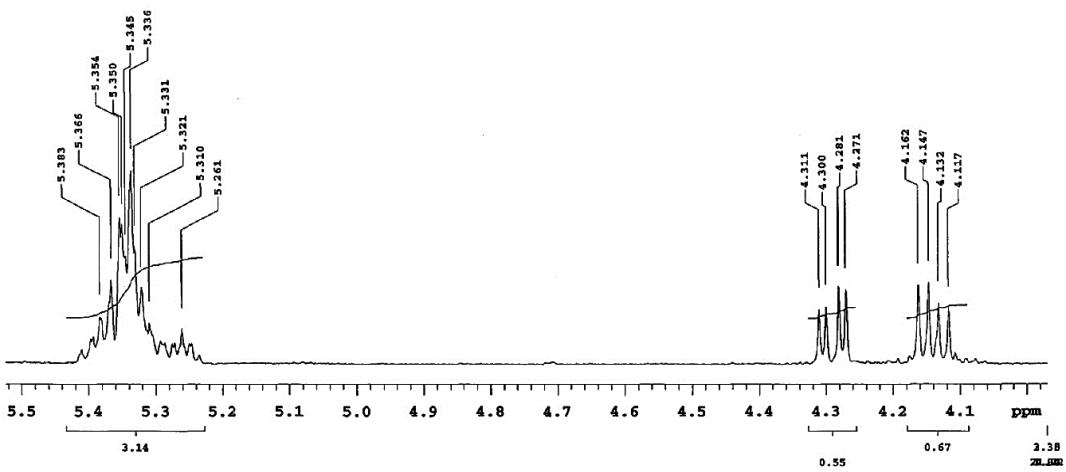

Appendix V (c): ^{1}H-NMR spectrum of sesame oil (chemical shift (δ) range 4.000-6.000 ppm).

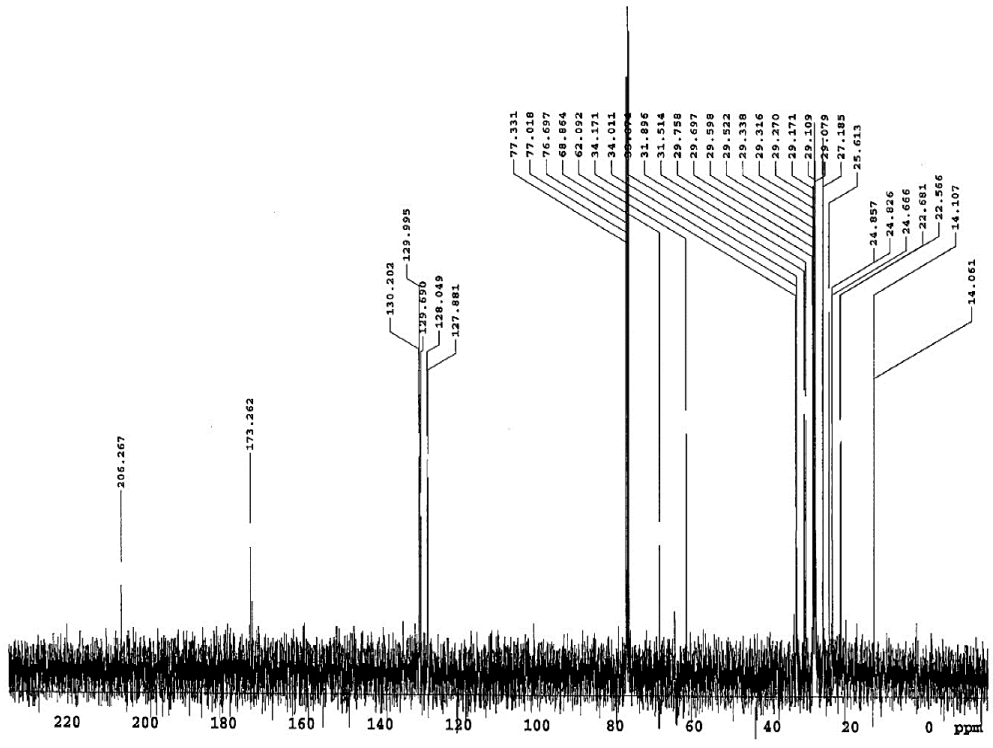

Appendix V (d): ^{13}C-NMR spectrum of sesame oil (chemical shift (δ) range 0.000-250 ppm).

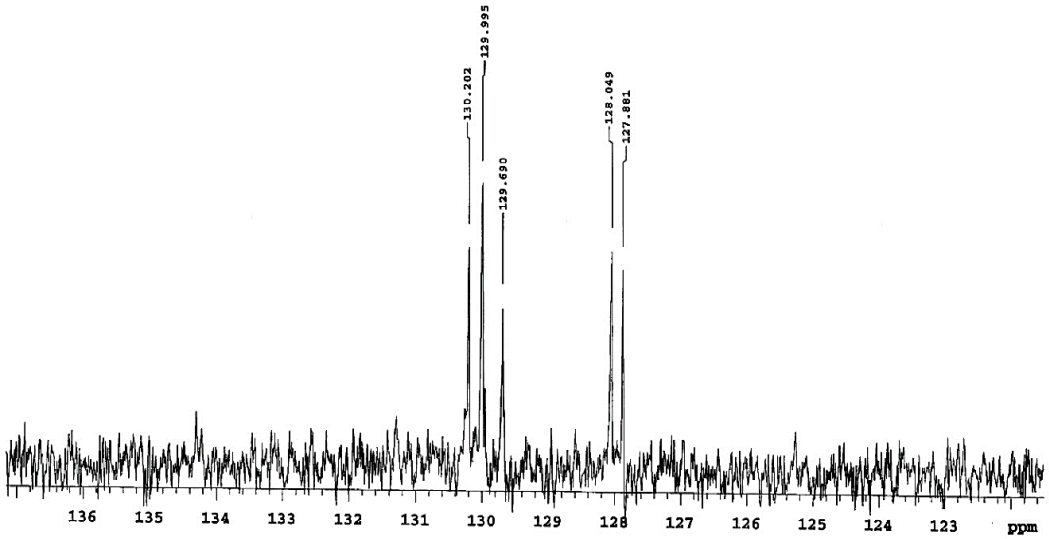

Appendix V (e): ^{13}C-NMR spectrum of sesame oil (chemical shift (δ) range 100-150 ppm).

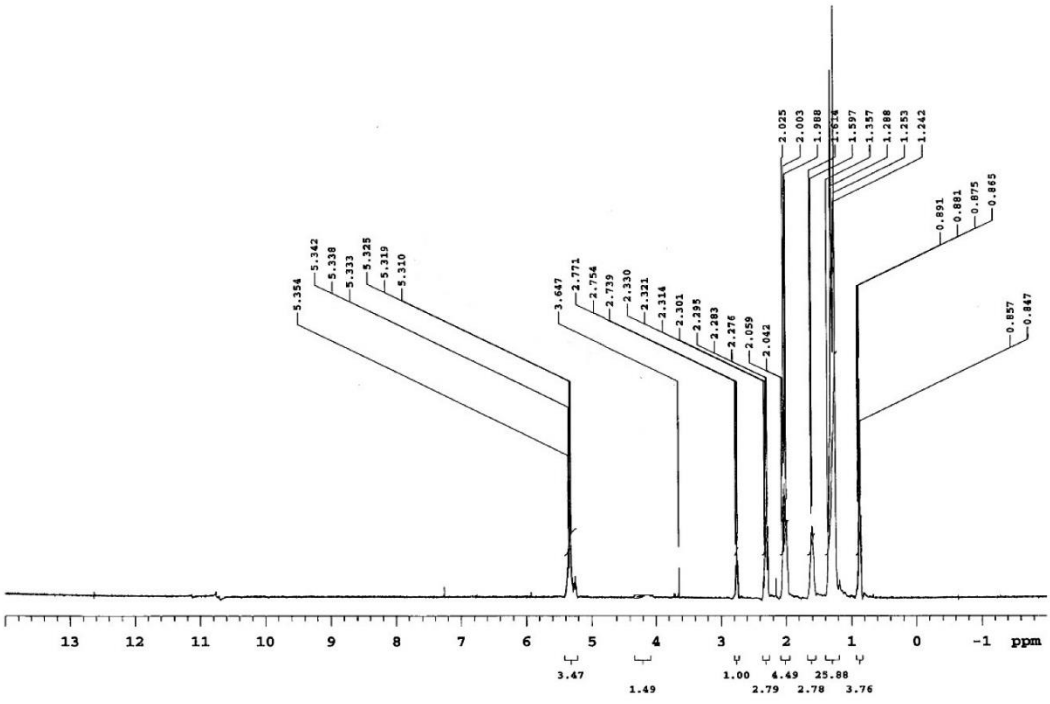

Appendix VI (a): ^{1}H-NMR spectrum of SEFAMEs biodiesel (chemical shift (δ) range-1.000-13.000 ppm).

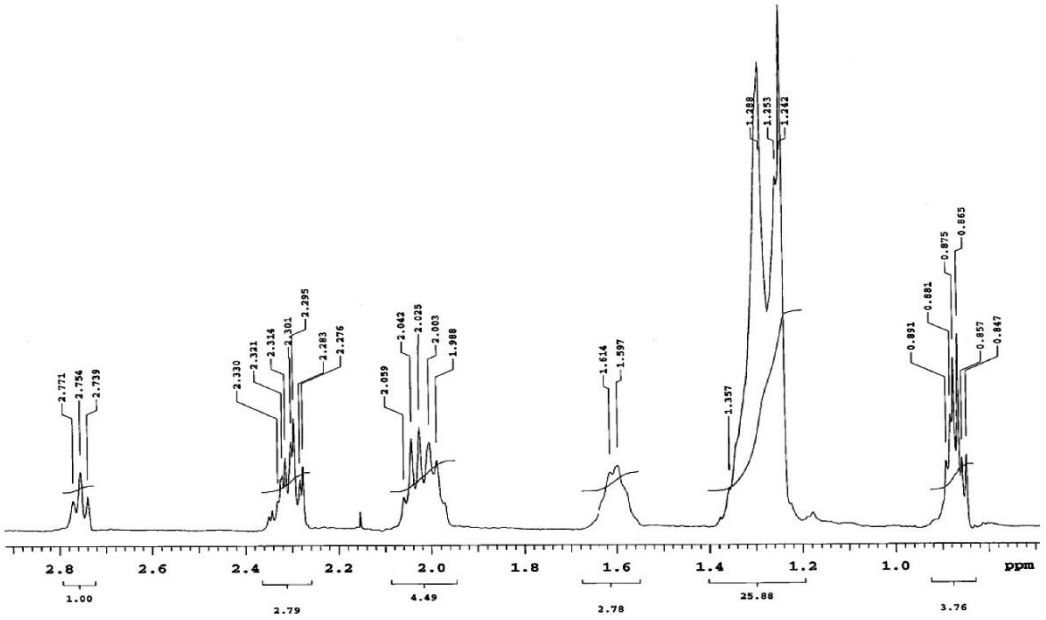

Appendix VI (b): ^{1}H-NMR spectrum of SEFAMEs biodiesel (chemical shift (δ) range 0.000-3.000 ppm).

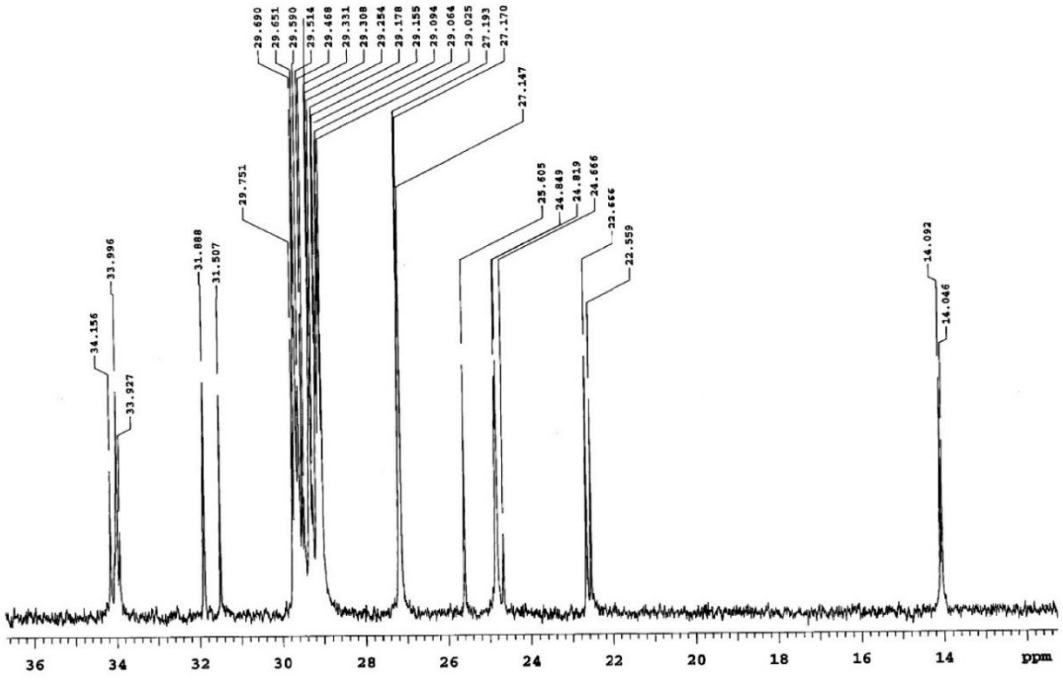

Appendix VI (c): ^{13}C-NMR spectrum of SEFAMEs biodiesel (chemical shift (δ) range 0.000-40.000 ppm).

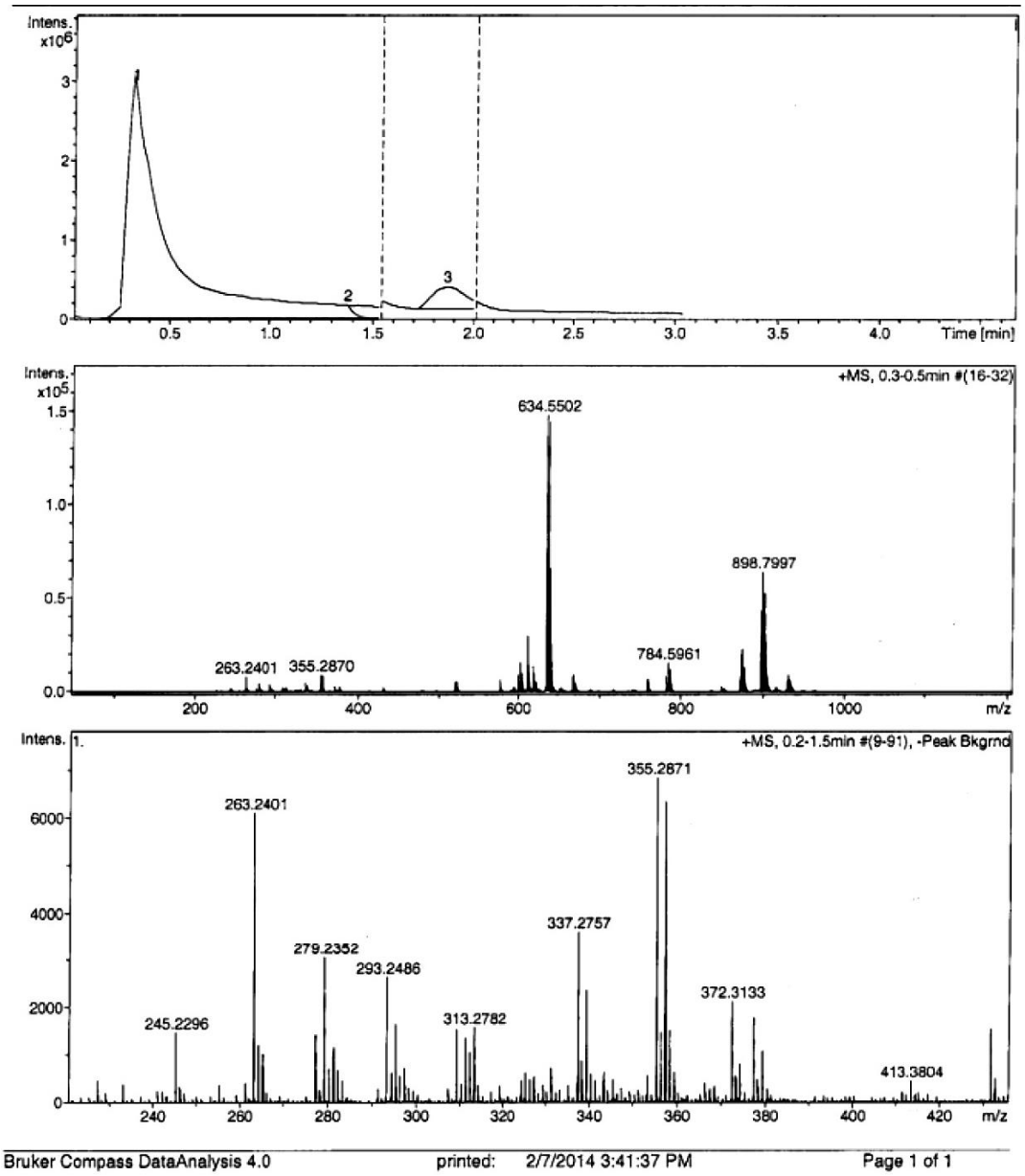

Appendix VII (a): HPLC-MS spectrum of Sesame oil (0-950 *m/z*)

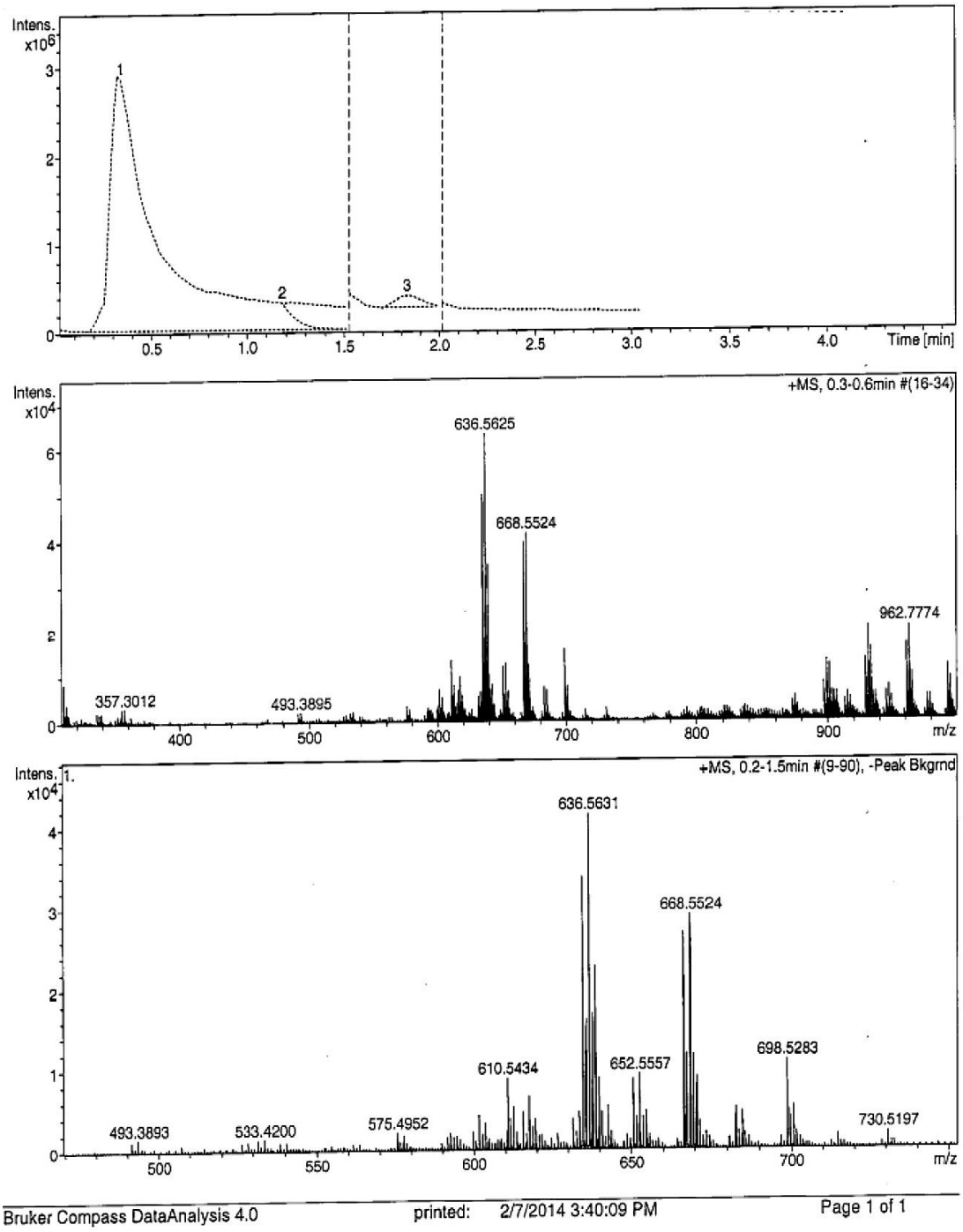

Appendix VII (b): HPLC-MS spectrum of SEFAMEs biodiesel (320-1000 *m/z*)

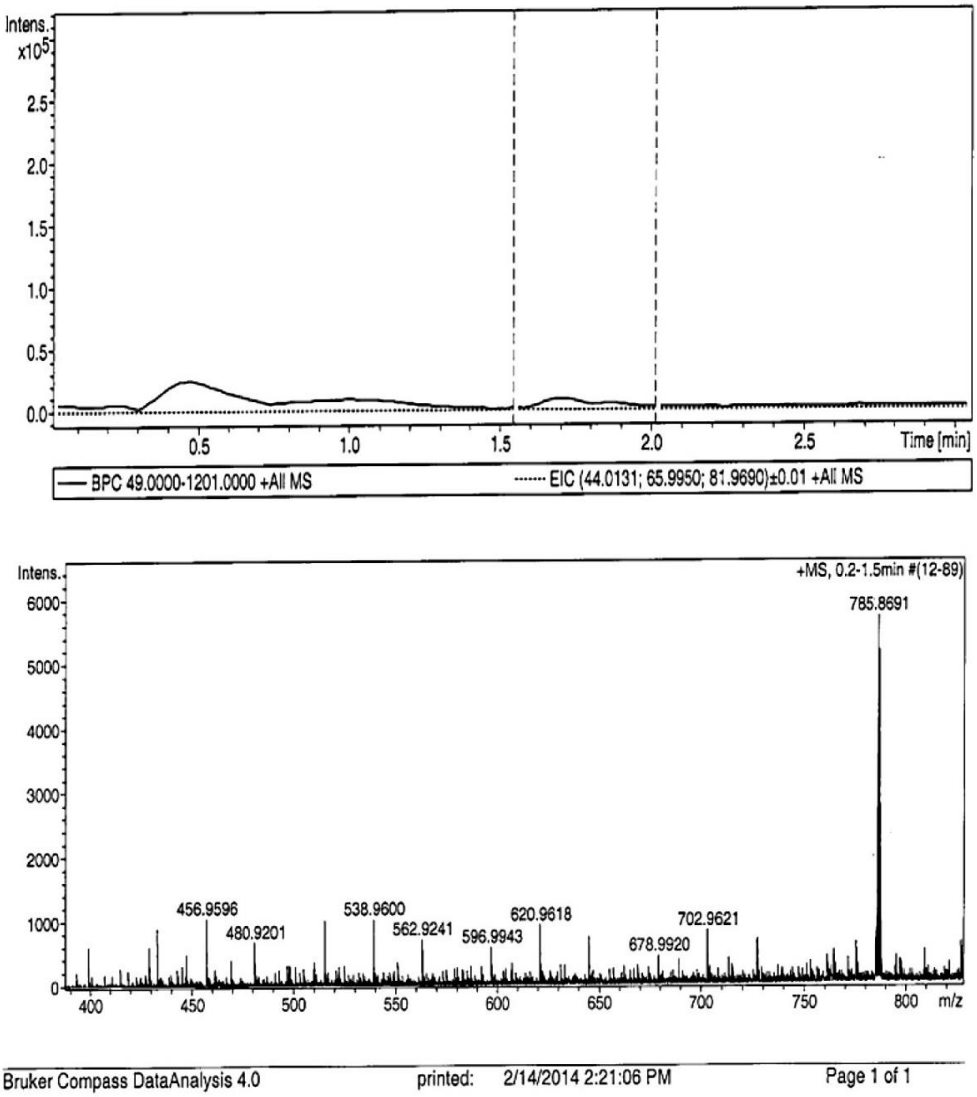

Appendix VII (c): HPLC-MS spectrum of the anionic SEFAMESO surfactant (350-900 *m/z*)

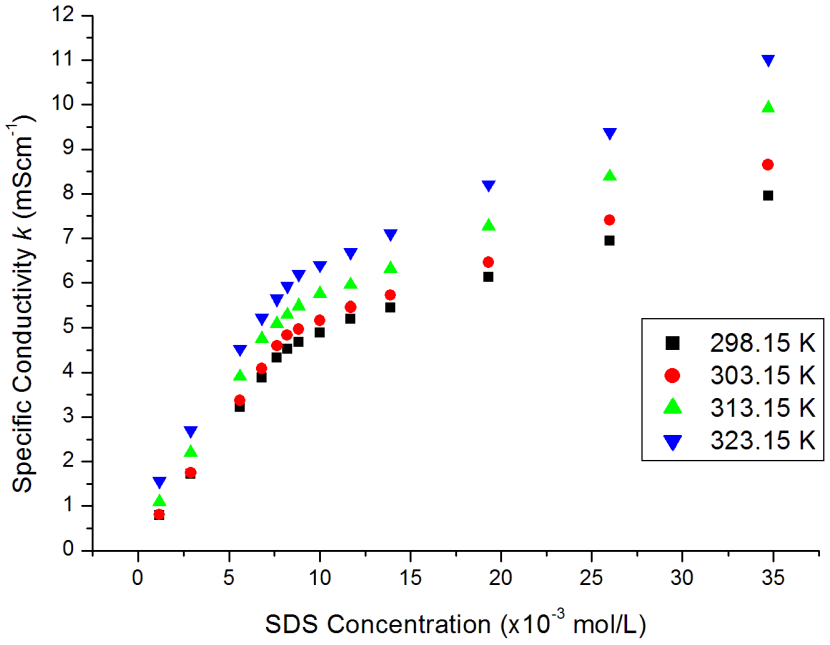

Appendix VIII (a): Plots of Specific Conductivity against SDS concentration at temperature ranges of 298.15-323.15 K.

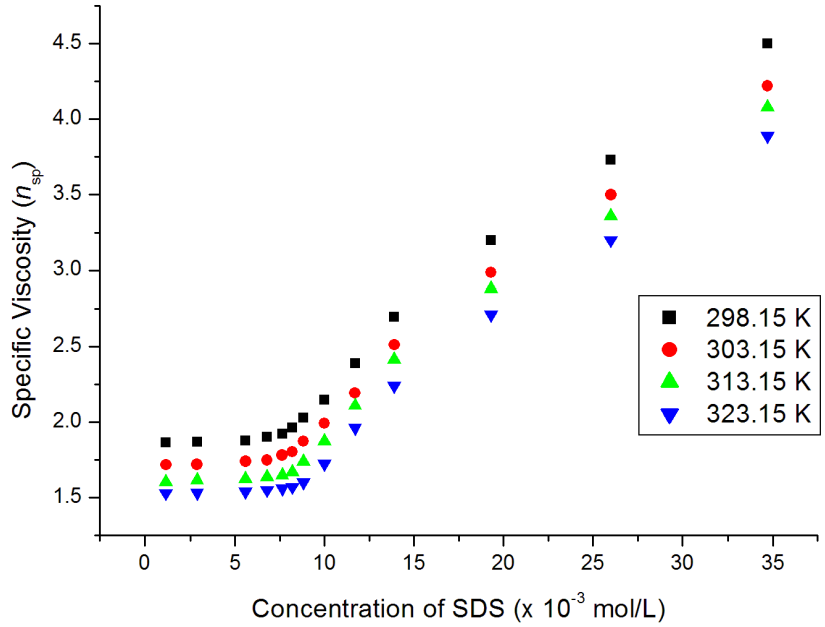

Appendix VIII (b): Plots of Specific Viscosity against SDS concentration at temperature ranges of 298.15-323.15 K.

Appendix IX: CMC values, β and Thermodynamic Properties of Micellization of SDS

SDS Standard							
Temp K	CMC Values ($x10^{-3}$ mol/L)		InX_{CMC}	β	ΔG°_{mic} (kJ mol^{-1})	ΔH°_{mic} (kJ mol^{-1})	ΔS°_{mic} (J $mol^{-1}K^{-1}$)
	From k	From n_{sp}					
298.15	8.318	8.535	-8.808	0.771	-38.64	-12.96	86.17
303.15	8.200	8.400	-8.821	0.756	-39.10	-13.29	85.18
313.15	8.530	8.834	-8.782	0.722	-39.95	-15.14	79.27
323.15	8.757	8.843	-8.746	0.700	-39.93	-16.91	71.27